Image Cover Sheet

CLASSIFICATION	SYSTEM NUMBER
UNCLASSIFIED	65834

TITLE

A NONLINEAR SIX DEGREE-OF-FREEDOM FLIGHT SIMULATION MODEL. VOLUME 1: THEORETICAL DEVELOPMENT

System Number:

Patron Number:

Requester:

Notes:

DSIS Use only:

Deliver to: JR

National Defence / Défense nationale

UNCLASSIFIED

DRES

SUFFIELD REPORT

NO. 446

UNLIMITED
DISTRIBUTION

A NONLINEAR SIX DEGREE-OF-FREEDOM FLIGHT SIMULATION MODEL VOLUME 1 THEORETICAL DEVELOPMENT (U)

by

A.B. Markov

PCN 031SE

May 1990

DEFENCE RESEARCH ESTABLISHMENT SUFFIELD : RALSTON : ALBERTA

Canada

UNCLASSIFIED

UNLIMITED
DISTRIBUTION

DEFENCE RESEARCH ESTABLISHMENT SUFFIELD
RALSTON, ALBERTA

SUFFIELD REPORT NO. 446

A NONLINEAR SIX DEGREE-OF-FREEDOM FLIGHT SIMULATION MODEL
VOLUME 1 THEORETICAL DEVELOPMENT (U)

by

A.B. Markov

PCN 031SE

ACKNOWLEDGEMENT

The current versions of the simulation software are the result of an evolutionary development that has taken place since 1981. During the course of this development there have been numerous contributions to the software by staff of the Systems Section (SS) of the Defence Research Establishment Suffield (DRES), by staff of the DRES computer group, by SS R&D contractors, and by a number of other outside agencies. The author is grateful for the contributions made by all of these sources.

The contributions of the following are especially noteworthy:

1. The software is loosely based on simulation software developed by the author at the University of Toronto Institute for Aerospace Studies while working as part of the Flight Transportation Group under Prof. L. Reid.

2. Preliminary ideas for the structure and features of the software were generated in discussions between the author and Mr. K. Schilling of West Germany. Mr. Schilling was a visiting NATO fellow to DRES in the period September 1980 to December 1981.

3. A significant portion of the ROBOT-X aerodynamic model is based on wind tunnel data collected at the facilities of the High Speed Aerodynamics Laboratory of the National Aeronautical Establishment of the National Research Council.

4. The plotting software package PLTSIM is based on the PLTNLSRBX plotting package developed by Mr. J. Erling. Mr. Erling was a Research Assistant under the supervision of the author from May 1983 to September 1983.

5. A number of SS R&D contractors have utilized the software extensively and have provided valuable feedback both in identifying and resolving a number of bugs and in improving the utility of the software. In this regard, Mr. K. Lee of Ballistech Systems Inc., Montreal and Mr. B. Gagnon formerly of Boeing of Canada Ltd. made particularly significant contributions in the February 1985 to September 1986 timeframe.

6. The careful reviews of the draft manuscripts by Dr. R. Herring and Dr. S. Barton of DRES were instrumental in finalizing the format and content of the report volumes.

7. The meticulous preparation of the manuscript volumes by Ms. C. Baumann, and patience through several extensive revisions, is particularly appreciated.

ABSTRACT

Six degree-of-freedom, rigid body equations of motion are described suitable for modeling the dynamic characteristics of multistaged rocket-boosted maneuvering aerial targets such as the DRES developed ROBOT-X. These equations of motion form the core of a Fortran simulation package called FLISIM. FLISIM is currently installed on a VAX 11/780 computer and allows for modeling of vehicle thrust and structural asymmetries, time-varying mass and inertia characteristics, autopilot control laws, autopilot update rates, autopilot sensor nonidealities, nonlinear aerodynamic characteristics, variable wind conditions, turbulence, nonstandard atmospheric conditions, stage and individual motor failures, different rocket motor types, and parachute deceleration dynamics. The FLISIM software package has been developed in two versions (FLISIMV1 and FLISIMV2) using two different aerodynamic models. Both are written in VAX 11 Fortran and run under the VMS Operating System. FLISIM is fully supported with a plotting software package (PLTSIM) developed around Tektronix PLOT 10 core software.

Volume 1 describes the development of the equations of motion. Volume 2 is the FLISIM software userbook. Volume 3 contains FLISIM source code listings.

VOLUME 1 - TABLE OF CONTENTS

VOLUME 1 - TABLE OF CONTENTS
(Continued)

VOLUME 2 - TABLE OF CONTENTS

VOLUME 2 - TABLE OF CONTENTS
(Continued)

VOLUME 2 - TABLE OF CONTENTS
(Continued)

VOLUME 3 - TABLE OF CONTENTS

VOLUME 3 - TABLE OF CONTENTS
(Continued)

VOLUME 1 - LIST OF TABLES

VOLUME 1 - LIST OF FIGURES

LIST OF SYMBOLS

The following is a list of important symbols. Some symbols, which are defined in the text and are used only once, or are secondary quantities related to a primary quantity that is apparent from the text or from the notation conventions to follow are not included. Numbers in parentheses refer to equations.

$\underset{\rightarrow}{A}$	Aerodynamic force vector applied to the vehicle not including thrust forces and parachute forces.
$\underset{\rightarrow}{a}$, $\underset{\rightarrow}{a}_B$	Vehicle centre-of-mass acceleration vector relative to inertial space.
a	Speed of sound (m/s).
b	Reference length (span of wing for winged flight vehicles) (m).
C_D	(Total drag) / ($q_D S$), vehicle drag coefficient.
C_{D_1}, $C_{D_1}^N$	Partial drag contributions, see Volume 1, Section 3.
C_L	(Total lift) / ($q_D S$), vehicle lift coefficient.

LIST OF SYMBOLS (cont'd)

C_{L_i}, $C^N_{L_i}$	Partial lift contributions, see Volume 1, Section 3.
C_{L_α}	$\frac{\partial C_L}{\partial \alpha}\Big\|_e$ (/rad).
C^B_ℓ, C^N_ℓ	$L_{A_B}/(q_D Sb)$, $L_{A_N}/(q_D Sb)$.
C^B_m, C^N_m	$M_{A_B}/(q_D S\bar{c})$, $M_{A_N}/(q_D S\bar{c})$.
C_{m_i}, C^N_m	Partial pitching moment contributions, see Volume 1, Section 3.
C^B_n, C^N_n	$N_{A_B}/(q_D Sb)$, $N_{A_N}/(q_D Sb)$.
C_T	$T/(q_D S)$, thrust coefficient.
C_W	$mg/(q_D S)$, weight coefficient.
C^B_x	$X_B/(q_D S)$.
C^B_y	$Y_B/(q_D S)$.
C^B_z	$Z_B/(q_D S)$.
$\bar{c}$	Mean geometric chord (m).

LIST OF SYMBOLS (cont'd)

$\bar{c}_A$	Mean aerodynamic chord (m).
D	Total drag.
$\underset{\rightarrow}{F}$	External force vector acting on the vehicle centre-of-mass.
F_B	Body-fixed reference frame with origin at the vehicle centre-of-mass, see Figure 3 of Volume 1.
F_E	North pointing Earth-fixed reference frame, see Section 2.2 and Figure 2 of Volume 1.
F_I	North pointing inertial reference frame, see Section 2.2 and Figure 2 of Volume 1.
F_L	Launch site reference frame, see Section 2.2 and Figure 2 of Volume 1.
F_{LA}	Launcher reference frame, see Section 2.2 and Figure 2 of Volume 1.
F_N	Body-fixed reference frame to which nominal aerodynamic characteristics are referenced, see Figure 3 of Volume 1.

LIST OF SYMBOLS (cont'd)

F_R	Structural body-fixed reference frame with origin at nose datum time, see Figure 3 of Volume 1.
F_T	Stand-off Earth-fixed reference frame, see Figure 2 of Volume 1.
F_W, F_{WN}	Wind axes reference frames, see Figure 4 and Section 2.2 of Volume 1.
g	Acceleration due to gravity (m/s^2).
g_o	Nominal sea level acceleration due to gravity (m/s^2).
$\underset{\rightarrow}{h}$	Vehicle angular momentum vector about centre-of-mass.
h_{ASL}	Altitude of vehicle centre-of-mass above sea level.
I_{sp_i}	Specific impulse of i-th rocket motor.
I^B_{xx}, I^B_{yy}, ...	Vehicle moments of inertia about its centre-of-mass written as components in F_B.
$(L_{A_B}, M_{A_B}, N_{A_B})$	Aerodynamic moment components in F_B not including thrust and parachute moments, about centre-of-mass.

LIST OF SYMBOLS (cont'd)

$(L_{T_B}, M_{T_B}, N_{T_B})$	Thrust moment components in F_B about centre-of-mass.
$(L_{T_B}, M_{T_B}, N_{T_B})_{cg}$	See Section 5 of Volume 1.
$(L_{T_B}, M_{T_B}, N_{T_B})_{nz}$	See Section 5 of Volume 1.
$\underset{\rightarrow}{M}_A$	Aerodynamic moment vector acting about the vehicle centre-of-mass not including thrust moments or parachute moments.
$\underset{\rightarrow}{M}_P$	Aerodynamic parachute moment vector acting about the vehicle centre-of-mass.
$\underset{\rightarrow}{M}_T$	Thrust moment vector acting about the vehicle centre-of-mass.
m	Vehicle total mass.
m_i	Mass of the i-th airframe component.
$(m_{RE})_i$	Mass of i-th rocket motor less propellant.
$(m_{PR})_i$	Mass of i-th rocket motor's propellant.
N_M	Total number of rocket motors.
p_A	Atmospheric pressure.

LIST OF SYMBOLS (cont'd)

(P_B, Q_B, R_B)	Angular velocity components of F_B with respect to F_I written as components in F_B.
q_D	Dynamic pressure, $\frac{1}{2}\rho V^2$ (Pa).
$\underset{\rightarrow}{R}$	Position vector of vehicle centre-of-mass relative to F_I.
$\underset{\rightarrow}{R}_T$	Position vector of vehicle centre-of-mass relative to F_T.
$\underset{\rightarrow}{R}_{IT}$	Position vector of R_T relative to F_I.
R	See equation (7,5) of Volume 1; also the magnitude of the range vector depending on the context.
r_E	Radius of the Earth to the nominal sea level datum plane (m).
S	Reference area (projected wing planform area for winged vehicles) (m^2).
s	Distance the vehicle has moved along the launcher from its rest position (see Section 8.1 of Volume 1) (m).

LIST OF SYMBOLS (cont'd)

s_G	Launch rail guide length (see Figure 14 of Volume 1) (m).
s_n	The length of vehicle in front of the launcher while the vehicle is at rest on the launcher (see Figure 14 of Volume 1) (m).
$\underset{\rightarrow}{T}$	Thrust vector.
T_A	Atmospheric temperature (degrees Kelvin).
T_i	Thrust of the i-th rocket motor (N).
(U_B, V_B, W_B)	Components of $\underset{\rightarrow}{V}$ in F_B.
$(U_{B_E}, V_{B_E}, W_{B_E})$	Components of $\underset{\rightarrow}{V}_E$ in F_B.
$(U_{B_g}, V_{B_g}, W_{B_g})$	Components of $\underset{\rightarrow}{W}$ in F_B.
$\underset{\rightarrow}{V}$	Airspeed vector.
$\underset{\rightarrow}{V}_E$	Velocity vector of the vehicle centre-of-mass with respect to F_I and F_E.
V	Magnitude of $\underset{\rightarrow}{V}$ (m/s).
V_{xz}	$(U_B^2 + W_B^2)^{1/2}$ (m/s).

LIST OF SYMBOLS (cont'd)

$\underset{\rightarrow}{W}$	Wind velocity vector with respect to F_I.
(W_1, W_2, W_3)	Components of $\underset{\rightarrow}{W}$ in F_I (m/s).
$(X_{A_B}, Y_{A_B}, Z_{A_B})$	Aerodynamic force components in F_B, acting at the vehicle centre-of-mass not including thrust and parachute contributions (N).
$(X_{P_B}, Y_{P_B}, Z_{P_B})$	Aerodynamic parachute force components in F_B acting at vehicle centre-of-mass (N).
$(X_{T_B}, Y_{T_B}, Z_{T_B})$	Thrust vector components in F_B (N).
(x_{cm}, y_{cm}, z_{cm})	Coordinates of the vehicle centre-of-mass in F_R (m).
(x_T, y_T, z_T)	Components of $\underset{\rightarrow}{R}_T$ in F_T (see Section 8.2 of Volume 1) (m).
(x_E, y_E, z_E)	Components of $\underset{\rightarrow}{R}$ in F_E (m).
(x_I, y_I, z_I)	Components of $\underset{\rightarrow}{R}$ in F_I (m).
$[(x_{RE})_i, (y_{RE})_i, (z_{RE})_i]$	Coordinates of the centre-of-mass of the empty motor case of the i-th rocket motor in F_R (m).

LIST OF SYMBOLS (cont'd)

(x_i, y_i, z_i)	Coordinates of the centre-of-mass of the i-th airframe component in F_R (m).
$[(x_{PR})_i, (y_{PR})_i, (z_{PR})_i]$	Coordinates of the centre-of-mass of the propellant of the i-th rocket motor in F_R (m).
α_f	Fuselage reference line angle of attack of vehicle.
β	Angle of sideslip of vehicle.
θ_B	Pitch Euler angle of F_B.
ξ_A	Aspect elevation angle of vehicle relative to F_T (see Figure 2 of Volume 1).
ξ_E	Aspect azimuth angle of vehicle relative to F_T (see Figure 2 of Volume 1).
ρ	Air density (kg/m^3).
ϕ_B	Euler bank angle for F_B.
ϕ	Cylindrical coordinate (see Figure 5 of Volume 1).
ψ_B	Euler azimuth angle for F_B.

LIST OF SYMBOLS (cont'd)

ψ_L	Euler azimuth angle for F_L.
ψ_{LW}	Euler azimuth angle for F_{LW}.
ψ_T	Euler azimuth angle for F_T.
$\underset{\rightarrow}{\omega}_B$	Angular velocity vector of F_B with respect to F_I.

NOTATION CONVENTIONS

$C^{C}_{A_s}$ Generalized aerodynamic derivative notation, $\left.\frac{\partial C^{C}_{A}}{\partial s}\right|_{e}$ where C_A is a nondimensional aerodynamic coefficient, specified by the subscript A, in reference frame F_C, s is a dynamic variable, and the 'e' notation indicates the aerodynamic derivative is evaluated at equilibrium.

F_A Reference frame A.

$\underline{L}_{AB}$ A rotation matrix rotating components of a vector expressed in F_B to the components of the same vector expressed in F_A.

$\underset{\rightarrow}{X}$ Vector quantity X.

$\underset{\rightarrow}{X} \times \underset{\rightarrow}{Y}$ Vector cross-product of X and Y.

$\underline{X}$ A matrix X.

$\underline{X}^{A}$ $\underset{\rightarrow}{X}$ expressed as components in F_A.

$\underline{X}^{T}$ The transpose of $\underline{X}$ or the components of a vector $\underset{\rightarrow}{X}$ expressed in the reference frame F_T(context will determine which interpretation is intended).

X* Indicates a parameter X estimated in the flight control system algorithms (used primarily in Volume 2).

$\underline{x}$ A column matrix x.

NOTATION CONVENTIONS (cont'd)

x_e A quantity x whose value is computed for an aerodynamic quasi-steady equilibrium condition.

x_s A quantity x sensed through the flight control system sensors (used primarily in Volume 2).

1. INTRODUCTION

Since 1979 DRES has been involved in the development of rocket boosted targets for use by the Canadian Forces (CF) in various high speed aerial target roles. This work included the development of ROBOT-5 in a joint US Army/DRES program that undertook to modify the US Army BATS target for use with the higher specific impulse C14 (CRV-7) rocket motors under the auspices of a joint US-Canadian TTCP agreement, the development of ROBOT-9, an all CRV-7 free-flight, multistage ballistic target, ROBOT-X, a maneuvering aerial target (Figure 1), capable of low altitude hold simulating an antiship missile, ROBOT-SX, a clipped wing supersonic dash ROBOT-X configuration and ROBOT-LRX, a novel short to medium range supersonic dash aerial target configuration. Of these systems, ROBOT-5, ROBOT-9 and ROBOT-X have flown, while ROBOT-SX and ROBOT-LRX have undergone wind tunnel testing.

To support the development of these targets computer simulation models were required that predicted the dynamic characteristics of the vehicles, modeled the closed-loop characteristics of the control system, and in general provided the means of modeling all of the relevant characteristics of the flight vehicle in determining performance, stability and control characteristics. Environmental effects (e.g. wind, nonstandard atmosphere and so forth) also had to be taken into account.

No existing software was available to DRES that met these requirements while at the same time permitting some configuration variation in terms of mass, aerodynamic, control system, propulsion unit and environmental characteristics. DRES thus undertook the development of the required simulation software.

As a result, two main simulation packages have been developed. The first, and less sophisticated package was developed in support of six degree-of-freedom (DOF) simulation of free-flight rocket boosted targets (e.g. ROBOT-5 and ROBOT-9) in the period September 1980 to December 1981 and, since this initial development, has undergone a gradual revision and improvement process that has included addition of extensive plotting software. This package was designated BALSIM (BALlistic SIMulation) and is currently resident on a VAX 11/780 computer at DRES. The initial version of the package is fully documented in Reference 1.

The second simulation package, referred to as FLISIM (FLIght SIMulation), was developed in response to the increasing sophistication of the rocket-boosted targets under development at DRES and in particular towards meeting the need to have six DOF simulation of "flying" systems including modeling of the closed-loop control characteristics. BALSIM has no capability for modeling nonballistic systems, and, in particular, systems with control surfaces.

The FLISIM software is based in part on simulation software developed at the University of Toronto Institute for Aerospace Studies (UTIAS) in support of the computations carried out for Reference 2. FLISIM software is resident on a VAX 11/780 at DRES, and was developed using DEC FORTRAN Version 4.8-276 (an extended version of FORTRAN 77) and run on the VMS Version 5.1 Operating System. It is available in two primary versions (FLISIMV1 and FLISIMV2), the differences in the two versions consisting solely of differences in the aerodynamic model formulation.

In addition to the FLISIM software itself, there are a number of associated software packages that may be used in conjunction with

FLISIM, including a plotting package developed around Tektronix PLOT 10 software, and aerodynamic model generation software. DRES six DOF simulation packages and associated software are summarized in Table I.

Both BALSIM and FLISIM software have command procedures that facilitate user set-up and execution in batch and interactive modes. Both packages, including software, have been successfully utilized using DEC VT100 (with Retrographics), Tektronix 4112, 4105, 4107 and 4114 terminals.

It is the intent of Volumes 1 and 2 to provide documentation of FLISIM and associated software in sufficient detail to permit users familiar with FORTRAN to run the program.

Volume 1 documents the simulation model. Section 2 develops the dynamic model and summarizes its limitations. Section 3 describes the aerodynamic models associated with FLISIMV1 and FLISIMV2. Section 4 describes the mass and moments of inertia models. Section 5 describes the thrust model. Section 6 describes the wind and turbulence models. Section 7 describes the atmospheric model. Section 8 describes equations developed to compute a number of auxiliary parameters. Finally, Section 9 gives a general software description.

Volume 2 is intended as an essentially self-contained userbook for FLISIM.

Volume 3 contains source code listings.

2. EQUATIONS OF MOTION

This section summarizes the key features of the dynamic model programmed into the FLISIM package. The basic six DOF equations are derived in the following subsections.

2.1 Fundamental Assumptions

Several overall simplifying assumptions have been made in the derivation of the equations of motion. They are valid for rocket-boosted flight vehicles that have rigid structures and relatively short ranges, i.e. less than 100 km (50 nm).

The assumptions are as follows:

1. The Earth is flat and any Earth-fixed reference frame is inertial.
2. The vehicle is a single rigid body.

Assumption 2 implies that there are no dynamically significant contributions due to rigid bodies spinning relative to each other, e.g. rotors.

2.2 Reference Frames, Rotation Matrices and Angular Velocities

In the general case both an Earth-fixed (say F_E) and an inertial reference frame (say F_I) must be defined. Because of the first simplifying assumption of the previous section, these reference frames are both inertial. Thus let F_I be an Earth-fixed inertial reference frame whose origin is at the centre-of-mass rest position of the vehicle on the launcher, whose x-axis points to True North, and whose

z-axis is nominally downwards (see Figure 2). The y-axis follows from the right hand rule.

F_E has axes that are parallel to F_I but an origin located on the sea level datum at the point where the z-axis of F_I intersects the datum.

A third, inertial Earth-fixed reference frame that is useful is the launcher reference frame F_{LA}. The origin of F_{LA} coincides with that of F_I with the x-axis pointing in the launch direction and the z-axis being nominally downwards (see Figure 2). The y-axis follows from the right hand rule.

A fourth Earth-fixed reference frame which is occasionally required is F_L, the launch site reference frame. As for F_{LA}, the origin of F_L coincides with F_I with the x-axis pointing along the projection of the initial flight path onto the horizontal plane and the z-axis being nominally downwards.

A fifth Earth-fixed reference frame which is occasionally required is that of a reference frame F_T placed at some distance from the launch site. This reference frame is used to compute the aspect angle of the flight vehicle relative to a designated site. Since the location and orientation of this reference will depend on the particular application, it is defined only generally in Figure 2.

Other Earth-fixed reference frames are used in specialized situations. These are defined as they arise in the text.

Since the aerodynamic forces are most conveniently expressed with respect to the vehicle, a body-fixed reference frame F_B will also

be used. The origin of F_B is located at the vehicle centre-of-mass. In vehicles that are axisymmetric, the x-axis is on the axis of symmetry and points forward through the nose. Otherwise the x-axis points in the nominal launch direction. The z-axis is nominally downward, while the y-axis follows from the right hand rule. This reference frame and some associated aerodynamic angles are shown in Figure 3.

A second body-fixed reference frame that is useful in specifying the vehicle's mass, inertia and configuration characteristics is a reference frame F_R whose origin is located on a nose datum plane on the vehicle. If the vehicle is axisymmetric, then the origin of F_R is on the axis of symmetry, and its x-axis points towards the rear of the vehicle on the axis of symmetry. Otherwise, the origin of F_R may be any convenient location on the nose datum plane, and the x-axis nominally points towards the rear of the vehicle. The z-axis is nominally upward and the y-axis follows from the right hand rule (see Figure 3).

A third body-fixed reference frame about which the nominal aerodynamic characteristics are expressed is the reference frame F_N. F_N has axes that are parallel to F_B but an origin that generally does not coincide with that of F_B.

Other body-fixed reference frames are occasionally used in the development of the simulation model. These are defined as they arise. They include the following:

1. F_{R_i} - A reference frame of arbitrary origin and orientation attached to the i-th airframe component.

2. F_{B_i} - A reference frame that has an origin located at the

centre-of-mass of the i-th component and axes that are parallel to F_B.

3. F_A - A reference frame whose origin is at a body-fixed accelerometer triad and whose axes are parallel to F_B.

4. F_{TH_i} - A reference frame whose origin is located at the point of action of the thrust vector of the i-th rocket motor, and its x-axis is in the negative thrust direction.

Wind axes F_W are used in specifying certain aspects of the aerodynamic forces and moments acting on the flight vehicle. The origin of F_W coincides with that of F_B, i.e. it is at the centre-of-mass, and its x-axis is always aligned with the velocity vector $\underrightarrow{V}$. Its z-axis is in the plane of symmetry and its y-axis orientation follows from the right hand rule (see Figure 4).

Wind axes F_{WN} are identical to F_W except that they have an origin located at the origin of F_N.

In the following, use is made of a number of notation conventions. In particular if $\underline{L}_{BA}$ denotes a rotation matrix relating the components of a vector $\underrightarrow{V}$ expressed in F_A ($\underline{v}^A$) to the components of the same vector in F_B ($\underline{v}^B$), then

$$\underline{v}^B = \underline{L}_{BA}\underline{v}^A \qquad (2.2,1)$$

The following definitions, geometric relationships and matrices, will be employed in the presentation of the equations of motion.

1. The rotation matrix relating F_I and F_B:

$$\underline{L}_{BI} = \begin{bmatrix} 1 & 0 & 0 \\ 0 & \cos\phi_B & \sin\phi_B \\ 0 & -\sin\phi_B & \cos\phi_B \end{bmatrix} \begin{bmatrix} \cos\theta_B & 0 & -\sin\theta_B \\ 0 & 1 & 0 \\ \sin\theta_B & 0 & \cos\theta_B \end{bmatrix} \begin{bmatrix} \cos\psi_B & \sin\psi_B & 0 \\ -\sin\psi_B & \cos\psi_B & 0 \\ 0 & 0 & 1 \end{bmatrix} \quad (2.2,2a)$$

or

$$\underline{L}_{BI} = \begin{bmatrix} \cos\theta_B\cos\psi_B & \cos\theta_B\sin\psi_B & -\sin\theta_B \\ \sin\phi_B\sin\theta_B\cos\psi_B - \cos\phi_B\sin\psi_B & \sin\phi_B\sin\theta_B\sin\psi_B + \cos\phi_B\cos\psi_B & \sin\phi_B\cos\theta_B \\ \cos\phi_B\sin\theta_B\cos\psi_B + \sin\phi_B\sin\psi_B & \cos\phi_B\sin\theta_B\sin\psi_B - \sin\phi_B\cos\psi_B & \cos\phi_B\cos\theta_B \end{bmatrix} \quad (2.2,2b)$$

$$= [l_{BI_{ij}}] \quad (2.2,2c)$$

where ϕ_B, θ_B and ψ_B are the Euler angles defined in References 4 and 5.

2. The rotation matrix relating F_I and F_{LA} (see Figure 2):

$$\underline{L}_{LAI} = \begin{bmatrix} \cos\theta_{B_o} & 0 & -\sin\theta_{B_o} \\ 0 & 1 & 0 \\ \sin\theta_{B_o} & 0 & \cos\theta_{B_o} \end{bmatrix} \qquad (2.2,3a)$$

$$= [l_{LAI_{ij}}] \qquad (2.2,3b)$$

3. The rotation matrix relating F_I and F_T (see Figure 2):

$$\underline{L}_{TI} = \begin{bmatrix} \cos\psi_T & \sin\psi_T & 0 \\ -\sin\psi_T & \cos\psi_T & 0 \\ 0 & 0 & 1 \end{bmatrix} \qquad (2.2,4a)$$

$$= [l_{TI_{ij}}] \qquad (2.2,4b)$$

4. The rotation matrix relating F_{TH_i} and F_B (see Figures 3 and 8 and cf. equation (2.2,2a)):

$$\underline{L}_{BTH_i} = \begin{bmatrix} -\cos\delta_{TH_i}\cos\theta_{TH_i} & \sin\delta_{TH_i}\cos\theta_{TH_i} & -\sin\theta_{TH_i} \\ \cos\delta_{TH_i}\sin\theta_{TH_i}\sin\phi_{TH_i} + \sin\delta_{TH_i}\cos\phi_{TH_i} & -\sin\delta_{TH_i}\sin\theta_{TH_i}\sin\phi_{TH_i} + \cos\delta_{TH_i}\cos\phi_{TH_i} & -\cos\theta_{TH_i}\sin\phi_{TH_i} \\ \cos\delta_{TH_i}\sin\theta_{TH_i}\cos\phi_{TH_i} - \sin\delta_{TH_i}\sin\phi_{TH_i} & -\sin\delta_{TH_i}\sin\theta_{TH_i}\cos\phi_{TH_i} - \cos\delta_{TH_i}\sin\phi_{TH_i} & -\cos\theta_{TH_i}\cos\phi_{TH_i} \end{bmatrix} \quad (2.2,5a)$$

$$= [(l_{BTH_i})_{ij}] \quad (2.2,5b)$$

5. The rotation matrix relating F_N and F_B:

$$\underline{L}_{BN} = \underline{I} \quad (2.2,6)$$

where $\underline{I}$ is the identity matrix. This implies that

$$\underline{L}_{NI} = \underline{L}_{BI} \quad (2.2,7)$$

6. The rotation matrix relating F_W and F_N, and F_W and F_B:

$$\underline{L}_{NW} = \underline{L}_{BW} = \begin{bmatrix} \cos\beta\cos\alpha_f & -\sin\beta\cos\alpha_f & -\sin\alpha_f \\ \sin\beta & \cos\beta & 0 \\ \cos\beta\sin\alpha_f & -\sin\beta\sin\alpha_f & \cos\alpha_f \end{bmatrix} \quad (2.2,8a)$$

$$= [l_{NW_{ij}}] = [l_{BW_{ij}}] \qquad (2.2,8b)$$

where the aerodynamic angles α_f and β have been interpreted as an ordered rotation $(-\beta, \alpha_f, 0)$.

7. The rotation matrix relating F_R and F_B:

$$\underline{L}_{BR} = \begin{bmatrix} -1 & 0 & 0 \\ 0 & 1 & 0 \\ 0 & 0 & -1 \end{bmatrix} \qquad (2.2,9a)$$

$$= [l_{BR_{ij}}] \qquad (2.2,9b)$$

8. The angular velocity of the vehicle with respect to F_I written as components in F_B:

$$\underline{\omega}^B = (P_B, Q_B, R_B)^T \qquad (2.2,10)$$

9. The angular rate cross-product matrices (Reference 4, Section 4.6), in F_B:

$$\underset{\sim}{\omega}^B = \begin{bmatrix} 0 & -R_B & Q_B \\ R_B & 0 & -P_B \\ -Q_B & P_B & 0 \end{bmatrix} \qquad (2.2,11)$$

10. The airspeed vector of the vehicle written as components in F_B:

$$\underline{V}^B = (U_B, V_B, W_B)^T \qquad (2.2,12)$$

11. The groundspeed vector of the vehicle with respect to F_I written as components in F_B and F_I:

$$\underline{V}_E^B = (U_{B_E}, V_{B_E}, W_{B_E})^T \qquad (2.2,13a)$$

$$\underline{V}_E^I = (\dot{x}_I, \dot{y}_I, \dot{z}_I)^T \qquad (2.2,13b)$$

12. The aerodynamic angles (see Figure 3):

$$\alpha_f = \arctan (W_B/U_B) \qquad (2.2,14)$$

$$\beta = \arctan (V_B/V_{xz}) \qquad (2.2,15)$$

where

$$V_{xz} = (U_B^2 + W_B^2)^{1/2} \qquad (2.2,16)$$

$$V = (U_B^2 + V_B^2 + W_B^2)^{1/2} \qquad (2.2,17)$$

Here α is the angle of attack of the x-axis of F_B, β is the angle of sideslip of the x-axis of F_B, V is the airspeed, and V_{xz} is the magnitude of the airspeed vector component along the x-z plane of F_B.

13. The geometric relationships (see Figure 3):

$$U_B = V\cos\beta\cos\alpha_f \qquad (2.2,18a)$$

$$V_B = V\sin\beta \qquad (2.2,18b)$$

$$W_B = V\cos\beta\sin\alpha_f \qquad (2.2,18c)$$

14. The wind velocity with respect to F_I (or F_E) written as components in F_I and F_B:

$$\underline{W}^E = \underline{W}^I = (W_1, W_2, W_3)^T \qquad (2.2,19a)$$

$$\underline{W}^B = (U_{B_g}, V_{B_g}, W_{B_g})^T \qquad (2.2,19b)$$

15. The acceleration due to gravity written as components in F_I (F_E):

$$\underline{g}^E = \underline{g}^I = (0, 0, g)^T \qquad (2.2,20)$$

16. The aerodynamic forces (not including thrust forces) written as components in F_B, F_N and F_W:

$$\underline{A}^B = \underline{A}^B_A = (X_{A_B}, Y_{A_B}, Z_{A_B})^T \qquad (2.2,21a)$$

$$\underline{A}^N_A = (X_{A_N}, Y_{A_N}, Z_{A_N})^T \qquad (2.2,21b)$$

$$\underline{A}^W_A = (-D, Y_W, -L)^T \qquad (2.2,21c)$$

17. The aerodynamic moments (not including thrust moments) written as components in F_B and F_N:

$$\underline{M}_A^B = (L_{A_B}, M_{A_B}, N_{A_B})^T \qquad (2.2,22a)$$

$$\underline{M}_A^N = (L_{A_N}, M_{A_N}, N_{A_N})^T \qquad (2.2,22b)$$

18. The inertia matrix of the vehicle with respect to its centre-of-mass expressed in F_B (see Reference 4, Section 5.4):

$$\underline{I}^B = \begin{bmatrix} I_{xx}^B & -I_{xy}^B & -I_{xz}^B \\ -I_{xy}^B & I_{yy}^B & -I_{yz}^B \\ -I_{xz}^B & -I_{yz}^B & I_{zz}^B \end{bmatrix} \qquad (2.2,23)$$

19. The total thrust forces written as components in F_B:

$$\underline{T}^B = (X_{T_B}, Y_{T_B}, Z_{T_B})^T \qquad (2.2,24)$$

20. The total thrust moments written as components in F_B:

$$\underline{M}_T^B = (L_{T_B}, M_{T_B}, N_{T_B})^T \qquad (2.2,25)$$

21. The total parachute forces written as components in F_B:

$$\underline{A}_P^B = (X_{P_B}, Y_{P_B}, Z_{P_B})^T \qquad (2.2,26)$$

22. The total parachute moments written as components in F_B:

$$\underline{M}_P^B = (L_{P_B}, M_{P_B}, N_{P_B})^T \qquad (2.2,27)$$

23. Cylindrical coordinates (Figure 5) of the centre-of-mass of the various vehicle components are as follows:

a) For the i-th airframe components they are denoted (x_i, r_i, ϕ_i).

b) For the i-th empty rocket motor they are denoted (x_{RE_i}, r_{RE_i}, ϕ_{RE_i}).

c) For the propellant of the i-th rocket motor they are denoted (x_{PR_i}, r_{PR_i}, ϕ_{PR_i}).

24. Cylindrical coordinates of the point of action of the thrust vector of the i-th rocket motor are given by (x_{TH_i}, r_{TH_i}, ϕ_{TH_i}).

2.3 Newton-Euler Development of the General Equations of Motion

Newton-Euler techniques begin with the fundamental equations (Reference 4, Chapter 5)

$$\underset{\rightarrow}{F} = m\underset{\rightarrow}{a} \qquad (2.3,1)$$

and

$$\dot{\underset{\rightarrow}{h}} = \underset{\rightarrow}{M} \qquad (2.3,2)$$

$\underset{\rightarrow}{a}$ is the acceleration vector of the body centre-of-mass relative to an inertial reference frame, $\underset{\rightarrow}{h}$ is the angular momentum of the body about its centre-of-mass, $\underset{\rightarrow}{F}$ is the external force vector acting at the centre-of-mass and $\underset{\rightarrow}{M}$ is the external moment vector about the centre-of-mass. $\underset{\rightarrow}{F}$ may be written

$$\underset{\rightarrow}{F} = m\dot{\underset{\rightarrow}{V}}_E \qquad (2.3,3)$$

where $\underset{\rightarrow}{V}_E$ is the velocity vector of the vehicle with respect to F_I and m is the mass of the vehicle. An expression for $\underset{\rightarrow}{h}$ follows from the fundamental relationship

$$\underset{\rightarrow}{h} = \int_{\text{mass}} [\underset{\rightarrow}{r} \times \dot{\underset{\rightarrow}{r}}] \, dm \qquad (2.3,4a)$$

or

$$\underset{\rightarrow}{h} = \int_{\text{mass}} [\underset{\rightarrow}{r} \times \overset{\circ}{\underset{\rightarrow}{r}} + \underset{\rightarrow}{r} \times (\underset{\rightarrow}{\omega}_B \times \underset{\rightarrow}{r})] \, dm \qquad (2.3,4b)$$

where $\underset{\rightarrow}{r}$ is the position vector of an element of mass dm of the body with respect to its centre-of-mass (see Figure 7), $\underset{\rightarrow}{\omega}_B$ is the angular velocity vector of F_B with respect to F_I, '$\cdot$' when applied to a vector represents rate of change with respect to F_I and '$\circ$' when applied to a vector represents rate of change with respect to F_B (see Reference 5,

Section 4.3, for a more thorough discussion of vector differentiation). Equation (2.3,4b) may be written in matrix notation as (replacing $\underset{\rightarrow}{\omega}_B \times \underset{\rightarrow}{r}$ by $-\underset{\rightarrow}{r} \times \underset{\rightarrow}{\omega}_B$ and dropping the subscript 'B' on $\underset{\rightarrow}{\omega}_B$ for the sake of brevity)*

$$\underline{h}^B = \int_{\text{mass}} [\underset{\sim}{\underline{r}}^B \dot{\underline{r}}^B - \underset{\sim}{\underline{r}}^B \underset{\sim}{\underline{r}}^B \underline{\omega}^B] \, dm \qquad (2.3,5)$$

But

$$\dot{\underline{r}}^B = \underline{0} \qquad (2.3,6)$$

for a rigid body. Since $\underline{\omega}^B$ is a constant with respect to the integration in (2.3,5), it follows that

$$\underline{h}^B = \underline{I}^B \underline{\omega}^B \qquad (2.3,7)$$

---

* Superscripts on matrix quantities refer to the reference frame in which the components of the matrix are expressed. Overscore '∿' refers to the matrix equivalent of the vector cross-product (Reference 4, Section 4.6):

$$\underset{\sim}{\underline{r}} = \begin{bmatrix} 0 & -z & y \\ z & 0 & -x \\ -y & x & 0 \end{bmatrix}$$

where

$$\underline{I}^B = -\int_{\text{mass}} \underset{\sim}{r}^B \underset{\sim}{r}^B dm \qquad (2.3,8)$$

$\underline{I}^B$ is, by convention, given by (2.2,23).

The externally applied force $\underset{\rightarrow}{F}$ is made up of an aerodynamic component $\underset{\rightarrow}{A}$, a thrust component $\underset{\rightarrow}{T}$, a parachute component $\underset{\rightarrow}{A}_P$, and a gravitational component $m\underset{\rightarrow}{g}$.

$$\underset{\rightarrow}{F} = \underset{\rightarrow}{A} + \underset{\rightarrow}{T} + \underset{\rightarrow}{A}_P + m\underset{\rightarrow}{g} \qquad (2.3,9)$$

The parachute contributions are treated separately for convenience.

Substituting (2.3,9) and (2.3,3) into (2.3,1), the vector force equation becomes

$$m\dot{\underset{\rightarrow}{V}}_E = \underset{\rightarrow}{A} + \underset{\rightarrow}{T} + \underset{\rightarrow}{A}_P + m\underset{\rightarrow}{g} \qquad (2.3,10)$$

The externally applied moment $\underset{\rightarrow}{M}$ is made up of an aerodynamic component $\underset{\rightarrow}{M}_A$, a thrust component $\underset{\rightarrow}{M}_T$, and a parachute component $\underset{\rightarrow}{M}_P$ such that

$$\underset{\rightarrow}{M} = \underset{\rightarrow}{M}_A + \underset{\rightarrow}{M}_T + \underset{\rightarrow}{M}_P \qquad (2.3,11)$$

Substituting (2.3,11) into (2.3,2) yields

$$\dot{\underset{\rightarrow}{h}} = \underset{\rightarrow}{M}_A + \underset{\rightarrow}{M}_T + \underset{\rightarrow}{M}_P \qquad (2.3,12)$$

Other than the gravitational force, the dominant forces and moments acting on the vehicle are aerodynamic, and are largely determined by its orientation and configuration. It is therefore advantageous to write the matrix equations of motion with respect to a body-fixed reference frame. This reference frame is chosen to be F_B. Since the origin of F_B and the centre-of-mass of the vehicle coincide, this choice avoids the introduction of gravitational moments.

Thus the matrix force and moment equations become

$$m(\dot{\underline{V}}_E^B + \tilde{\underline{\omega}}^B \underline{V}_E^B) = \underline{A}^B + \underline{T}^B + \underline{A}_P^B + m\underline{L}_{BI}\underline{g}^I \qquad (2.3,13)$$

and

$$\dot{\underline{h}}^B + \tilde{\underline{\omega}}^B \underline{h}^B = \underline{M}_A^B + \underline{M}_T^B + \underline{M}_P^B \qquad (2.3,14)$$

Substituting for $\underline{h}_B$ from (2.3,7), the moment equation becomes

$$\underline{I}^B \dot{\underline{\omega}}^B + \dot{\underline{I}}^B \underline{\omega}^B + \tilde{\underline{\omega}}^B \underline{I}^B \underline{\omega}^B = \underline{M}_A^B + \underline{M}_T^B + \underline{M}_P^B \qquad (2.3,15)$$

Writing out the equation (2.3,13) in scalar form yields

$$m(\dot{U}_{B_E} + Q_B W_{B_E} - R_B V_{B_E}) = X_{A_B} + X_{T_B} + X_{P_B} + mgl_{BI_{13}} \qquad (2.3,16a)$$

$$m(\dot{V}_{B_E} + R_B U_{B_E} - P_B W_{B_E}) = Y_{A_B} + Y_{T_B} + Y_{P_B} + mgl_{BI_{23}} \qquad (2.3,16b)$$

$$m(\dot{W}_{B_E} + P_B V_B - Q_B U_{B_E}) = Z_{A_B} + Z_{T_B} + Z_{P_B} + mgl_{BI_{33}} \qquad (2.3,16c)$$

for the force equations, and similarly for equation (2.3,15) yields

$$I^B_{xx}\dot{P}_B - I^B_{xy}\dot{Q}_B - I^B_{xz}\dot{R}_B + \dot{I}^B_{xx}P_B - \dot{I}^B_{xy}Q_B - \dot{I}^B_{xz}R_B$$
$$+ I_{yz}(R_B^2 - Q_B^2) + (I^B_{zz} - I^B_{yy})R_BQ_B + I^B_{xy}R_BP_B - I^B_{xz}Q_BP_B$$
$$= L_{A_B} + L_{T_B} + L_{P_B} \qquad (2.3,17a)$$

$$-I^B_{xy}\dot{P}_B + I^B_{yy}\dot{Q}_B - I^B_{yz}\dot{R}_B - \dot{I}^B_{xy}P_B + \dot{I}^B_{yy}Q_B - \dot{I}^B_{yz}R_B$$
$$+ I^B_{xz}(P_B^2 - R_B^2) + (I^B_{xx} - I^B_{zz})P_BR_B + I^B_{yz}P_BQ_B - I^B_{xy}R_BQ_B$$
$$= M_{A_B} + M_{T_B} + M_{P_B} \qquad (2.3,17b)$$

$$-I^B_{xz}\dot{P}_B - I^B_{yz}\dot{Q}_B + I^B_{zz}\dot{R}_B - \dot{I}^B_{xz}P_B - \dot{I}^B_{yz}Q_B + \dot{I}^B_{zz}R_B$$
$$+ I^B_{xy}(Q_B^2 - P_B^2) + (I^B_{yy} - I^B_{xx})P_BQ_B + I^B_{xz}Q_BR_B - I^B_{yz}P_BR_B$$
$$= N_{A_B} + N_{T_B} + N_{P_B} \qquad (2.3,17c)$$

for the moment equations.

Kinematic equations are also required for the linear and rotational position of the aircraft. The linear position equations follow from

$$\underline{V}_E^I = \underline{L}_{IB}\underline{V}_E^B \qquad (2.3,18)$$

The rotational position equations are the Euler angle rate equations and are derived in (Reference 4, Section 5.2). The resulting scalar kinematic equations of motion are thus seen to be

$$\dot{x}_I = l_{BI_{11}}U_{B_E} + l_{BI_{21}}V_{B_E} + l_{BI_{31}}W_{B_E} \qquad (2.3,19a)$$

$$\dot{y}_I = l_{BI_{12}}U_{B_E} + l_{BI_{22}}V_{B_E} + l_{BI_{32}}W_{B_E} \qquad (2.3,19b)$$

$$\dot{z}_I = l_{BI_{13}}U_{B_E} + l_{BI_{23}}V_{B_E} + l_{BI_{33}}W_{B_E} \qquad (2.3,19c)$$

for linear position, and

$$\dot{\phi}_B = P_B + Q_B\sin\phi_B\tan\theta_B + R_B\cos\phi_B\tan\theta_B \qquad (2.3,20a)$$

$$\dot{\theta}_B = Q_B\cos\phi_B - R_B\sin\phi_B \qquad (2.3,20b)$$

$$\dot{\psi}_B = [Q_B\sin\phi_B + R_B\cos\phi_B]\ \sec\theta_B \qquad (2.3,20c)$$

for angular position.

It should be stressed that the variables (U_{B_E}, V_{B_E}, W_{B_E}) in equations (2.3,16), (2.3,17) and (2.3,19) are the body-axes components of the vehicle's ground velocity vector. This is not the same as the equations developed in Reference 2 where airspeed vector components in body-axes are used. Also, no assumptions have been made, up to this

point, regarding vehicle planes of symmetry and the symmetry of the thrust and aerodynamic forces and moments. Finally, it should be noted that unlike Reference 2 no assumptions have been made about the mass and inertia characteristics of the vehicle, i.e. in general

$$\dot{m} \neq 0$$

and

$$\dot{I}^B_{ij} \neq 0$$

A number of simplifications may be made to these equations if certain symmetry conditions are satisfied. If the vehicle has mass symmetry about the xy and xz planes, then

$$I^B_{xz} = I^B_{xy} = I^B_{yz} = 0 \qquad (2.3,21)$$

If the vehicle mass characteristics are also axisymmetric, then in addition to (2.3,21) we also have

$$I^B_{yy} = I^B_{zz} \qquad (2.3,22)$$

Applying assumption (2.3,21) to the moment equations (2.3,17a) through to (2.3,17c) results in the simplified set of equations

$$\dot{P}_B = [-\dot{I}^B_{xx} P_B - (I^B_{zz} - I^B_{yy}) R_B Q_B + L_{A_B} + L_{T_B} + L_{P_B}]/I^B_{xx} \qquad (2.3,23a)$$

$$\dot{Q}_B = [-\dot{I}^B_{yy} Q_B - (I^B_{xx} - I^B_{zz}) P_B R_B + M_{A_B} + M_{T_B} + M_{P_B}]/I^B_{yy} \qquad (2.3,23b)$$

$$\dot{R}_B = [-\dot{I}^B_{zz} R_B - (I^B_{yy} - I^B_{xx}) P_B Q_B + N_{A_B} + N_{T_B} + N_{P_B}]/I^B_{zz} \qquad (2.3,23c)$$

Applying the axisymmetry assumption (2.3,22) to these equations simplifies (2.3,23a) even further by eliminating the $(I^B_{zz} - I^B_{yy}) R_B Q_B$ term, i.e.

$$\dot{P}_B = [-\dot{I}^B_{xx} P_B + L_{A_B} + L_{T_B} + L_{P_B}]/I^B_{xx} \qquad (2.3,24)$$

2.4 Wind Contributions

The equations of motion developed in Section 2.3 have not explicitly included terms taking into account wind effects. If it is assumed that the spatial variation of the wind velocity from one point of the flight vehicle's surface to another is negligible (in many cases this is reasonable, see the discussion in Reference 2), then the uniform gust approximation applies. In this situation, the aerodynamic and kinematic effects of the wind may be determined by considering its interaction with the vehicle's centre-of-mass dynamic variables (e.g. U_{B_E}, V_{B_E}, W_{B_E}), and by utilizing the fundamental vector relationship

$$\underset{\rightarrow}{V}_E = \underset{\rightarrow}{V} + \underset{\rightarrow}{W} \qquad (2.4,1)$$

Equation (2.4,1) states that the ground velocity vector $\underset{\rightarrow}{V}_E$ equals the airspeed vector $\underset{\rightarrow}{V}$ plus the wind velocity vector $\underset{\rightarrow}{W}$.

Equation (2.4,1) may be used directly in (2.3,10) to obtain equations of motion that include wind terms. Alternatively, defining $(U_{B_g}, V_{B_g}, W_{B_g})$ to be the components of the wind velocity vector $\underset{\rightarrow}{W}$ expressed in F_B, one may substitute

$$U_{B_E} = U_B + U_{B_g} \tag{2.4,2a}$$

$$V_{B_E} = V_B + V_{B_g} \tag{2.4,2b}$$

$$W_{B_E} = W_B + W_{B_g} \tag{2.4,2c}$$

into equations (2.3,16) and (2.3,19) to obtain the desired result. Here (U_B, V_B, W_B) are the components of the airspeed vector $\underrightarrow{V}$ expressed in F_B, and

$$(U_{B_g}, V_{B_g}, W_{B_g})^T = \underline{L}_{BI}(W_1, W_2, W_3)^T \tag{2.4,3}$$

Making these substitutions, the force equations that result are

$$m\,(\dot{U}_B + Q_B W_B - R_B V_B + l_{BI_{11}}\dot{W}_1 + l_{BI_{12}}\dot{W}_2 + l_{BI_{13}}\dot{W}_3) = X_{A_B} + X_{T_B} + X_{P_B} + mgl_{BI_{13}} \tag{2.4,4a}$$

$$m\,(\dot{V}_B + R_B U_B - P_B W_B + l_{BI_{21}}\dot{W}_1 + L_{BI_{22}}\dot{W}_2 + l_{BI_{23}}\dot{W}_3) = Y_{A_B} + Y_{T_B} + Y_{P_B} + mgl_{BI_{23}} \tag{2.4,4b}$$

$$m\,(\dot{W}_B + P_B V_B - Q_B U_B + l_{BI_{31}}\dot{W}_1 + l_{BI_{32}}\dot{W}_2 + l_{BI_{33}}\dot{W}_3) = Z_{A_B} + Z_{T_B} + Z_{P_B} + mgl_{BI_{33}} \tag{2.4,4c}$$

and the inertial position equations are

$$\dot{x}_I = l_{BI_{11}} U_B + l_{BI_{21}} V_B + l_{BI_{31}} W_B + W_1 \qquad (2.4,5a)$$

$$\dot{y}_I = l_{BI_{12}} U_B + l_{BI_{22}} V_B + l_{BI_{32}} W_B + W_2 \qquad (2.4,5b)$$

$$\dot{z}_I = l_{BI_{13}} U_B + l_{BI_{23}} V_B + l_{BI_{33}} W_B + W_3 \qquad (2.4,5c)$$

The $(\dot{W}_1, \dot{W}_2, \dot{W}_3)$ terms represent the dynamic (or shear) effects of the wind.

It is frequently more convenient to treat equation (2.4,5c) as an altitude equation, i.e.

$$\dot{h} = -\dot{z}_I \qquad (2.4,6)$$

It is noted that in this formulation wind terms do not arise in the moment equations (2.3,17) or in the Euler angle equations (2.3,20).

3. AERODYNAMIC MODELS

The equations of motion developed in the previous section contain terms (e.g. X_{A_B}) that represent the aerodynamic forces and moments acting on the vehicle. In the following sections these terms are defined as functions of the vehicle's state.

Two aerodynamic models have been developed. The first, named AERO1, is used in FLISIMV1. The second, named AERO2, is used in

FLISIMV2. Both models make extensive use of quasisteady aerodynamic modeling techiques based partially on Bryan's aerodynamic derivative technique. Although more sophisticated techniques are available (see the discussion in Reference 2), for the purposes of rigid body six degree-of-freedom simulation, it is usually adequate to use this approach. This is particularly so as both models have features that are designed to take into account nonlinear aerodynamic characteristics associated with Mach number and with angle of attack.

No attempt has been made here to generalize these models so that they apply equally well to all types of air vehicles. The models apply to a broad class of high speed vehicles, including vehicles in the ROBOT-X class, but certain important effects associated with some flight vehicles (e.g. aerodynamic coupling effects between longitudinal and lateral characteristics) have not been taken into account. These additional features can usually be incorporated with relatively minor changes to the models.

3.1 AERO1 Aerodynamic Model

The AERO1 aerodynamic model associated with the simulation program FLISIMV1 is summarized in the following. The expressions for the aerodynamic forces and moments are presented in the reference frame F_N (see Section 2.2 and Figure 3), or, for the drag and lift characteristics, in wind- axes F_W (Figure 4). Recall that F_N is a body-fixed reference frame about which the nominal aerodynamic characteristics are expressed. These nominal characteristics must be transformed to the body-fixed reference frame F_B, located at the vehicle centre-of-gravity; in general, F_B and F_N are not the same.

Sections 3.3 through 3.5 derive generalized transformation

relationships between F_N and F_B, and F_W and F_B.

The nominal longitudinal aerodynamic forces and moments of the AERO1 aerodynamic model, in nondimensional form, are specified by

$$C_D^N(M_a, C_T, \alpha_f, \beta, C_{D_q}^N, C_{D_{\dot{\alpha}}}^N, C_{D_{\delta_E}}^N, C_{D_{i_H}}^N) = C_{D_1}^N(M_a, C_T, \alpha_f, \beta)$$

$$+ C_{D_q}^N(M_a, C_T, \alpha_f)\frac{Q_B\bar{c}}{2V} + C_{D_{\dot{\alpha}}}^N(M_a, C_T, \alpha_f)\frac{\dot{\alpha}_f\bar{c}}{2V}$$

$$+ C_{D_{\delta_E}}^N(M_a, C_T, \alpha_f)\delta_E + C_{D_{i_H}}^N(M_a, C_T, \alpha_f)i_H \qquad (3.1,1a)$$

$$C_L^N(M_a, C_T, \alpha_f, \beta, C_{L_q}^N, C_{L_{\dot{\alpha}}}^N, C_{L_{\delta_E}}^N, C_{L_{i_H}}^N) = C_{L_1}^N(M_a, C_T, \alpha_f, \beta)$$

$$+ C_{L_q}^N(M_a, C_T, \alpha_f)\frac{Q_B\bar{c}}{2V} + C_{L_{\dot{\alpha}}}^N(M_a, C_T, \alpha_f)\frac{\dot{\alpha}_f\bar{c}}{2V}$$

$$+ C_{L_{\delta_E}}^N(M_a, C_T, \alpha_f)\delta_E + C_{L_{i_H}}^N(M_a, C_T, \alpha_f)i_H \qquad (3.1,1b)$$

$$C_m^N(M_a, C_T, \alpha_f, \beta, C_{m_q}^N, C_{m_{\dot{\alpha}}}^N, C_{m_{\delta_E}}^N, C_{m_{i_H}}^N) = C_{m_1}^N(M_a, C_T, \alpha_f, \beta)$$

$$+ C_{m_q}^N(M_a, C_T, \alpha_f)\frac{Q_B\bar{c}}{2V} + C_{m_{\dot{\alpha}}}^N(M_a, C_T, \alpha_f)\frac{\dot{\alpha}_f\bar{c}}{2V}$$

$$+ C_{m_{\delta_E}}^N(M_a, C_T, \alpha_f)\delta_E + C_{m_{i_H}}^N(M_a, C_T, \alpha_f)i_H \qquad (3.1,1c)$$

The model is presented as a function of Mach number M_a, thrust coefficient C_T, fuselage reference line angle-of-attack α_f, fuselage reference line angle-of-sideslip β and aerodynamic derivatives associated with pitching rate Q_B, angle-of-attack rate of change $\dot{\alpha}_f$, elevator angular position δ_E and horizontal stabilizer (or canard) angular position i_H. The aerodynamic derivates themselves have a functional dependence on M_a, C_T and α_f.

The first term on the right hand side of equations (3.1,1a), (3.1,1b) and (3.1,1c) represents the contribution due to static effects (e.g. α_f) with control contributions set to zero (i.e. $\delta_E = i_H = 0$).

The model is formulated with control contributions due to an elevator and an all-moving surface (e.g. a horizontal stabilizer or a canard). It may be readily adapted to other types of longitudinal control (e.g. engine throttles) either by interpreting the δ_E and/or i_H terms differently, or by adding extra control terms.

From a fundamental point of view, the drag coefficient C_D^N and the lift coefficient C_L^N are actually force components in wind-axes F_{WN}.

$$C_y^N(M_a, C_T, \alpha_f, \beta, C_{y_\beta}^N, C_{y_p}^N, C_{y_r}^N, C_{y_{\delta_A}}^N, C_{y_{\delta_R}}^N)$$

$$= C_{y_\beta}^N(M_a, C_T, \alpha_f)\beta + C_{y_p}^N(M_a, C_T, \alpha_f)\frac{P_B b}{2V}$$

$$+ C_{y_r}^N(M_a, C_T, \alpha_f)\frac{R_B b}{2V} + C_{y_{\delta_A}}^N(M_a, C_T, \alpha_f)\delta_A$$

$$+ C_{y_{\delta_R}}^N(M_a, C_T, \alpha_f)\delta_R \qquad (3.1,2a)$$

$$C_\ell^N(M_a, C_T, \alpha_f, \beta, C_{\ell_\beta}^N, C_{\ell_p}^N, C_{\ell_r}^N, C_{\ell_{\delta_A}}^N, C_{\ell_{\delta_R}}^N)$$

$$= C_{\ell_\beta}^N(M_a, C_T, \alpha_f)\beta + C_{\ell_p}^N(M_a, C_T, \alpha_f)\frac{P_B b}{2V}$$

$$+ C_{\ell_r}^N(M_a, C_T, \alpha_f)\frac{R_B b}{2V} + C_{\ell_{\delta_A}}^N(M_a, C_T, \alpha_f)\delta_A$$

$$+ C_{\ell_{\delta_R}}^N(M_a, C_T, \alpha_f)\delta_R \qquad (3.1,2b)$$

$$C_n^N(M_a, C_T, \alpha_f, \beta, C_{n_\beta}^N, C_{n_p}^N, C_{n_r}^N, C_{n_{\delta_A}}^N, C_{n_{\delta_R}}^N)$$

$$= C_{n_\beta}^N(M_a, C_T, \alpha_f)\beta + C_{n_p}^N(M_a, C_T, \alpha_f)\frac{P_B b}{2V}$$

$$+ C_{n_r}^N(M_a, C_T, \alpha_f)\frac{R_B b}{2V} + C_{n_{\delta_A}}^N(M_a, C_T, \alpha_f)\delta_A$$

$$+ C_{n_{\delta_R}}^N(M_a, C_T, \alpha_f)\delta_R \qquad (3.1,2c)$$

The lateral portion of the AERO1 model is presented as a function of M_a, C_T, α_f, β and aerodynamic derivatives associated with β, rolling rate P_B, yawing rate R_B, aileron angular position δ_A and rudder angular position δ_R. The aerodynamic derivatives themselves have a functional dependence on M_a, C_T and α_f.

The lateral model is presented with control contributions due to aileron and rudders. As was the case for the longitudinal model, it may be readily adapted to other types of lateral control (e.g. spoilers) by either interpreting the δ_A and δ_R terms differently, or by adding extra control terms.

3.2 The AERO2 Aerodynamic Model

The AERO1 aerodynamic model defined in Section 3.1 has been utilized in the FLISIMV1 simulation software, and has proven invaluable in many aspects of ROBOT-X proof-of-concept development including design, control law synthesis and flight testing. It was not, however,

in a form that could take full advantage of available ROBOT-X wind tunnel data.

As a consequence, the AERO1 model was modified. The new model that resulted has been named the AERO2 model and is utilized by the FLISIMV2 simulation software. The AERO2 model and the FLISIMV2 software were used to check the AERO1 aerodynamic model and the FLISIMV1 software. Since this comparison proved very favourable, only the more efficient FLISIMV1 software has been used extensively on ROBOT-X.

The nominal longitudinal aerodynamic forces and moments of the AERO2 aerodynamic model, in nondimensional form, are specified by

$$C_D^N(M_a, C_T, i_H, \alpha_f, \beta, C_{D_q}^N, C_{D_{\dot{\alpha}}}^N, C_{D_{\delta_E}}^N) = C_{D_1}^N(M_a, C_T, i_H, \alpha_f, \beta)$$

$$+ C_{D_q}^N(M_a, C_T, \alpha_f)\frac{Q_B\bar{c}}{2V} + C_{D_{\dot{\alpha}}}^N(M_a, C_T, \alpha_f)\frac{\dot{\alpha}_f\bar{c}}{2V}$$

$$+ C_{D_{\delta_E}}^N(M_a, C_T, \alpha_f)\delta_E \qquad (3.2,1a)$$

$$C_L^N(M_a, C_T, i_H, \alpha_f, \beta, C_{L_q}^N, C_{L_{\dot{\alpha}}}^N, C_{L_{\delta_E}}^N) = C_{L_1}^N(M_a, C_T, i_H, \alpha_f, \beta)$$

$$+ C_{L_q}^N(M_a, C_T, \alpha_f)\frac{Q_B\bar{c}}{2V} + C_{L_{\dot{\alpha}}}^N(M_a, C_T, \alpha_f)\frac{\dot{\alpha}_f\bar{c}}{2V}$$

$$+C_{L_{\delta_E}}^N(M_a, C_T, \alpha_f)\delta_E \qquad (3.2,1b)$$

$$C_m^N(M_a, C_T, i_H, \alpha_f, \beta, C_{m_q}^N, C_{m_{\dot{\alpha}}}^N, C_{m_{\delta_E}}^N) = C_{m_1}^N(M_a, C_T, i_H, \alpha_f, \beta)$$

$$+ C_{m_q}^N(M_a, C_T, \alpha_f)\frac{Q_B\bar{c}}{2V} + C_{m_{\dot{\alpha}}}^N(M_a, C_T, \alpha_f)\frac{\dot{\alpha}_f\bar{c}}{2V}$$

$$+ C_{m_{\delta_E}}^N(M_a, C_T, \alpha_f)\delta_E \qquad (3.2,1c)$$

The main difference between the AERO1 and AERO2 longitudinal aerodynamic models is that for the AERO2 model, i_H contributions are included in the first term on the right hand side of equations (3.2,1a), (3.2,1b) and (3.2,1c). This was done to allow direct use of available ROBOT-X wind tunnel data for a number of i_H settings, and thus avoid the AERO1 model's simplified treatment through the use of the aerodynamic control derivatives $C_{D_{i_H}}^N$, $C_{L_{i_H}}^N$ and $C_{m_{i_H}}^N$. The available wind tunnel data also allowed some β effects to be present in the first term on the right hand side of equations (3.2,1a), (3.2,1b) and (3.2,1c).

The nominal lateral aerodynamic forces and moments of the AERO2 aerodynamic model, in nondimensional form, are specified by

$$C_y^N(M_a, C_T, i_H, \alpha_f, \beta, C_{y_p}^N, C_{y_r}^N, C_{y_{\delta_A}}^N, C_{y_{\delta_R}}^N)$$

$$= C_{y_1}^N(M_a, C_T, i_H, \alpha_f, \beta) + C_{y_p}^N(M_a, C_T, \alpha_f)\frac{P_B b}{2V}$$

$$+ C_{y_r}^N(M_a, C_T, \alpha_f)\frac{R_B b}{2V} + C_{y_{\delta_A}}^N(M_a, C_T, \alpha_f)\delta_A$$

$$+ C_{y_{\delta_R}}^N(M_a, C_T, \alpha_f)\delta_R \qquad (3.2,2a)$$

$$C_\ell^N(M_a, C_T, i_H, \alpha_f, \beta, C_{\ell_p}^N, C_{\ell_r}^N, C_{\ell_{\delta_A}}^N, C_{\ell_{\delta_R}}^N)$$

$$= C_{\ell_1}^N(M_a, C_T, i_H, \alpha_f, \beta) + C_{\ell_p}^N(M_a, C_T, \alpha_f)\frac{P_B b}{2V}$$

$$+ C_{\ell_r}^N(M_a, C_T, \alpha_f)\frac{R_B b}{2V} + C_{\ell_{\delta_A}}^N(M_a, C_T, \alpha_f)\delta_A$$

$$+ C_{\ell_{\delta_R}}^N(M_a, C_T, \alpha_f)\delta_R \qquad (3.2,2b)$$

$$C_n^N(M_a, C_T, i_H, \alpha_f, \beta, C_{n_p}^N, C_{n_r}^N, C_{n_{\delta_A}}^N, C_{n_{\delta_R}}^N)$$

$$= C_{n_1}^N(M_a, C_T, i_H, \alpha_f, \beta) + C_{n_p}^N(M_a, C_T, \alpha_f)\frac{P_B b}{2V}$$

$$+ C_{n_r}^N(M_a, C_T, \alpha_f)\frac{R_B b}{2V} + C_{n_{\delta_A}}^N(M_a, C_T, \alpha_f)\delta_A$$

$$+ C_{n_{\delta_R}}^N(M_a, C_T, \alpha_f)\delta_R \qquad (3.2,2c)$$

The main difference between the AERO1 and AERO2 lateral aerodynamic models is that for the AERO2 model, i_H and β contributions are included in the first term on the right hand side of the equations (3.2,2a), (3.2,2b) and (3.2,2c). Use of the β aerodynamic derivatives $C_{y_\beta}^N$, $C_{\ell_\beta}^N$ and $C_{n_\beta}^N$ is not explicit in the AERO2 model in order to take advantage of available aerodynamic data.

For both the AERO1 and AERO2 aerodynamic models, aerodynamic derivatives that are part of the model formulation may be estimated by utilizing the best available aerodynamic data sources. For ROBOT-X this has typically meant wind tunnel data for static (M_a, α_f and β) and some control (i_H) characteristics, and DATCOM (Reference 6) type methods for estimating the remaining characteristics, using available wind tunnel data wherever possible.

3.3 Transformation of Aerodynamic Moments from F_N to F_B

In general the vehicle centre-of-mass will not coincide with

the origin of F_N but will in fact be located at the origin of a second reference frame F_B. Since it is most convenient to write the equations of motion in F_B, the aerodynamic moments must be transformed accordingly. (No transformation is required on the forces since the axes of F_N and F_B are parallel; see Section 2.2.)

A third reference frame F_R, located on the nose datum plane and on the fuselage reference line (frl), will be used to define vehicle structural and mass coordinates.

All of these reference frames are illustrated in Figure 3.

Let $\underset{\rightarrow}{r}_N$ be the position vector from the origin of F_R to the origin of F_N (Figure 6).

Let $\underset{\rightarrow}{r}_B$ be the position vector from the origin of F_R to the origin of F_B (Figure 6).

Define

$$\underset{\rightarrow}{r}_{BN} = \underset{\rightarrow}{r}_N - \underset{\rightarrow}{r}_B \qquad (3.3,1)$$

$\underset{\rightarrow}{r}_{BN}$ represents the position vector from the origin of F_B to the origin of F_N.

Furthermore, let

$\underset{\rightarrow}{A}$ = vector of aerodynamic forces acting at the origin of F_N).

$\underset{\rightarrow}{M}_A$ = vector of aerodynamic moments acting about the centre-of-mass (i.e. at the origin of F_B).

$\underline{M}_{AN}$ = vector of aerodynamic moments acting about the origin of F_N.

$\underline{L}_{BN}$ = rotation matrix rotating F_N components to F_B components.

We have, based on fundamental force and moment mechanics

$$\underline{A}^B = \underline{L}_{BN}\underline{A}^N \tag{3.3,2}$$

$$\underline{M}_A^B = \underline{\tilde{r}}_{BN}^B \underline{A}^B + \underline{M}_{AN}^B$$

$$= \underline{\tilde{r}}_{BN}^B \underline{L}_{BN}\underline{A}^N + \underline{M}_{AN}^B$$

$$\underline{M}_A^B = \underline{\tilde{r}}_{BN}^B \underline{L}_{BN}\underline{A}^N + \underline{L}_{BN}\underline{M}_{AN}^N \tag{3.3,3}$$

For the typical case, $\underline{L}_{BN} = \underline{I}$ (this has been assumed throughout this report) and thus equation (3.3,3) becomes

$$\underline{M}_A^B = \underline{\tilde{r}}_{BN}^B \underline{A}^N + \underline{M}_{AN}^N \tag{3.3,4}$$

But

$$\underline{r}_{BN}^B = \underline{r}_N^B - \underline{r}_B^B \tag{3.3,5}$$

$$\underline{r}^B_{BN} = \underline{L}_{BR}\underline{r}^R_N - \underline{L}_{BR}\underline{r}^R_B$$

$$= \underline{L}_{BR}(\underline{r}^R_N - \underline{r}^R_B)$$

$$= \underline{L}_{BR}\underline{r}^R_{BN} \qquad (3.3,6)$$

Typically

$$\underline{L}_{BR} = \begin{bmatrix} \cos\pi & 0 & -\sin\pi \\ 0 & 1 & 0 \\ \sin\pi & 0 & \cos\pi \end{bmatrix}$$

$$= \begin{bmatrix} -1 & 0 & 0 \\ 0 & 1 & 0 \\ 0 & 0 & -1 \end{bmatrix} \qquad (3.3,7)$$

Therefore, letting $\underline{r}^R_N = (x_N, y_N, z_N)^T$, $\underline{r}^R_B = (x_{cm}, y_{cm}, z_{cm})^T$, we have

$$\underline{r}^B_{BN} = \begin{bmatrix} -(x_N - x_{cm}) \\ y_N - y_{cm} \\ -(z_N - z_{cm}) \end{bmatrix} \qquad (3.3,8)$$

Using the matrix equivalent of the vector cross-product, it may also be shown that

$$\underset{\sim}{r}_{BN}{}^{\tilde{}}\,\underset{\sim}{A}^{N} = \begin{bmatrix} 0 & (z_N - z_{cm}) & (y_N - y_{cm}) \\ -(z_N - z_{cm}) & 0 & (x_N - x_{cm}) \\ -(y_N - y_{cm}) & -(x_N - x_{cm}) & 0 \end{bmatrix} \begin{bmatrix} X_{AN} \\ Y_{AN} \\ Z_{AN} \end{bmatrix} \qquad (3.3,9)$$

It follows that the aerodynamic moments about the origin of F_B expressed as components in F_B are given by

$$L_{AB} = (z_N - z_{cm})Y_{AN} + (y_N - y_{cm})Z_{AN} + L^N_{AN} \qquad (3.3,10a)$$

$$M_{AB} = -(z_N - z_{cm})X_{AN} + (x_N - x_{cm})Z_{AN} + M^N_{AN} \qquad (3.3,10b)$$

$$N_{AB} = -(y_N - y_{cm})X_{AN} - (x_N - x_{cm})Y_{AN} + N^N_{AN} \qquad (3.3,10c)$$

These relationships may be made nondimensional by dividing by $\frac{1}{2}\rho V^2 \bar{c}$ for M_{AB} and $\frac{1}{2}\rho V^2 b$ for L_{AB} and N_{AB} to yield

$$C^B_\ell = \frac{(z_N - z_{cm})}{b} C^N_y + \frac{(y_N - y_{cm})}{b} C^N_z + C^N_\ell \qquad (3.3,11a)$$

$$C^B_m = -\frac{(z_N - z_{cm})}{\bar{c}} C^N_x + \frac{(x_N - x_{cm})}{\bar{c}} C^N_z + C^N_m \qquad (3.3,11b)$$

$$C^B_n = -\frac{(y_N - y_{cm})}{b} C^N_x - \frac{(x_N - x_{cm})}{b} C^N_y + C^N_n \qquad (3.3,11c)$$

The relationships (3.3,10a) through to (3.3,11c) are based on the assumptions that $\underline{\underline{L}}_{BN} = \underline{\underline{I}}$ and that $\underline{\underline{L}}_{BR}$ is given by (3.3,7). As has already been stated, these assumptions are typically the case, and are made throughout this report.

3.4 Transformation of Aerodynamic Forces from Wind Axes to Body Axes

The longitudinal aerodynamic forces are frequently available as lift and drag rather than as force components in F_N or F_B. Lift and drag are force components in a reference frame F_{WN} (or F_W, see Section 2.2) referred to as the wind axes. The origin of F_W is fixed to the vehicle (typically at the centre-of-mass) but has an x-axis that parallels the freestream airspeed vector $\underline{V}$, a z-axis that is nominally downwards and a y-axis that follows from the right hand rule. F_{WN} is identical to F_W except that its origin is at the origin of F_N (see Figure 4).

In the sense of Euler angles, the aerodynamic angle-of-sideslip β and fuselage reference line angle-of-attack α_f will carry F_{WN} (or F_W) to F_N (or F_B) (see Figure 4) by the ordered rotations $(-\beta, \alpha_f, 0)$, i.e.

$$\underline{\underline{L}}_{NW} = \begin{bmatrix} \cos\beta\cos\alpha_f & -\sin\beta\cos\alpha_f & -\sin\alpha_f \\ \sin\beta & \cos\beta & 0 \\ \cos\beta\sin\alpha_f & -\sin\beta\sin\alpha_f & \cos\alpha_f \end{bmatrix} \qquad (3.4,1)$$

Let the aerodynamic force vector expressed as components in F_{WN} be given by

$$\underline{A}^{WN} = (-D_N, Y_{WN}, -L_N)^T \qquad (3.4,2)$$

Here D and L are the drag and lift respectively, and Y_{WN} is the wind axes side force. Using the relationship

$$\underline{A}^{N} = \underline{L}_{NW}\underline{A}^{WN} \qquad (3.4,3)$$

we may obtain the relationships relating force components in F_N to aerodynamic drag D_N and lift L_N, i.e.

$$X_{AN} = -\cos\beta\cos\alpha_f D_N - \sin\beta\cos\alpha_f Y_{WN} + \sin\alpha_f L_N \qquad (3.4,4a)$$

$$Y_{AN} = -\sin\beta D_N + \cos\beta Y_{WN} \qquad (3.4,4b)$$

$$Z_{AN} = -\cos\beta\sin\alpha_f D_N - \sin\beta\sin\alpha_f Y_{WN} - \cos\alpha_f L_N \qquad (3.4,4c)$$

Nondimensionally, (3.4,4a) through (3.4,4c) become

$$C_x^N = -\cos\beta\cos\alpha_f C_D^N - \sin\beta\cos\alpha_f C_y^{WN} + \sin\alpha_f C_L^N \qquad (3.4,5a)$$

$$C_y^N = -\sin\beta C_D^N + \cos\beta C_y^{WN} \qquad (3.4,5b)$$

$$C_z^N = -\cos\beta\sin\alpha_f C_D^N - \sin\beta\sin\alpha_f C_y^{WN} - \cos\alpha_f C_L^N \qquad (3.4,5c)$$

In practice, C_L^N and C_D^N models and/or wind tunnel data are frequently available only for symmetric flight, i.e. for $\beta = 0$. If this is the case, these relationships simplify to

$$C_x^N = -\cos\alpha_f C_D^N + \sin\alpha_f C_L^N \qquad (3.4,6a)$$

$$C_y^N = C_y^{WN} \qquad (3.4,6b)$$

$$C_z^N = -\sin\alpha_f C_D^N - \cos\alpha_f C_L^N \qquad (3.4,6c)$$

The 'N' subscript/superscript notation, although cumbersome, has been retained to emphasize that the forces and moments are related to the nominal reference frame F_N. The relationships for body-axes (F_B) components may be derived in an analogous fashion.

3.5 The Aerodynamic Models in Body Axes F_B

As well as correcting the nominal aerodynamic model for actual centre-of-mass position, the FLISIMV1 and FLISIMV2 software packages have provision for introducing a number of changes to the nominal model that facilitate parametric variation. This may be required to provide a convenient means of modifying the nominal aerodynamic characteristics to adjust for changes in vehicle configuration (e.g. addition of equipment that alters drag characteristics) and to obtain a better fit with flight test data.

In addition, it has been found useful to add a simplified model of the ROBOT-X parachute dynamics to the simulation software.

Table II summarizes the nominal aerodynamic characteristics provided by the AERO1 model. These parameters form the baseline from which the aerodynamic characteristics utilized in FLISIMV1 are derived.

All of the parameters of Table II are adjusted by a multiplicative factor m_{lon_i} and an offset b_{lon_i} for the i-th longitudinal para-

meter. Analogous factors are used for the lateral parameters. To designate parameters with correction applied, prime notation is used, e.g. C'_{D_1}.

Following this adjustment, the nominal base drag coefficient $C^N_{D_{base}}$ is extracted and corrected by the multiplicative factor $f_{C_{D_{base}}}$.

This corrected base drag is adjusted for the base drag reduction that results due to the rocket motor burn by utilizing the parameter $\partial C_D/\partial(T_i/T_{i_{max}})$, i.e. drag coefficient reduction due to the thrust of the i-th motor.

An excrescence drag ($C_{D_{ex}}$) correction is introduced to the nominal drag through the factor $f_{C_{D_{ex}}}$. This factor represents the off-nominal drag contribution, due to excrescence drag, relative to the zero lift, zero base drag coefficient $(C_{D_o})_{C_{D_{base}}} = 0$.

It is only at this point that the F_N to F_B centre-of-mass transformation relationships of Section 3.3 are introduced, and this in turn is followed by the introduction of total nondimensional coefficient offsets $C_{D_{os}}$, $C_{L_{os}}$, $C^B_{m_{os}}$, $C^B_{y_{os}}$, $C^B_{\ell_{os}}$ and $C^B_{n_{os}}$.

Finally, the parachute system forces and moments are computed in body-axes F_B and introduced into the totals. To summarize, for the AERO1 model we have the following ($\beta \approx 0$ has been assumed):

$$C_x^B = -\cos\alpha_f(C_D + C_{D_{os}}) + \sin\alpha_f(C_L + C_{L_{os}}) + C_{x_P}^B \qquad (3.5,1a)$$

$$C_y^B = C_y^{N'} + C_{y_{os}}^B + C_{y_P}^B \qquad (3.5,1b)$$

$$C_z^B = -\sin\alpha_f(C_D + C_{D_{os}}) - \cos\alpha_f(C_L + C_{L_{os}}) + C_{z_P}^B \qquad (3.5,1c)$$

$$C_\ell^B = \frac{(z_N - z_{cm})}{b} C_y^{N'} + \frac{(y_N - y_{cm})}{b} C_z^{N'} + C_\ell^{N'} + C_{\ell_{os}}^B + C_{\ell_P}^B \qquad (3.5,2a)$$

$$C_m^B = -\frac{(z_N - z_{cm})}{\bar{c}} C_x^{N'} + \frac{(x_N - x_{cm})}{\bar{c}} C_z^{N'} + C_m^{N'} + C_{m_{os}}^B + C_{m_P}^B \qquad (3.5,2b)$$

$$C_n^B = -\frac{(y_N - y_{cm})}{b} C_x^{N'} - \frac{(x_N - x_{cm})}{b} C_y^{N'} + C_n^{N'} + C_{n_{os}}^B + C_{n_P}^B \qquad (3.5,2c)$$

$$C_x^{N'} = -\cos\alpha_f C_D + \sin\alpha_f C_L \qquad (3.5,3a)$$

$$C_y^{N'} = C_{y_\beta}^{N'}\beta + C_{y_p}^{N'}\frac{P_B b}{2V} + C_{y_r}^{N'}\frac{R_B b}{2V} + C_{y_{\delta_A}}^{N'}\delta_A + C_{y_{\delta_R}}^{N'}\delta_R \qquad (3.5,3b)$$

$$C_z^{N'} = -\sin\alpha_f C_D - \cos\alpha_f C_L \qquad (3.5,3c)$$

$$C_D^{N'} = C_{D_1} + C_{D_q}^{N'}\frac{Q_B \bar{c}}{2V} + C_{D_{\dot{\alpha}}}^{N'}\frac{\dot{\alpha}_f \bar{c}}{2V} + C_{D_{\delta_E}}^{N'}\delta_E + C_{D_{i_H}}^{N'} i_H \qquad (3.5,4)$$

$$C_L^{N'} = C_{L_1}^{N'} + C_{L_q}^{N'} \frac{Q_B \bar{c}}{2V} + C_{L_{\dot{\alpha}}}^{N'} \frac{\dot{\alpha}_f \bar{c}}{2V} + C_{L_{\delta_E}}^{N'} \delta_E + C_{L_{i_H}}^{N'} i_H \qquad (3.5,5)$$

$$C_\ell^{N'} = C_{\ell_\beta}^{N'} \beta + C_{\ell_p}^{N'} \frac{P_B b}{2V} + C_{\ell_r}^{N'} \frac{R_B b}{2V} + C_{\ell_{\delta_A}}^{N'} \delta_A + C_{\ell_{\delta_R}}^{N'} \delta_R \qquad (3.5,6a)$$

$$C_m^{N'} = C_{m_1}^{N'} + C_{m_q}^{N'} \frac{Q_B \bar{c}}{2V} + C_{m_{\dot{\alpha}}}^{N'} \frac{\dot{\alpha}_f \bar{c}}{2V} + C_{m_{\delta_E}}^{N'} \delta_E + C_{m_{i_H}}^{N'} i_H \qquad (3.5,6b)$$

$$C_n^{N'} = C_{n_\beta}^{N'} \beta + C_{n_p}^{N'} \frac{P_B b}{2V} + C_{n_r}^{N'} \frac{R_B b}{2V} + C_{n_{\delta_A}}^{N'} \delta_A + C_{n_{\delta_R}}^{N'} \delta_R \qquad (3.5,6c)$$

$$C_{D_1} = C'_{D_1} - C^N_{D_{base}} + f_{C_{D_{base}}} C'_{D_{base}} + \sum_{i=1}^{N_M} [\partial C_D / \partial (T_i/T_{i_{max}})] T_i/T_{i_{max}}$$

$$+ f_{C_{D_{ex}}} (C_{D_o}) C_{D_{base}} = 0 \qquad (3.5,7)$$

$$C'_{D_1} = m_{lon_1} C_{D_1} + b_{lon_1} \qquad (3.5,8)$$

$$C^N_{D_{base}} = 0.13 S^N_{base}/S \qquad (3.5,9)$$

$$C'_{D_{base}} = 0.13 S_{base}/S \qquad (3.5,10)$$

$$C_{D_{base}} = f_{C_{D_{base}}} C'_{D_{base}} \qquad (3.5,11)$$

The expressions for base factor in (3.5,9) and (3.5,10) are based on an empirical formula taken from Torenbeek (Reference 8). It is valid for subsonic conditions.

The parachute system force coefficients $C^B_{x_P}$, $C^B_{y_P}$ and $C^B_{z_P}$ and moment coefficients $C^B_{\ell_P}$, $C^B_{m_P}$ and $C^B_{n_P}$ are derived in Section 3.6.

The AERO2 model in F_B is identical to the AERO1 model except for a number of minor changes that are required to accommodate the different form of the AERO2 model as presented in Section 3.2. These changes arise in equations (3.5,3b), (3.5,4), (3.5,5), (3.5,6a), (3.5,6b) and (3.5,6c). These become,

$$C^{N'}_y = C^{N'}_{y_1} + C^{N'}_{y_p}\frac{P_B b}{2V} + C^{N'}_{y_r}\frac{R_B b}{2V} + C^{N'}_{y_{\delta_A}}\delta_A + C^{N'}_{y_{\delta_R}}\delta_R \qquad (3.5,12)$$

$$C^{N'}_D = C^{N'}_{D_1} + C^{N'}_{D_q}\frac{Q_B \bar{c}}{2V} + C^{N'}_{D_{\dot{\alpha}}}\frac{\dot{\alpha}_f \bar{c}}{2V} + C^{N'}_{D_{\delta_E}}\delta_E \qquad (3.5,13)$$

$$C^{N'}_L = C^{N'}_{L_1} + C^{N'}_{L_q}\frac{Q_B \bar{c}}{2V} + C^{N'}_{L_{\dot{\alpha}}}\frac{\dot{\alpha}_f \bar{c}}{2V} + C^{N'}_{L_{\delta_E}}\delta_E \qquad (3.5,14)$$

$$C^{N'}_\ell = C^{N'}_{\ell_1} + C^{N'}_{\ell_p}\frac{P_B b}{2V} + C^{N'}_{\ell_r}\frac{R_B b}{2V} + C^{N'}_{\ell_{\delta_A}}\delta_A + C^{N'}_{\ell_{\delta_R}}\delta_R \qquad (3.5,15a)$$

$$C^{N'}_m = C^{N'}_{m_1} + C^{N'}_{m_q}\frac{Q_B \bar{c}}{2V} + C^{N'}_{m_{\dot{\alpha}}}\frac{\dot{\alpha}_f \bar{c}}{2V} + C^{N'}_{m_{\delta_E}}\delta_E \qquad (3.5,15b)$$

$$C_n^{N'} = C_{n_1}^{N'} + C_{n_p}^{N'} \frac{P_B B}{2V} + C_{n_r}^{N'} \frac{R_B b}{2V} + C_{n_{\delta_A}}^{N'} \delta_A + C_{n_{\delta_R}}^{N'} \delta_R \qquad (3.5,15c)$$

In certain circumstances, it is convenient to interpret the individual aerodynamic parameters associated with the AERO1 and AERO2 models as parameters in the reference frame F_B. The force parameters transfer directly, but the moment parameters require transformation to take into account the different moment reference point.

Again assuming $\beta \approx 0$, the results are summarized in the following:

$$C_{m_1}^B = -\left(\frac{z_N - z_{cm}}{\bar{c}}\right)\left(-\cos\alpha_f C_{D_1} + \sin\alpha_f C_{L_1}^{N'}\right) + \frac{(x_N - x_{cm})}{\bar{c}}\left(-\sin\alpha_f C_{D_1} - \cos\alpha_f C_{L_1}^{N'}\right) + C_{m_1}^{N'} \qquad (3.5,16)$$

$$C_{m_{\dot{\alpha}}}^B = -\left(\frac{z_N - z_{cm}}{\bar{c}}\right)\left(-\cos\alpha_f C_{D_{\dot{\alpha}}}^{N'} + \sin\alpha_f C_{L_{\dot{\alpha}}}^{N'}\right) + \left(\frac{x_N - x_{cm}}{\bar{c}}\right)\left(-\sin\alpha_f C_{D_{\dot{\alpha}}}^{N'} - \cos\alpha_f C_{L_{\dot{\alpha}}}^{N'}\right) + C_{m_{\dot{\alpha}}}^{N'} \qquad (3.5,17)$$

$$C_{m_q}^B = -\left(\frac{z_N - z_{cm}}{\bar{c}}\right)\left(-\cos\alpha_f C_{D_q}^{N'} + \sin\alpha_f C_{L_q}^{N'}\right) + \left(\frac{x_N - x_{cm}}{\bar{c}}\right)\left(-\sin\alpha_f C_{D_q}^{N'} - \cos\alpha_f C_{L_q}^{N'}\right) + C_{m_q}^{N'} \qquad (3.5,18)$$

$$C^B_{m_{\delta_E}} = -\left(\frac{z_N - z_{cm}}{\bar{c}}\right)\left(-\cos\alpha_f C^{N'}_{D_{\delta_E}} + \sin\alpha_f C^{N'}_{L_{\delta_E}}\right)$$

$$+ \left(\frac{x_N - x_{cm}}{\bar{c}}\right)\left(-\sin\alpha_f C^{N'}_{D_{\delta_E}} - \cos\alpha_f C^{N'}_{L_{\delta_E}}\right) + C^{N'}_{m_{\delta_E}} \qquad (3.5,19)$$

$$C^B_{m_{i_H}} = -\left(\frac{z_N - z_{cm}}{\bar{c}}\right)\left(-\cos\alpha_f C^{N'}_{D_{i_H}} + \sin\alpha_f C^{N'}_{L_{i_H}}\right)$$

$$+ \left(\frac{x_N - x_{cm}}{\bar{c}}\right)\left(-\sin\alpha_f C^{N'}_{D_{i_H}} - \cos\alpha_f C^{N'}_{L_{i_H}}\right) + C^{N'}_{m_{i_H}} \qquad (3.5,20)$$

$$C^B_{\ell_{\bullet_\alpha}} = \left(\frac{y_N - y_{cm}}{b}\right)\left(-\sin\alpha_f C^{N'}_{D_{\bullet_\alpha}} - \cos\alpha_f C^{N'}_{L_{\bullet_\alpha}}\right) + C^{N'}_{\ell_{\bullet_\alpha}} \qquad (3.5,21)$$

$$C^B_{\ell_1} = \left(\frac{y_N - y_{cm}}{b}\right)\left(-\sin\alpha_f C_{D_1} - \cos\alpha_f C^{N'}_{L_1}\right) + C^{N'}_{\ell_1} \qquad (3.5,22)$$

$$C^B_{\ell_q} = \left(\frac{y_N - y_{cm}}{b}\right)\left(-\sin\alpha_f C^{N'}_{D_q} - \cos\alpha_f C^{N'}_{L_q}\right) + C^{N'}_{\ell_q} \qquad (3.5,23)$$

$$C^B_{\ell_{\delta_E}} = \left(\frac{y_N - y_{cm}}{b}\right)\left(-\sin\alpha_f C^{N'}_{D_{\delta_E}} - \cos\alpha_f C^{N'}_{L_{\delta_E}}\right) + C^{N'}_{\ell_{\delta_E}} \qquad (3.5,24)$$

$$C^B_{\ell_{i_H}} = \left(\frac{y_N - y_{cm}}{b}\right)\left(-\sin\alpha_f C^{N'}_{D_{i_H}} - \cos\alpha_f C^{N'}_{L_{i_H}}\right) + C^{N'}_{\ell_{i_H}} \qquad (3.5,25)$$

$$C^B_{\ell_\beta} = \left(\frac{z_N - z_{cm}}{b}\right) C^{N'}_{y_\beta} + C^{N'}_{\ell_\beta} \qquad (3.5,26)$$

$$C^B_{\ell_p} = \left(\frac{z_N - z_{cm}}{b}\right) C^{N'}_{y_p} + C^{N'}_{\ell_p} \qquad (3.5,27)$$

$$C^B_{\ell_r} = \left(\frac{z_N - z_{cm}}{b}\right) C^{N'}_{y_r} + C^{N'}_{\ell_r} \qquad (3.5,28)$$

$$C^B_{\ell_{\delta_A}} = \left(\frac{z_N - z_{cm}}{b}\right) C^{N'}_{y_{\delta_A}} + C^{N'}_{\ell_{\delta_A}} \qquad (3.5,29)$$

$$C^B_{\ell_{\delta_R}} = \left(\frac{z_N - z_{cm}}{b}\right) C^{N'}_{y_{\delta_R}} + C^{N'}_{\ell_{\delta_R}} \qquad (3.5,30)$$

$$C^B_{n_i} = -\left(\frac{y_N - y_{cm}}{b}\right)\left(-\cos\alpha_f C_{D_i} + \sin\alpha_f C^{N'}_{L_i}\right) + C^{N'}_{n_i} \qquad (3.5,31)$$

$$C^B_{n_{\dot{\alpha}}} = -\left(\frac{y_N - y_{cm}}{b}\right)\left(-\cos\alpha_f C^{N'}_{D_{\dot{\alpha}}} + \sin\alpha_f C^{N'}_{L_{\dot{\alpha}}}\right) + C^{N'}_{n_{\dot{\alpha}}} \qquad (3.5,32)$$

$$C^B_{n_q} = -\left(\frac{y_N - y_{cm}}{b}\right)\left(-\cos\alpha_f C^{N'}_{D_q} + \sin\alpha_f C^{N'}_{L_q}\right) + C^{N'}_{n_q} \qquad (3.5,33)$$

$$C^B_{n_{\delta_E}} = -\left(\frac{y_N - y_{cm}}{b}\right)\left(-\cos\alpha_f C^{N'}_{D_{\delta_E}} + \sin\alpha_f C^{N'}_{L_{\delta_E}}\right) + C^{N'}_{n_{\delta_E}} \qquad (3.5,34)$$

$$C^B_{n_{i_H}} = -\left(\frac{y_N - y_{cm}}{b}\right)\left(-\cos\alpha_f C^{N'}_{D_{i_H}} + \sin\alpha_f C^{N'}_{L_{i_H}}\right) + C^{N'}_{n_{i_H}} \qquad (3.5,35)$$

$$C^B_{n_\beta} = -\left(\frac{x_N - x_{cm}}{b}\right) C^{N'}_{y_\beta} + C^{N'}_{n_\beta} \qquad (3.5,36)$$

$$C^B_{n_p} = -\left(\frac{x_N - x_{cm}}{b}\right) C^{N'}_{y_p} + C^{N'}_{n_p} \qquad (3.5,37)$$

$$C^B_{n_r} = -\left(\frac{x_N - x_{cm}}{b}\right) C^{N'}_{y_r} + C^{N'}_{n_r} \qquad (3.5,38)$$

$$C^B_{n_{\delta_A}} = -\left(\frac{x_N - x_{cm}}{b}\right) C^{N'}_{y_{\delta_A}} + C^{N'}_{n_{\delta_A}} \qquad (3.5,39)$$

$$C^B_{n_{\delta_R}} = -\left(\frac{x_N - x_{cm}}{b}\right) C^{N'}_{y_{\delta_R}} + C^{N'}_{n_{\delta_R}} \qquad (3.5,40)$$

It is interesting to note that in the process of transforming moments expressed about F_N to equivalent moments expressed about F_B, longitudinal and lateral coupling terms arise. For example, in equation (3.5,33) although the coupling aerodynamic derivative $C^N_{n_q}$ (yawing moment due to pitching rate) is usually negligible, the $(y_N - y_{cm})$ term can be significant if the lateral centre-of-mass is significantly off the nominal position y_N. This intuitively makes sense in that if the lateral centre-of-mass position is significantly away from the drag and lift points of action, then a significant yawing moment could result relative to F_B (recall that F_B has an origin that is located at the centre-of-mass). The other coupling terms may be interpreted in a similar fashion.

3.6 Parachute Aerodynamics

The equations of motion presented in Sections 2.3 and 2.4 contain terms (e.g. X_{P_B}) representing the forces and moments generated by

the parachute system. The model for these forces and moments is summarized in this section.

The model that has been utilized is relatively simple and is intended only to model the main dynamic characteristics associated with the ROBOT-X parachute system deployment. A number of assumptions have been made in its formulation, as follows:

a) Tension acts at aft end of vehicle at the centre of the fuselage.
b) The parachute is either fully inflated and deployed or is fully stowed (i.e. instantaneous deployment dynamics).
c) Line dynamics are negligible (the parachute lines are adequately described by a single straight line along which a tension force T_p acts).
d) The tension vector $\underset{\rightarrow}{T}_p$ is perfectly aligned with the airspeed vector at all times. Thus the angles that $\underset{\rightarrow}{T}_p$ makes with the fuselage reference line can be described adequately by the aerodynamic angles α_f and β.
e) The aerodynamic torque generated by the parachute is negligible.

Let a reference frame F_p be defined with its origin at the nominal parachute attachment point to the vehicle and with its axes parallel to those of wind-axes F_W. Then we have

$$\begin{bmatrix} X_{P_B} \\ Y_{P_B} \\ Z_{P_B} \end{bmatrix} = \begin{bmatrix} \cos\alpha_f\cos\beta & \cos\alpha_f\sin\beta & -\sin\alpha_f \\ \sin\beta & \cos\beta & 0 \\ \sin\alpha_f\cos\beta & -\sin\alpha_f\sin\beta & \cos\alpha_f \end{bmatrix} \begin{bmatrix} -T_P \\ 0 \\ 0 \end{bmatrix} \qquad (3.6,1)$$

or

$$X_{P_B} = -\cos\alpha_f\cos\beta T_P \qquad (3.6,2a)$$

$$Y_{P_B} = -T_P\sin\beta \qquad (3.6,2b)$$

$$Z_{P_B} = -T_P\sin\alpha_f\cos\beta \qquad (3.6,2c)$$

The parachute deployment moments may be computed with the knowledge of $(X_{P_B}, Y_{P_B}, Z_{P_B})$ and the geometry. From fundamental vector mechanics, we have

$$\underset{\rightarrow}{M}_{P_B} = \underset{\rightarrow}{r}_{BP} \times \underset{\rightarrow}{T}_P \qquad (3.6,3)$$

where $\underset{\rightarrow}{r}_{BP}$ is the position vector of F_P relative to F_B. We have

$$\underset{\rightarrow}{r}_P^R = \begin{bmatrix} l_B \\ 0 \\ 0 \end{bmatrix} \qquad (3.6,4)$$

$$\underline{r}_B^R = \begin{bmatrix} x_{cm} \\ y_{cm} \\ z_{cm} \end{bmatrix} \tag{3.6,5}$$

$$\underline{r}_{BP}^R = \begin{bmatrix} l_B - x_{cm} \\ -y_{cm} \\ -z_{cm} \end{bmatrix} \tag{3.6,6}$$

$$\underline{r}_{BP}^B = \begin{bmatrix} x_{cm} - l_B \\ -y_{cm} \\ z_{cm} \end{bmatrix} \tag{3.6,7}$$

and

$$\begin{bmatrix} L_{P_B} \\ M_{P_B} \\ N_{P_B} \end{bmatrix} = \begin{bmatrix} 0 & -z_{cm} & -y_{cm} \\ z_{cm} & 0 & l_B - x_{cm} \\ y_{cm} & x_{cm} - l_B & 0 \end{bmatrix} \begin{bmatrix} X_{P_B} \\ Y_{P_B} \\ Z_{P_B} \end{bmatrix} \tag{3.6,8}$$

or

$$L_P^B = -z_{cm}Y_{P_B} - y_{cm}Z_{P_B} \qquad (3.6,9a)$$

$$M_P^B = z_{cm}X_{P_B} + (l_B - x_{cm})Z_{P_B} \qquad (3.6,9b)$$

$$N_P^B = y_{cm}X_{P_B} + (x_{cm} - l_B)Y_{P_B} \qquad (3.6,9c)$$

This completes the description of the dynamic model of the parachute system.

The aerodynamics are modeled as

$$T_P = C_{D_D} q_D S_D \qquad (3.6,10)$$

for the drogue parachute, and

$$T_P = C_{D_M} q_D S_M \qquad (3.6,11)$$

for the main parachute.

These equations are readily implemented in the ROBOT-X simulation. The main limitation arises in that as the vehicle slows down and adopts a near nose down attitude, $\theta_B \approx \pi/2$, and the Φ_B and ψ_B Euler equations (2,3,20a) and (2.3,20c) have singularities. Unless a singularity-free attitude representation (e.g. quaternions) is used, the simulation should be stopped prior to reaching the singularity.

4. MASS AND MOMENTS OF INERTIA MODEL

The equations of motion have been written so that variations in the vehicle's mass and inertia characteristics are permitted. Component methods are used to compute the total vehicle mass and moments of inertia. The components considered are N_c airframe components, N_M vehicle rocket motors (less propellant) and the rocket motor's propellant. Of these components, only the propellant characteristics are considered to be variable with time.

The model has provision for defining the mass, centre-of-mass, and moments of inertia characteristics of each of the components. The moments of inertia characteristics are defined with respect to an arbitrary, component-fixed reference frame F_{R_i}. By utilizing an appropriate moment of inertia transformation, these are transformed to the component-fixed reference frame F_{B_i}. F_{B_i} has an origin located at the centre-of-mass of the i-th component and axes that are parallel to F_B. The moments of inertia expressed about F_{B_i} may be readily transformed to equivalent moments of inertia expressed about F_B if the orientation of F_{B_i} relative to F_B is known (Figure 6).

The main assumptions that have been made in the formulation of this model are as follows:

1. Only the rocket motor propellant characteristics are considered to be variable with time.
2. The propellant centre-of-mass position of the i-th rocket motor relative to F_R (see Figure 3) does not change signi-

ficantly during the rocket motor burn. This would be the case in rocket motors that are not end burners.

3. There is only one type of rocket motor.
4. The rate of change of a particular moment of inertia of the i-th rocket motor relative to the motor's centre-of-mass during a rocket motor burn is constant.

Under these conditions, expressions for the vehicle mass and inertia characteristics have been developed as summarized in the following. The subscripts used to reference the different components are as follows:

1. 'i' or 'R_i' - i-th airframe component, not including rocket motors (if no risk of confusion exists, the 'R' is dropped).
2. 'PR' - rocket motor propellant.
3. 'RE' - rocket motor less propellant, i.e. rocket motor empty.

Since all component positions are given with respect to F_R while the moments of inertia are with respect to F_B, the inertia expressions involve incremental position terms describing the cartesian coordinates of each component relative to F_B.

For a component denoted generically by ξ, these incremental position terms may be written in F_B as

$$\Delta x_\xi = x_{cm} - x_\xi \qquad (4,1a)$$

$$\Delta y_\xi = y_\xi - y_{cm} \qquad (4,1b)$$

$$\Delta z_\xi = z_{cm} - z_\xi \qquad (4,1c)$$

Here (x_ξ, y_ξ, z_ξ) are the cartesian coordinates of the centre-of-mass of the ξ-component in reference frame F_R, (x_{cm}, y_{cm}, z_{cm}) are the cartesian coordinates of the vehicle centre-of-mass in F_R and $(\Delta x_\xi, \Delta y_\xi, \Delta z_\xi)$ are the cartesian coordinates of the centre-of-mass of the ξ-component in reference frame F_B. The sign changes take into account the fact that F_R is related to F_B through a 180° rotation about the F_B y-axis.

The expressions for the mass and inertia characteristics are as follows:

$$m = \sum_{i=1}^{N_c} m_i + N_M m_{RE} + \sum_{i=1}^{N_M} (m_{PR})_i \qquad (4,2)$$

$$x_{cm} = [\sum_{i=1}^{N_c} m_i x_i + m_{RE} \sum_{i=1}^{N_M} (x_{RE})_i + \sum_{i=1}^{N_M} (m_{PR})_i (x_{PR})_i]/m \qquad (4,3a)$$

$$y_{cm} = [\sum_{i=1}^{N_c} m_i y_i + m_{RE} \sum_{i=1}^{N_M} (y_{RE})_i + \sum_{i=1}^{N_M} (m_{PR})_i (y_{PR})_i]/m \qquad (4,3b)$$

$$z_{cm} = [\sum_{i=1}^{N_c} m_i z_i + m_{RE} \sum_{i=1}^{N_M} (z_{RE})_i + \sum_{i=1}^{N_M} (m_{PR})_i (z_{PR})_i]/m \qquad (4,3c)$$

$$I^B_{xx} = \sum_{i=1}^{N_c} \{(I^B_{xx})_i + m_i[(\Delta y)_i^2 + (\Delta z)_i^2]\} + \sum_{i=1}^{N_M} [(I^B_{xx_{RE}})_i + (I^B_{xx_{PR}})_i] + \sum_{i=1}^{N_M} \{(m_{RE})_i [(\Delta y_{RE})_i^2 + (\Delta z_{RE})_i^2] + (m_{PR})_i [(\Delta y_{PR})_i^2 + (\Delta z_{PR})_i^2]\} \quad (4,4a)$$

$$I^B_{yy} = \sum_{i=1}^{N_c} \{(I^B_{yy})_i + m_i[(\Delta x)_i^2 + (\Delta z)_i^2]\} + \sum_{i=1}^{N_M} [(I^B_{yy_{RE}})_i + (I^B_{yy_{PR}})_i] + \sum_{i=1}^{N_M} \{(m_{RE})_i [(\Delta x_{RE})_i^2 + (\Delta z_{RE})_i^2] + (m_{PR})_i [(\Delta x_{PR})_i^2 + (\Delta z_{PR})_i^2]\} \quad (4,4b)$$

$$I^B_{zz} = \sum_{i=1}^{N_c} \{(I^B_{zz})_i + m_i[(\Delta x)_i^2 + (\Delta y)_i^2]\} + \sum_{i=1}^{N_M} [(I^B_{zz_{RE}})_i + (I^B_{zz_{PR}})_i] + \sum_{i=1}^{N_M} \{(m_{RE})_i [(\Delta x_{RE})_i^2 + (\Delta y_{RE})_i^2] + (m_{PR})_i [(\Delta x_{PR})_i^2 + (\Delta y_{PR})_i^2]\} \quad (4,4c)$$

$$I^B_{xy} = \sum_{i=1}^{N_c} [(I^B_{xy})_i - m_i \Delta x_i \Delta y_i] + \sum_{i=1}^{N_M} [(I^B_{xy_{RE}})_i + (I^B_{xy_{PR}})_i] - \sum_{i=1}^{N_M} [(m_{RE})_i (\Delta x_{RE})_i (\Delta y_{RE})_i + (m_{PR})_i (\Delta x_{PR})_i (\Delta y_{PR})_i] \quad (4,4d)$$

$$I^B_{xz} = \sum_{i=1}^{N_c} [(I^B_{xz})_i - m_i \Delta x_i \Delta z_i] + \sum_{i=1}^{N_M} [(I^B_{xz_{RE}})_i + (I^B_{xz_{PR}})_i] - \sum_{i=1}^{N_M} [(m_{RE})_i (\Delta x_{RE})_i (\Delta z_{RE})_i + (m_{PR})_i (\Delta x_{PR})_i (\Delta z_{PR})_i] \quad (4,4e)$$

$$I^B_{yz} = \sum_{i=1}^{N_c} [(I^B_{yz})_i - m_i \Delta y_i \Delta z_i] + \sum_{i=1}^{N_M} [(I^B_{yz_{RE}})_i + (I^B_{yz_{PR}})_i] - \sum_{i=1}^{N_M} [(m_{RE})_i (\Delta y_{RE})_i (\Delta z_{RE})_i + (m_{PR})_i (\Delta y_{PR})_i (\Delta z_{PR})_i] \quad (4,4f)$$

Because it has been assumed that the only mass changes are due to propellant burn, in these expressions the only time variable quantities will be $(m_{PR})_i$ and $(x_{PR_i}, y_{PR_i}, z_{PR_i})$. As has already been

indicated, if we further assume that the propellant burns in such a way that the centre-of-mass of the propellant of a given rocket motor does not change significantly, then $(x_{PR_i}, y_{PR_i}, z_{PR_i})$ are not time variable and only $(\dot{m}_{PR})_i$ need be considered. The latter is related to the specific impulse of the rocket motor through the relationship (Reference 7)

$$(\dot{m}_{PR})_i = -T_i(t)/(I_{sp_i} g) \qquad (4,5)$$

where g is the acceleration due to gravity, $T_i(t)$ is the thrust of the i-th rocket motor as a function of time t, and I_{sp_i} is the specific impulse of the i-th motor.

Under these assumptions and with (4,5), $\dot{m}$, the moment of inertia time derivatives, and $(\dot{x}_{cm}, \dot{y}_{cm}, \dot{z}_{cm})$ may be readily computed. For the sake of brevity, an exhaustive set of equations will not be given. Typically we have

$$\dot{m} = \sum_{i=1}^{N_M} [-T_i(t)/(I_{sp_i} g)] \qquad (4,6)$$

$$\dot{x}_{cm} = \{ \sum_{i=1}^{N_M} [-T_i(t)/(I_{sp_i} g)] \; (x_{PR})_i - x_{cm}\dot{m}\}/m \qquad (4,7a)$$

$$\dot{y}_{cm} = \{ \sum_{i=1}^{N_M} [-T_i(t)/(I_{sp_i} g)] \; (y_{PR})_i - y_{cm}\dot{m}\}/m \qquad (4,7b)$$

$$\dot{z}_{cm} = \{ \sum_{i=1}^{N_M} [-T_i(t)/(I_{sp_i} g)] (z_{PR})_i - z_{cm}\dot{m}\}/m \qquad (4,7c)$$

$$\dot{I}^B_{xx} = 2 \sum_{i=1}^{N_c} m_i(-\Delta y_i \dot{y}_{cm} + \Delta z_i \dot{z}_{cm}) + \sum_{i=1}^{N_M} (\dot{I}^B_{xx_{PR}})_i$$

$$+ \sum_{i=1}^{N_M} \{2(m_{RE})_i[-(\Delta y_{RE})_i \dot{y}_{cm} + (\Delta z_{RE})_i \dot{z}_{cm}]$$

$$+ (\dot{m}_{PR})_i[(\Delta y_{PR})_i^2 + (\Delta z_{PR})_i^2] + 2(m_{PR})_i[-(\Delta y_{PR})_i \dot{y}_{cm}$$

$$+ (\Delta z_{PR})_i \dot{z}_{cm}]\} \qquad (4,8a)$$

$$\dot{I}^B_{xy} = \sum_{i=1}^{N_c} m_i(-\dot{x}_{cm}\Delta y_i + \Delta x_i \dot{y}_{cm}) + \sum_{i=1}^{N_M} (\dot{I}^B_{xy_{PR}})_i$$

$$+ \sum_{i=1}^{N_M} \{(m_{RE})_i[-\dot{x}_{cm}(\Delta y_{RE})_i + \dot{y}_{cm}(\Delta x_{RE})_i]$$

$$+ (\dot{m}_{PR})_i(\Delta x_{PR})_i(\Delta y_{PR})_i + (m_{PR})_i[-\dot{x}_{cm}(\Delta y_{PR})_i$$

$$+ \dot{y}_{cm}(\Delta x_{PR})_i]\} \qquad (4,8b)$$

In general it will not be convenient to specify the moments of inertia of the individual airframe components, empty rocket motors and the propellant of the rocket motors in, respectively, component reference frames F_{B_i}, F_{BRE_i} and F_{BPR_i} whose axes are parallel to F_B.

Rather, it is assumed that the component moments of inertia are specified in the generalized reference frames F_{R_i}, F_{RE_i} and F_{PR_i} whose axes are orientated in a fashion that makes for the convenient specification of the moment of inertia of the i-th component (e.g. an orientation for which data is available or a principle axes orientation for which cross-moments are zero).

Knowing the Euler angles rotating F_{R_i}, F_{RE_i} and F_{PR_i} to, respectively, F_{B_i}, F_{BRE_i} and F_{BPR_i}, it is possible to transform the component moments of inertia in F_{R_i}, F_{RE_i} and F_{PR_i} to component moments of inertia in F_B. These transformed moments of inertia may then be used directly in the moment of inertia equations defined previously (e.g. the term $(I^B_{yy})_i$ in equation (4,4b)).

This process is illustrated for airframe components. The relationships for the empty rocket motors and the propellant are identical with subscripts 'i' or 'R_i' replaced with, respectively, 'RE_i' and 'PR_i'.

Let $\underline{L}_{BR_i}$ be the rotation matrix rotating components expressed in F_{R_i} to components expressed in F_{B_i}. F_{R_i} is related to F_R through the ordered rotation $(\phi_i, \theta_i, \delta_i)$, and F_R to F_{B_i} through (2.2,9) (note that the axes of F_{B_i} are parallel to F_B). It may be shown that (Reference 4, Section 5.4)

$$\underline{I}^{B_i} = \underline{L}_{BR_i} \underline{I}^{R_i} \underline{L}_{RB_i} \qquad (4,9)$$

where

$$\underline{L}_{RB_i} = (\underline{L}_{BR_i})^T \tag{4,10}$$

$$\underline{I}^{R_i} = \begin{bmatrix} (I^R_{xx})_i & -(I^R_{xy})_i & -(I^R_{xz})_i \\ -(I^R_{yx})_i & (I^R_{yy})_i & -(I^R_{yz})_i \\ -(I^R_{zx})_i & -(I^R_{zy})_i & (I^R_{zz})_i \end{bmatrix} \tag{4,11}$$

and (cf. equation (2.2,5a))

$$\underline{L}_{BR_i} = \begin{bmatrix} -\cos\delta_{R_i}\cos\theta_{R_i} & \sin\delta_{R_i}\cos\theta_{R_i} & -\sin\theta_{R_i} \\ \cos\delta_{R_i}\sin\theta_{R_i}\sin\phi_{R_i} + \sin\delta_{R_i}\cos\phi_{R_i} & -\sin\delta_{R_i}\sin\theta_{R_i}\sin\phi_{R_i} + \cos\delta_{R_i}\cos\phi_{R_i} & -\cos\theta_{R_i}\sin\phi_{R_i} \\ \cos\delta_{R_i}\sin\theta_{R_i}\cos\phi_{R_i} - \sin\delta_{R_i}\sin\phi_{R_i} & -\sin\delta_{R_i}\sin\theta_{R_i}\cos\phi_{R_i} - \cos\delta_{R_i}\sin\phi_{R_i} & -\cos\theta_{R_i}\cos\phi_{R_i} \end{bmatrix} \tag{4.12}$$

The equations that have been presented for the mass and moment of inertia characteristics extensively utilize component centre-of-mass locations (x_i, y_i, z_i). (x_i, y_i, z_i) (Figure 6) represents the compon-

ents of the vector $\underset{\rightarrow}{r}_i$ expressed in reference frame F_R. $\underset{\rightarrow}{r}_i$ is the vector position of the origin of the component centre-of-mass reference frame F_{R_i} relative to F_R (Figure 6). The orientation of the axes of F_{R_i} relative to axes of the structural reference frame F_R is given by the ordered Euler angle rotations $(\phi_{R_i}, \theta_{R_i}, \delta_{R_i})$, i.e. a rotation ϕ_{R_i} about the x-axis of F_R, a rotation θ_{R_i} about the y-axis of the reference frame resulting from the first rotation, and a rotation δ_{R_i} about the z-axis of the reference frame resulting from the second rotation.

As a consequence of the way that the F_R and F_{R_i} have been defined, the order selected for the Euler angle rotations relating F_{R_i} and F_R, and the definition of the cylindrical coordinate system of Figure 5, the Euler angle ϕ_{R_i} also corresponds to the angular cylindrical coordinate. This formulation reduces the total number of parameters required without affecting the generality of the formulation.

The cartesian coordinates (x_i, y_i, z_i) may be obtained from the cylindrical coordinates $(x_{R_i}, r_{R_i}, \phi_{R_i})$ through the relationships

$$x_i = x_{R_i} \tag{4,13a}$$

$$y_i = r_{R_i} \cos\phi_{R_i} \tag{4,13b}$$

$$z_i = r_{R_i} \sin\phi_{R_i} \tag{4,13c}$$

It is emphasized that the x-axis cylindrical and cartesian coordinates are identical.

5. THRUST FORCES AND MOMENTS MODEL

In Section 2.3 the equations of motion are written in the reference frame F_B with the thrust forces and moments written, respectively, as $(X_{T_B}, Y_{T_B}, Z_{T_B})$ and $(L_{T_B}, M_{T_B}, N_{T_B})$. In this section these terms are examined in more detail.

The force terms $(X_{T_B}, Y_{T_B}, Z_{T_B})$ depend on the time domain thrust characteristics and the physical location and orientation of the rocket motors. This data must be know **a priori** to the simulation and is provided as input data to the computer program in the form of a thrust versus time look-up table and a number of parameters associated with the full definition of the rocket motor configuration.

The thrust moments require a somewhat more detailed examination. They are considered to consist of two components:

1) A moment due to the location and orientation of the thrust vector relative to F_B (see Figure 8).
2) A moment induced due to fixed vanes or nozzle grooves onto which the exhaust jet impinges.

Thus we have

$$L_{T_B} = (L_{T_B})_{cm} + (L_{T_B})_{nz} \qquad (5,1a)$$

$$M_{T_B} = (M_{T_B})_{cm} + (M_{T_B})_{nz} \qquad (5,1b)$$

$$N_{T_B} = (N_{T_B})_{cm} + (N_{T_B})_{nz} \qquad (5,1c)$$

These characteristics are rocket motor specific. It is assumed that such data is available for the rocket motors used in the simulation. It then follows that once the orientation and location of the rocket motor thrust vectors relative to the vehicle are specified, enough information is available to determine (L_{T_B}, M_{T_B}, N_{T_B}) as given by (5,1a) to (5,1c).

An assumption that has tacitly been made in this description of the thrust effects is that Coriolis forces and moments on the vehicle generated by the rocket motor exhaust are negligible. This need not always be the case, particularly for the moments, if the exhaust mass flow rate $\dot{m}$ and the exhaust velocity vector relative to the vehicle $\underset{\rightarrow}{V}_E$ are large. However, for vehicles in the class of ROBOT-X using short burn duration 70 mm (2.75 inch) rocket motors, these effects are negligible and will not be considered further in this report.

In order to obtain the body-axes components of the thrust forces and moments, a transformation is required taking the thrust vector and transforming it into components in F_B, then using these components and the location of the point of action of the thrust vector relative to F_B to compute the thrust moments. The following summarizes this analysis.

Only the case for one rocket motor of arbitrary orientation relative to the fuselage reference line (FRL) is considered. The

results for several rocket motors follow with an algebraic summation of each motor's contributions.

A reference frame F_{TH_i} is defined in Figure 8. F_{TH_i} has its origin located at the point of action on the airframe of the thrust vector of the i-th rocket motor, and its x-axis in the negative thrust direction. The orientation of the axes of F_{TH_i} relative to the axes of the structural reference frame F_R is given by the ordered Euler angle rotations (ϕ_{TH_i}, θ_{TH_i}, δ_{TH_i}), i.e. a rotation ϕ_{TH_i} about the x-axis of F_R, a rotation θ_{TH_i} about the y-axis of the reference frame resulting from the first rotation, and a rotation δ_{TH_i} about the z-axis of the reference resulting from the second rotation. A further, important constraint is that the rotation ϕ_{TH_i} corresponds to the angular cylindrical coordinate of the point of action of the thrust vector of the i-th rocket motor relative to the fuselage reference line (see Figure 5).

Since the orientation of F_B is related to the orientation of F_R by a π rotation about the y-axis of F_R (see equation (2.2,9)), it may be shown that the rotation matrix $\underline{L}_{BTH_i}$ relating components of a vector expressed in F_{TH_i} to the components of the same vector expressed in F_B is given by

$$\underline{L}_{BTH_i} = \begin{bmatrix} -\cos\delta_{TH_i}\cos\theta_{TH_i} & \sin\delta_{TH_i}\cos\theta_{TH_i} & -\sin\theta_{TH_i} \\ \cos\delta_{TH_i}\sin\theta_{TH_i}\sin\phi_{TH_i} + \sin\delta_{TH_i}\cos\phi_{TH_i} & -\sin\delta_{TH_i}\sin\theta_{TH_i}\sin\phi_{TH_i} + \cos\delta_{TH_i}\cos\phi_{TH_i} & -\cos\theta_{TH_i}\sin\phi_{TH_i} \\ \cos\delta_{TH_i}\sin\theta_{TH_i}\cos\phi_{TH_i} - \sin\delta_{TH_i}\sin\phi_{TH_i} & -\sin\delta_{TH_i}\sin\theta_{TH_i}\cos\phi_{TH_i} - \cos\delta_{TH_i}\sin\phi_{TH_i} & -\cos\theta_{TH_i}\cos\phi_{TH_i} \end{bmatrix} \quad (5,2)$$

From the definition of F_{TH_i} it follows that the thrust of the i-th rocket motor is given by

$$\underline{T}_i^{TH_i} = (-T_i, 0, 0)^T \quad (5,3)$$

and the nozzle moment of the i-th rocket motor is given by

$$(\underline{M}_{T_i}^{TH_i})_{nz} = (-L_{nz_i}, 0, 0)^T \quad (5,4)$$

Using (5,2) and summing over all the rocket motors, it follows that

$$X_{T_B} = \sum_{i=1}^{N_M} T_i \cos\delta_{TH_i}\cos\theta_{TH_i} \quad (5,5a)$$

$$Y_{T_B} = \sum_{i=1}^{N_M} - T_i(\cos\delta_{TH_i}\sin\theta_{TH_i}\sin\phi_{TH_i} + \sin\delta_{TH_i}\cos\phi_{TH_i}) \qquad (5,5b)$$

$$Z_{T_B} = \sum_{i=1}^{N_M} - T_i(\cos\delta_{TH_i}\sin\theta_{TH_i}\cos\phi_{TH_i} - \sin\delta_{TH_i}\sin\phi_{TH_i}) \qquad (5,5c)$$

and

$$(L_{T_B})_{nz} = \sum_{i=1}^{N_M} L_{nz_i}\cos\delta_{TH_i}\cos\theta_{TH_i} \qquad (5,6a)$$

$$(M_{T_B})_{nz} = \sum_{i=1}^{N_M} - L_{nz_i}(\cos\delta_{TH_i}\sin\theta_{TH_i}\sin\phi_{TH_i} + \sin\delta_{TH_i}\cos\phi_{TH_i}) \qquad (5,6b)$$

$$(N_{T_B})_{nz} = \sum_{i=1}^{N_M} - L_{nz_i}(\cos\delta_{TH_i}\sin\theta_{TH_i}\cos\phi_{TH_i} - \sin\delta_{TH_i}\sin\phi_{TH_i}) \qquad (5,6c)$$

What remains is to compute the thrust moment $(\underset{\rightarrow}{M}_{T_i})_{cm}$ generated by the i-th rocket motor due to the displacement of its point of action relative to the vehicle centre-of-mass. Let $\underset{\rightarrow}{r}_{BTH_i}$ be the vector from the vehicle centre-of-mass to the origin of F_{TH_i} (see Figure 8), $(x_{TH_i}, y_{TH_i}, z_{TH_i})$ are the coordinates of the origin of F_{TH_i} in F_R, and (x_{cm}, y_{cm}, z_{cm}) are the coordinates of the vehicle centre-of-mass in F_R. $(\underset{\rightarrow}{M}_{T_i})_{cm}$ is given by

$$(\underset{\rightarrow}{M}_{T_i})_{cm} = \underset{\rightarrow}{r}_{BTH_i} \times \underset{\rightarrow}{T}_i \qquad (5,7)$$

or

$$\underline{M}^{B}_{T_i} = \underline{\tilde{r}}^{B}_{BTH_i} \underline{T}^{B}_{i} \tag{5,8}$$

where $\underline{\tilde{r}}^{B}_{BTH_i}$ is the matrix equivalent of the vector cross-product (Reference 4, Section 4.6). Using the definitions of the previous paragraph and Figure 8, it may be shown that (cf. equation (3.3,9))

$$\underline{\tilde{r}}^{B}_{BTH_i} = \begin{bmatrix} 0 & (z_{TH_i} - z_{cm}) & (y_{TH_i} - y_{cm}) \\ -(z_{TH_i} - z_{cm}) & 0 & (x_{TH_i} - x_{cm}) \\ -(y_{TH_i} - y_{cm}) & -(x_{TH_i} - x_{cm}) & 0 \end{bmatrix} \tag{5,9}$$

From (5,5), (5,8) and (5,9), it follow that

$$\begin{aligned} (L_{T_B})_{cm} = \sum_{i=1}^{N_M} [&-(z_{TH_i} - z_{cm}) T_i (\cos\delta_{TH_i} \sin\theta_{TH_i} \sin\phi_{TH_i} \\ &+ \sin\delta_{TH_i} \sin\phi_{TH_i}) - (y_{TH_i} - y_{cm}) T_i (\cos\delta_{TH_i} \sin\theta_{TH_i} \cos\phi_{TH_i} \\ &- \sin\delta_{TH_i} \sin\phi_{TH_i})] \end{aligned} \tag{5,10a}$$

$$(M_{T_B})_{cm} = \sum_{i=1}^{N_M} [-(z_{TH_i} - z_{cm})T_i \cos\delta_{TH_i} \cos\theta_{TH_i}$$

$$- (x_{TH_i} - x_{cm})T_i (\cos\delta_{TH_i} \sin\theta_{TH_i} \cos\phi_{TH_i}$$

$$- \sin\delta_{TH_i} \sin\phi_{TH_i})] \qquad (5,10b)$$

$$(N_{T_B})_{cm} = \sum_{i=1}^{N_M} [-(y_{TH_i} - y_{cm})T_i \cos\delta_{TH_i} \cos\theta_{TH_i}$$

$$+ (x_{TH_i} - x_{cm})T_i (\cos\delta_{TH_i} \sin\theta_{TH_i} \cos\phi_{TH_i}$$

$$+ \sin\delta_{TH_i} \cos\phi_{TH_i})] \qquad (5,10c)$$

All the terms that are required to specify the total thrust moments (L_{T_B}, M_{T_B}, N_{T_B}) as given by equations (5,1a), (5,1b) and (5,1c) have now been specified.

As was the case for the mass and moment of inertia formulation of the previous section, the cartesian coordinates (x_{TH_i}, y_{TH_i}, z_{TH_i}) of the point of action of the thrust vector of the i-th rocket motor are more conveniently specified in cylindrical coordinates (x_{TH_i}, r_{TH_i}, ϕ_{TH_i}) (see Figure 5) through the relationships

$$y_{TH_i} = r_{TH_i} \cos\phi_{TH_i} \qquad (5,11a)$$

$$z_{TH_i} = r_{TH_i} \sin\phi_{TH_i} \qquad (5,11b)$$

The x-axis cylindrical and cartesian coordinates are identical.

6. WIND AND TURBULENCE MODELS

The equations of motion developed in Section 2 include terms that take into account wind effects. In Section 2.4 it was indicated that those terms could be written as wind velocities in F_B or F_I (F_E). It is generally more convenient to define the wind velocity vector in terms of components expressed in F_I (F_E), that is

$$\underset{\rightarrow}{W} = W_1 \underset{\rightarrow}{i}_E + W_2 \underset{\rightarrow}{j}_E + W_3 \underset{\rightarrow}{k}_E \qquad (6,1)$$

where we note that in the definition of F_E and F_I used in the report (see Section 2.2), the components of the wind velocity vector expressed in F_E are identical to those expressed in F_I.

In general, $\underset{\rightarrow}{W}$ will be a function of both position and time, that is

$$\underset{\rightarrow}{W} = \underset{\rightarrow}{W}(x_E, y_E, z_E, t) \qquad (6,2)$$

It is common practice to separate this vector into two components, a mean wind and a zero-mean random turbulence component (Reference 2). This separation may be written

$$\underset{\rightarrow}{W}(x_E, y_E, z_E, t) = \underset{\rightarrow}{W}_M(x_E, y_E, z_E, t) + \underset{\rightarrow}{w}(x_E, y_E, z_E, t) \qquad (6,3)$$

Here $\underset{\rightarrow}{W}_M$ is the mean wind and $\underset{\rightarrow}{w}$ is the turbulence component of the wind. The mean wind is frequently assumed to be time-independent, i.e. (6,3) may be written

$$\underset{\rightarrow}{W}(x_E, y_E, z_E, t) = \underset{\rightarrow}{W}_M(x_E, y_E, z_E) + \underset{\rightarrow}{w}(x_E, y_E, z_E, t) \qquad (6,4)$$

The wind models that are provided as part of the simulation software are based on (6,4). The standard models are provided as a matter of convenience. They are not exhaustive but they do provide a framework around which users can customize the wind models to their particular requirements.

A detailed review of wind modeling in flight vehicle response study is given in Chapter 2 of Reference 2. This is the basis of the wind models that are defined in this report.

Three standard mean wind models are provided as part of the simulation package. Model 1 consists of a neutrally stable atmospheric boundary layer wind speed model with speed and direction jets superimposed. Model 2 is the simplest and consists of constant, generally nonzero wind components. Finally, Model 3 consists of mean wind characteristics that are user defined based on altitude dependant look-up tables. Linear interpolation is used to obtain wind velocity characteristics between look-up table data points.

For all three models the mean wind vector is given by

$$\underset{\rightarrow}{W}_M = -W_H \cos\zeta \underset{\rightarrow}{i}_E - W_H \sin\zeta \underset{\rightarrow}{j}_E + W_V \underset{\rightarrow}{k}_E \qquad (6,5)$$

where W_H is the horizontal mean wind, speed W_V is the vertical mean wind speed, and ζ is the direction from which the wind is coming measured relative to True North (see Figure 9).

6.1 Detailed Description of Model 1

For a neutrally stable atmospheric boundary layer (ABL) (this is usually the case with higher wind velocities) the mean horizontal wind speed altitude profile is approximated by (Reference 2)

$$\frac{W_N}{W_G} = \left(\frac{h}{h_G}\right)^n \qquad (6.1,1)$$

Here W_N = wind speed for neutral ABL
W_G = wind speed at the top of the ABL
h = height above the ground
h_G = height above the ground of the top of the ABL.

Typical values of h_G and n for several terrain types are given in the following table (Reference 2).

terrain	h_G (meters)	n
smooth (water, prairie)	300	0.16
woodland	400	0.28
city	500	0.40

These neutral profiles result in mild wind shears and will generally not lead to great control difficulties. Severe wind shears may be modeled by headwind and tailwind discontinuities superimposed onto this profile. This technique will be adopted here by adding hypertangent profiles. In particular, two half jets of the form

$$W_{J_1} = W_{i_1}[1 - \tanh\{(h - h_{i_1})/\Delta s_{H_1}\}] \qquad (6.1,2)$$

$$W_{J_2} = W_{i_2}[\tanh\{(h - h_{i_2})/\Delta s_{H_2}\} - 1] \qquad (6.1,3)$$

will be added. Here W_{J_1}, W_{J_2} = wind speed contributions of the first and second jets respectively; W_{i_1}, W_{i_2} = inflection point heights above ground level for first and second jets respectively; and Δs_{H_1}, Δs_{H_2} = depth of shear zones for first and second jets respectively.

In this model the total horizontal mean wind speed is given by

$$W_H = W_N + W_{J_1} + W_{J_2} \qquad (6.1,4)$$

Equation (6.1,4) is qualitatively plotted in Figure 10*. If the overall mean wind is a headwind, then if $h_{i_1} > h_{i_2}$ the model approximates an increasing headwind discontinuity and if $h_{i_1} < h_{i_2}$ the model approximates a decreasing headwind discontinuity. As Δs_{H_1}, Δs_{H_2} approach zero these approximations approach true headwind and tailwind discontinuities.

The mean wind direction may be modeled similarly.

In the northern hemisphere the wind direction tends to turn in a clockwise direction with height if we are looking down onto the Earth (in other words ζ increases with height). The total change in direction of this turn from the bottom to the top of the ABL is usually between 10 and 45 degrees, but has been measured to be as much as 180 degrees.

---

* Note that in general $W_{J_1}(0) \neq -W_{J_2}(0)$ and thus $W_H(0) \neq 0$.

A family of turning profiles whose parameters may be adjusted to be representative of modest to abrupt direction changes of the wind that a flight vehicle might encounter can be defined as follows:

$$\zeta = \zeta_0 + \kappa_\zeta h + \zeta_{J_1} + \zeta_{J_2}, \quad h \leq h_G \tag{6.1,5a}$$

$$\zeta = \zeta_0 + \kappa_\zeta h_G + \zeta_{J_1} + \zeta_{J_2}, \quad h > h_G \tag{6.1,5b}$$

ζ_{J_1}, ζ_{J_2} are analogous to W_{J_1}, W_{J_2} and are given by

$$\zeta_{J_1} = \zeta_{i_1}[1 - \tanh\{(h - h_{\zeta_{i_1}})/\Delta s_{\zeta_1}\}] \tag{6.1,6}$$

$$\zeta_{J_2} = \zeta_{i_2}[\tanh\{(h - h_{\zeta_{i_2}})/\Delta s_{\zeta_2}\} - 1] \tag{6.1,7}$$

Here ζ_{i_1}, ζ_{i_2} = inflection point values of the direction perturbation magnitudes of the first and second direction shift jets respectively; $h_{\zeta_{i_1}}$, $h_{\zeta_{i_2}}$ = inflection point heights above ground level for first and second direction shift jets respectively; and Δs_{ζ_1}, Δs_{ζ_2} = depth of shear zones for first and second direction shift jets respectively.

Figure 11 presents the qualitative characteristics of the horizontal mean wind direction profiles. If $h_{\zeta_{i_1}} > h_{\zeta_{i_2}}$, an increasing ζ with height direction shift occurs and vice versa for $h_{\zeta_{i_1}} < h_{\zeta_{i_2}}$.

To this point, updrafts and downdrafts have not been considered. These may also be modeled with hypertangent profiles.

Consider Figure 12 where the geometry of the updraft/downdraft region is defined. This may be thought of as a model downburst cell. The vertical mean wind velocity model will then be given by

$$\underset{\sim}{W}_V = W_V \underset{\sim}{k}_E \qquad (6.1,8)$$

where

$$W_V = W_{V_0}[\tanh\{(x_E - x_{E_{i_1}})/\Delta s_{V_1}\} - \tanh\{(x_E - x_{E_{i_2}})/\Delta s_{V_1}\}]$$

$$\cdot [\tanh\{(y_E - y_{E_{i_1}})/\Delta s_{V_2}\} - \tanh\{(y_E - y_{E_{i_2}})/\Delta s_{V_2}\}] \qquad (6.1,9)$$

The terms of this profile are defined analogously to those of the previous hypertangent profiles. The profile is plotted qualitatively in Figure 13.

Physically the updraft or downdraft velocities must be zero at the ground. Terms which cause W_V to go to zero as h approaches zero may readily be added to (6.1,9) (e.g. by multiplying (6.1,9) by tanh(ch) for suitably chosen $c > 0$). Other physical characteristics, such as outflow near the ground level in a downdraft, may be included by appropriate combinations of (6.1,8) and the horizontal wind profiles.

6.2 Detailed Description of Model 2

The mean wind speed for Model 2 consists of constant components given in a reference frame F_{LW} (Figure 9). The orientation of the axes of F_{LW} may be obtained from F_E (F_I) through a rotation ψ_{LW} about the z-axis of F_E (F_I).

We have

$$\underset{\rightarrow}{W}_M = W_{1_{LW_M}} \underset{\rightarrow}{i}_{LW} + W_{2_{LW_M}} \underset{\rightarrow}{j}_{LW} + W_{3_{LW_M}} \underset{\rightarrow}{k}_{LW} \qquad (6.2,1)$$

Equation (6.2,1) may be transformed to provide the mean wind vector expressed in F_E (F_I) components. The result is

$$\underset{\rightarrow}{W}_M = W_{1_M} \underset{\rightarrow}{i}_E + W_{2_M} \underset{\rightarrow}{j}_E + W_{3_M} \underset{\rightarrow}{k}_E \qquad (6.2,2)$$

where

$$W_{1_M} = W_{1_{LW_M}} \cos\psi_{LW} + W_{2_{LW_M}} \sin\psi_{LW} \qquad (6.2,3a)$$

$$W_{2_M} = -W_{1_{LW_M}} \sin\psi_{LW} + W_{2_{LW_M}} \cos\psi_{LW} \qquad (6.2,3b)$$

$$W_{3_M} = W_{3_{LW_M}} \qquad (6.2,3c)$$

The equations (6.2,3a), (6.2,3b) and (6.2,3c) are used in the simulation software.

6.3 Detailed Description of Model 3

As has been indicated, Model 3 consists of look-up table data given as a function of height above sea level (h_{ASL}) fully defining the mean wind characteristics. The input data consists of N_W data points defining the following:

$$W_{H_i} = W_{H_i}(h_{ASL}) \qquad (6.3,1a)$$

$$\zeta_i = \zeta_i(h_{ASL}) \qquad (6.3,1b)$$

$$W_{V_i} = W_{\zeta_i}(h_{ASL}) \qquad (6.3,1c)$$

for $i = 1, N_W$.

Linear interpolation is used to determine values between data points.

Equations (6.3,1a) through (6.3,1c) inclusive may be related to F_E (F_I) mean wind components through equation (6,5), i.e.

$$W_{1M} = -W_H \cos\zeta \qquad (6.3,2a)$$

$$W_{2M} = -W_H \sin\zeta \qquad (6.3,2b)$$

$$W_{3M} = W_V \qquad (6.3,2c)$$

Equations (6.3,2a) through (6.3,2c) are used in the simulation software.

6.4 Turbulence Model

The term $\underset{\rightarrow}{w}$ arising in equations (6,3) and (6,4) represents zero-mean atmospheric turbulence. The simulation package has provision for modeling the three components of the turbulence velocity vector through the definition of three turbulence time histories, one for each component of the turbulence vector.

These time histories are user-defined. They may be created using an appropriate method for generating random time histories. One such method, described in Reference 9, consists of filtering white noise to produce turbulence records whose spectral characteristics are representative of atmospheric turbulence.

The turbulence model used in the simulation software assumes that the three user files have a zero-mean and a standard deviation of 1 m/s. Program input parameters include the definition of the desired standard deviation. This may be used to alter the intensity of the turbulence without changing the basic input files themselves.

The turbulence files are defined with respect to F_E for models 1 and 3 and with respect to F_{LW} for model 2.

6.5 Miscellaneous Wind Model Remarks

The absolute intensity of these wind phenomena may be related in an imprecise way to the hazard posed to flight vehicles. One classification scheme for reporting wind shear in the atmospheric boundary layer (relevant to aircraft, see Reference 2) is as follows:

Category	Vertical Shear Magnitude ($ms^{-1}/30$ m)
Light	0 - 2.5
Moderate	2.5 - 4.5
Strong	4.5 - 6.0
Severe	>6

It is stressed that the effect of such shears on a flight vehicle depends on many factors unrelated to the shear magnitude itself. These include airspeed, configuration, engine response characteristics, and the presence of other meteorological factors. The last may, in fact, lead to somewhat misleading situations. For example, if a flight vehicle encounters a downdraft cell of 4 ms^{-1} strength at 100 m altitude, the mean vertical shear of the downdraft will be 4/100 = 0.04 s^{-1}. In terms of the vertical shear of the horizontal wind which results from the divergence of the downdraft, the equivalent average value is 1.2 m/s per 30 meters. Such a vertical shear on its own would not be considered significant but in combination with the downdraft and the aircraft's low altitude may still cause significant control difficulties.

Downdrafts that have a vertical wind velocity greater than 3.6 m/s (12 fps) at an altitude of 91 m (300 ft) AGL are considered to be downbursts (Reference 2).

7. ATMOSPHERIC MODEL

Since the flight envelope of most flight vehicles spans a large altitude regime, an atmospheric model is required that takes into account variations in density (ρ), temperature (T_A), pressure (P_A), and the speed of sound (a) as a function of altitude above sea level (h_{ASL}).

The model used is based on the US standard atmosphere (1962), as is common practice in aeronautical engineering, and is valid within the troposphere, i.e. for $h_{ASL} \leq 11{,}100$ m (36,000 ft) (see Reference 7). It is given by

$$T_A = 288.15 - 0.0065\, h_{ASL} R \qquad (7,1)$$

$$P_A = 101300(T_A/288.15)^{5.255} \qquad (7,2)$$

$$a = 20.0463\ (T_A)^{1/2} \qquad (7,3)$$

$$\rho = 0.00348454\ P_A/T_A \qquad (7,4)$$

where

$$R = r_E/(h_{ASL} + r_E) \qquad (7,5)$$

T_A is in degrees Kelvin, P_A is in Pascals, a is in meters per second, ρ is in kilograms per cubic meter, h_{ASL} is in meters, and r_E is the Earth's radius to the sea level datum, $r_E = 6.3567658 \times 10^6$ m (2.0855531×10^7 ft).

For altitudes between 11 and 20 km, this model continues to be valid if the temperature T_A is set to 226.65°K (-56.5°C). This corresponds to the isothermal region of the stratosphere.

From the factor R it is also convenient to compute the variation of the acceleration due to gravity as a function of altitude, i.e.

$$g = g_o R^2 \qquad (7,6)$$

where g_o = 9.80667 m/s² (32.1741 f/s²).

Provision has been made in the simulation package to vary the temperature and pressure (and thus the density) from the standard values by allowing altitude dependent deviations from standard conditions.

8. AUXILIARY PARAMETERS AND EQUATIONS

This section describes a number of auxiliary dynamic, kinematic and control system paramters and equations that are used in the simulation software.

8.1 Vehicle Kinematic Restrictions While on Launcher

The presence of the launcher during the initial portion of the flight places a number of kinematic constraints on the vehicle's motion. This section considers these constraints for a rail launcher such as that used for ROBOT-X.

The basic geometrical quantities are defined in Figure 14. The equations of motion while the vehicle is on the rail are presented for the following assumptions:

1) The vehicle is mechanically constrained from rolling while on the launcher by guides until the guides clear the launch rail (i.e. the vehicle is initially constrained to move along the x-axis of reference frame F_{LA}).

2) The quantity s_G represents the distance and vehicle must move in the x-direction of F_B before the guides clear the launch rail.

3) The vehicle may not move backwards on the launcher rail (i.e. $\dot{U}_{B_E}$ is never less than zero).

Under these assumptions it follows that if the distance that the vehicle centre-of-mass has travelled, denoted by s, is less than or equal to s_G, then the vehicle is physically constrained to move only in the launch rail direction, i.e. for $s \leq s_G$ we have

$$\dot{P}_{B_E} = \dot{Q}_{B_E} = \dot{R}_{B_E} = \dot{V}_{B_E} = \dot{W}_{B_E} = 0 \qquad (8.1,1a)$$

$$\dot{U}_{B_E} \geq 0 \qquad (8.1,1b)$$

$$V_{B_E} = V_{B_E}(0) \qquad (8.1,2a)$$

$$W_{B_E} = W_{B_E}(0) \qquad (8.1,2b)$$

$$P_{B_E} = P_{B_E}(0) \qquad (8.1,2c)$$

$$Q_{B_E} = Q_{B_E}(0) \qquad (8.1,2d)$$

$$R_{B_E} = R_{B_E}(0) \qquad (8.1,2e)$$

The nonzero conditions (8.1,2a) to (8.1,2e) allow for a non-stationary launcher, i.e. as would be the case for a launch from a ship in linear and angular motion.

The quantity s is defined precisely as

$$s = [(x_I - x_{I_o})^2 + (y_I - y_{I_o})^2 + z_I^2]^{1/2} \qquad (8.1,3)$$

where (x_I, y_I, z_I) are the vehicle centre-of-mass coordinates in F_I and $(x_{I_o}, y_{I_o}, 0)$ are the centre-of-mass coordinates when the vehicle is at rest on the launcher prior to first stage ignition.

For $s > s_G$, the governing equations are the unconstrained equations of motion developed in Section 2.3.

It is emphasized that this is a simplified model that only considers the gross effects of the launcher constraints on the system during the launch process. A number of potentially important effects have not been modeled. These effects include the tip-off dynamics, i.e. effects that arise when the vehicle centre-of-mass is in front of the launcher but the aft portions of the vehicle are still under the influence of the launcher.

These effects become more important for launch from a moving platform, e.g. as would be the case in a ROBOT-X launch from a ship.

8.2 Aspect Angle Equations

For aerial target and flight test applications, it is frequently necessary that the vehicle's aspect azimuth (ξ_A) and elevation (ξ_E) angles be known with respect to an observer at F_T (see Figure 2). This section presents equations for ξ_A and ξ_E in terms of the location and orientation of F_T relative to that of F_I.

It is assumed that the x-y planes of F_I and F_T are parallel, i.e. that F_I may be rotated to F_T through a rotation ψ_T about the z-axis of F_I.

Let the vector position of F_T relative to F_I be $\underset{\rightarrow}{R}_{IT}$, and that of the vehicle centre-of-mass relative to the origin of F_I be $\underset{\rightarrow}{R}$ (see Figure 15). It follows that the vector position of the vehicle relative to F_T is given by

$$\underset{\rightarrow}{R}_T = \underset{\rightarrow}{R} - \underset{\rightarrow}{R}_{IT} \qquad (8.2,1)$$

or in matrix notation

$$\underline{R}_T^T = \underline{L}_{TI}\underline{R}^I - \underline{L}_{TI}\underline{R}_{IT}^I \qquad (8.2,2)$$

where $\underline{L}_{TI}$ is the rotation matrix rotating vector components in F_I to components in F_T, and is given by (2.2,4a).

Equations (8.2,2) may be written in scalar form as

$$x_T = (x_I - x_{IT})\cos\psi_T + (y_I - y_{IT})\sin\psi_T \qquad (8.2,3a)$$

$$y_T = -(x_I - x_{IT})\sin\psi_T + (y_I - y_{IT})\cos\psi_T \qquad (8.2,3b)$$

$$z_T = z_I - z_{IT} \qquad (8.2,3c)$$

From the definition of ξ_A and ξ_E in Figure 2, it follows that

$$\xi_A = \arctan\,(y_T/x_T) \qquad (8.2,4a)$$

$$\xi_E = \arctan\,(-z_T/x_T) \qquad (8.2,4b)$$

8.3 Vehicle Acceleration

The accelerations that are present on the flight vehicle are frequently required, e.g. in modeling accelerometer inputs to the flight control system computer.

The inertial accelerations sensed at the centre-of-mass may be derived from (2.3,16a) through (2.3,16c), i.e.

$$a_{x_B} = (X_{A_B} + X_{T_B} + X_{P_B})/m + gl_{BI_{13}} \qquad (8.3,1a)$$

$$a_{y_B} = (Y_{A_B} + Y_{T_B} + Y_{P_B})/m + gl_{BI_{23}} \qquad (8.3,1b)$$

$$a_{z_B} = (Z_{A_B} + Z_{T_B} + Z_{P_B})/m + gl_{BI_{33}} \qquad (8.3,1c)$$

where $(a_{x_B}, a_{y_B}, a_{z_B})$ are the components of the vehicle inertial acceleration vector $\underset{\rightarrow}{a}$ expressed in F_B.

Equations (8.3,1a) through (8.3,1c) may also be written

$$a_{x_B} = \dot{U}_{B_E} + Q_B W_{B_E} - R_B V_{B_E} \qquad (8.3,2a)$$

$$a_{y_B} = \dot{V}_{B_E} + R_B U_{B_E} - P_B W_{B_E} \qquad (8.3,2b)$$

$$a_{z_B} = \dot{W}_{B_E} + P_B V_{B_E} - Q_B U_{B_E} \qquad (8.3,2c)$$

Both the inertial and gravitational forces are proportional to the vehicle's mass. If these terms are grouped together, the resulting expressions represent accelerations that would be sensed by instruments located at the centre-of-mass, i.e. at the origin of F_B. The result is

$$a_{x_{cm}} = a_{x_B} - gl_{BI_{13}} \qquad (8.3,3a)$$

$$a_{y_{cm}} = a_{y_B} - gl_{BI_{23}} \qquad (8.3,3b)$$

$$a_{z_{cm}} = a_{z_B} - gl_{BI_{33}} \qquad (8.3,3c)$$

or

$$a_{x_{cm}} = (X_{A_B} + X_{T_B} + X_{P_B})/m \qquad (8.3,4a)$$

$$a_{y_{cm}} = (Y_{A_B} + Y_{T_B} + Y_{P_B})/m \qquad (8.3,4b)$$

$$a_{z_{cm}} = (Z_{A_B} + Z_{T_B} + Z_{P_B})/m \qquad (8.3,4c)$$

These are often written as load factors $n_{x_{cm}}$, $n_{y_{cm}}$, $n_{z_{cm}}$, i.e.

$$n_{x_{cm}} = a_{x_B}/g - 1_{BI_{13}} \qquad (8.3,5a)$$

$$n_{y_{cm}} = a_{y_B}/g - 1_{BI_{23}} \qquad (8.3,5b)$$

$$n_{z_{cm}} = -a_{z_B}/g + 1_{BI_{33}} \qquad (8.3,5c)$$

where the z-equation for load factor has been negated to conform with the convention typically used in aeronautics, i.e. a flight vehicle pull-up is a positive $n_{z_{cm}}$.

In general, the accelerometer triad will not be at the vehicle centre-of-mass, and thus the sensed accelerations must be corrected for apparent accelerations due to angular rate and position. Let $\underset{\rightarrow}{r}_A$ be the position vector of the reference frame F_A relative to F_B. F_A is a body-fixed reference frame whose origin is at the accelerometer triad and whose axes are parallel to F_B. In reference frame F_B, $\underset{\rightarrow}{r}_A$ may be expressed

$$\underset{\rightarrow}{r}_A = x_A \underset{\rightarrow}{i}_B + y_A \underset{\rightarrow}{j}_B + z_A \underset{\rightarrow}{k}_B \qquad (8.3,6)$$

In general it may be shown that the acceleration at F_A ($\underset{\rightarrow}{a}_A$) is related to the acceleration at F_B through the relationship (Reference 4, Section 5.1)

$$\underset{\rightarrow}{a}_A = \underset{\rightarrow}{a}_B + \dot{\underset{\rightarrow}{\omega}}_B \times \underset{\rightarrow}{r}_A + 2\underset{\rightarrow}{\omega}_B \times \dot{\underset{\rightarrow}{r}}_A + \underset{\rightarrow}{\omega} \times \underset{\rightarrow}{\omega} \times \underset{\rightarrow}{r}_A \qquad (8.3,7)$$

Since the vehicle is assumed to be a rigid body,

$$\dot{\underset{\rightarrow}{r}}_A = 0 \qquad (8.3,8)$$

and this term drops out of (8.3,7). Substituting the equivalent matrix relationships into (8.3,7), solving for centre-of-mass acceleration, and dividing by g, the resulting scalar equations may be shown to be

$$n_{x_{cm}} = n_{x_s} + [x_A(Q_B^2+R_B^2) - y_A(P_BQ_B-\dot{R}_B) - z_A(P_BR_B+\dot{Q}_B)]/g \qquad (8.3,9a)$$

$$n_{y_{cm}} = n_{y_s} + [-x_A(P_BQ_B+\dot{R}_B) + y_A(P_B^2+R_B^2) - z_A(Q_BR_B-\dot{P}_B)]/g \qquad (8.3,9b)$$

$$n_{z_{cm}} = n_{z_s} + [x_A(P_BR_B-\dot{Q}_B) + y_A(Q_BR_B+\dot{P}_B) - z_A(P_B^2+Q_B^2)]/g \qquad (8.3,9c)$$

where n_{x_s}, n_{y_s} and n_{z_s} are the accelerations sensed at F_A (normalized by g) and n_{z_s} is defined as a load factor in the conventional aeronautical sense (i.e. the negative of the z-acceleration sense in F_A).

Equations (8.3,9a), (8.3,9b) and (8.3,9c) are important if a very accurate estimate of acceleration at the centre-of-mass is required (e.g. in strapdown inertial navigation algorithms).

In terms of the structural datum reference frame F_R, (x_A, y_A, z_A) may be written

$$x_A = -(x_{R_A} - x_{cm}) \qquad (8.3,10a)$$

$$y_A = y_{R_A} - y_{cm} \qquad (8.3,10b)$$

$$z_A = -(z_{R_A} - z_{cm}) \qquad (8.3,10c)$$

where $(x_{R_A}, y_{R_A}, z_{R_A})$ are the coordinates of the origin of reference frame F_A in F_R.

8.4 Homing Beacon Geometry

The simulation software has provision for modeling a nondirectional homing beacon (NDB) in order to simulate a homing signal for an autopilot automatic direction finder (ADF). The homing angle η is defined in Figure 16 and is given by

$$\eta = \psi_{rel} - \psi_B, \quad 0 \leq \eta < 2\pi \qquad (8.4,1)$$

where

$$\psi_{rel} = \arctan(\Delta y_I / \Delta x_I), \quad 0 \leq \psi_{rel} < 2\pi \qquad (8.4,2)$$

$$\Delta x_I = x_{I_{be}} - x_I \qquad (8.4,3)$$

$$\Delta y_I = y_{I_{be}} - y_I \qquad (8.4,4)$$

The location of the beacon relative to F_I is given by the vector $\underset{\rightarrow}{R}_{be}$ where

$$\underset{\rightarrow}{R}_{be} = x_{I_{be}} \underset{\rightarrow}{i}_I + y_{I_{be}} \underset{\rightarrow}{j}_I + (h_{o_{ASL}} - h_{be_{ASL}}) \underset{\rightarrow}{k}_I \qquad (8.4,5)$$

where $h_{o_{ASL}}$ is the elevation above sea level of the origin of F_I and $h_{be_{ASL}}$ is the elevation above sea level of the NDB.

It is noted that this model assumes that for the homing distances of interest, a flat earth assumption is valid.

If more sophisticated homing systems are utilized (e.g. TACAN or LORAN C), then a more elaborate homing model would be required.

8.5 Servo Dynamics Model

The simulation package models servo dynamics as a first order lag, and takes advantage of the fact that the flight control system updates the commanded servo position once every Δt seconds. Δt is the autopilot update rate.

The resulting models for throttle position δ_T, elevator position δ_E, horizontal stabilizer (or canard) position i_H, aileron position δ_A and rudder position δ_R are given by

$$\delta_T = (\delta_{T_i} - \delta_T{}^c)e^{-\Delta t_i/T_{\delta_T}} + \delta_T{}^c \qquad (8.5,1)$$

$$\delta_E = (\delta_{E_i} - \delta_E{}^c)e^{-\Delta t_i/T_{\delta_E}} + \delta_E{}^c \qquad (8.5,2)$$

$$i_H = (i_{H_i} - i_H{}^c)e^{-\Delta t_i/T_{i_H}} + i_H{}^c \qquad (8.5,3)$$

$$\delta_A = (\delta_{A_i} - \delta_A{}^c)e^{-\Delta t_i/T_{\delta_A}} + \delta_A{}^c \qquad (8.5,4)$$

$$\delta_R = (\delta_{R_i} - \delta_R{}^c)e^{-\Delta t_i/T_{\delta_R}} + \delta_R{}^c \qquad (8.5,5)$$

where the subscript 'i' on a control position indicates the value of the actual control position at the beginning of the i-th Δt interval, a superscript 'c' on a control position indicates the commanded control position for the i-th Δt interval, and

$$\Delta t_i = t - t_i \qquad (8.5,6)$$

Here t is time and t_i is the time at which the i-th time interval begins. Equations (8.5,1) through (8.5,5) are valid in the time interval $t_i \leq t < t_i + \Delta t$. $\delta_T{}^c$, $\delta_E{}^c$, $i_H{}^c$, $\delta_A{}^c$ and $\delta_R{}^c$ are assumed to be updated at the beginning of each Δt interval.

The actual control deflections that result are limited to values appropriate to the physical limits of the servos.

If higher order or nonlinear features (other than limiting) are important to the vehicle dynamics, this model may be modified to take such effects into account with a corresponding increase in the complexity of the model.

9. GENERAL SOFTWARE DESCRIPTION

The simulation model described in the previous sections has been implemented on a VAX 11/780 computer located at DRES. It has been named FLISIM (FLIght SIMulation) and has been developed in two versions

(FLISIMV1 and FLISIMV2) using, respectively, the AERO1 and AERO2 aerodynamic models of Sections 3.1 and 3.2.

Both FLISIMV1 and FLISIMV2 are written in VAX 11 Fortran Version 4.8-276 and run using the VMS Version 5.1 Operating System. Both make use of IMSL subroutines (Reference 10).

FLISIM is fully supported with a plotting software package developed around Tektronix PLOT 10 core software. The plotting software has been used successfully on a number of graphics terminals including DEC VT 100 (with Retrographics), Tektronix 4105, 4107, 4112 and 4114 terminals.

FLISIM has been designed to be highly modular in order to facilitate user defined changes. This is particularly important in certain areas (e.g. in the flight control system modules).

FLISIMV2 size and performance are similar to FLISIMV1. The input aerodynamic files required for FLISIMV2 are generally of considerably greater size.

A version of FLISIM is currently being implemented as part of the DRES real time simulation facility (SIMFAC). This version will be geared to real time operation and will, as a secondary benefit, lead to a more efficient code for use on the VAX 11/780 as well as on the SIMFAC computer. The SIMFAC version will run in a UNIX environment.

Both FLISIMV1 and FLISIMV2 have VMS command procedures to facilitate compilation and execution, and to provide a user-friendly environment.

The FLISIM software was designed not only to provide a six degree-of-freedom simulation capability but also to provide the high degree of flexibility required in applications requiring its use as a flight control algorithm and flight vehicle design tool, and in parametric and monte carlo simulation of flight vehicles. The software has been used very extensively and successfully in these roles in support of ROBOT-X design, development and flight test and, to a lesser degree, in other DRES RPV and drone activities. In the course of these applications there have been many changes introduced to improve the utility of the software, to enhance its modularity and remove identified bugs, and to develop user-friendly command procedures.

The high degree of flexibility that has been built into the software also results in a software subset that is of some complexity. This requires a concentrated initial effort by new users in order to become familiar with the software and its various options and features. It has been the DRES experience that users familiar with the VMS Operating System and Fortran typically required 3-4 weeks to acquire a good working familiarity with the software.

The IMSL subroutine DGEAR (Reference 10) is used to solve the twelfth order nonlinear system of differential equations. DGEAR allows a number of solution modes as determined by its input parameters. These include an Adams-Moulton predictor-corrector method and Gear's backward differentiation method (Reference 11).

For simulations in which speed of computation is essential, DGEAR is not particularly efficient, in part due to its variable step size and complexity of options. A fixed step size fourth order Runge-Kutta method is usually satisfactory for flight vehicle simulation applications and could be used in place of DGEAR.

The simulation includes features that model flight control systems that discretely update control and navigation parameters. The update time Δt is user-defined thus facilitating parametric evaluation of the effect of various update intervals on flight control system performance, and allowing for the introduction of lags associated with "stale" sensor data and flight control computer computations.

In summary, the main features of the FLISIM simulation software are as follows:

a) Time varying mass and moment of inertia characteristics.
b) Time varying thrust characteristics.
c) Two standard aerodynamic models that allow input of the characteristics of a wide variety of flight configurations based on predicted, wind tunnel and flight test aerodynamic data.
d) Modeling of ripple rocket firing characteristics.
e) Modeling of control dynamics of flight vehicles that have any combination of throttle, elevator, all-flying stabilizer or canard, ailerons and rudder.
f) Modeling of digital autopilot control algorithms including discrete sensor and control command updates.
g) Modeling of sensor nonidealities including sensor lag and bias.
h) Modeling of variable wind characteristics including discrete gusts, wind shear and turbulence.
i) An atmospheric model based on the standard ICAO atmosphere.
j) An input data file conveniently structured for parametric and sensitivity variation of critical thrust, mass and aerodynamic characteristics.

k) An interactively structured command procedure that allows convenient variation of autopilot control algorithms and control gains, and wind and turbulence models.

l) An interactive plotting package developed around Tektronix PLOT 10.

A detailed userbook for the simulation software and the associated plotting package has been developed and is given as Volume 2.

Volume 3 gives source code listings.

10. SUMMARY AND FUTURE WORK

Six degree-of-freedom, rigid body equations of motion have been described suitable for modeling the dynamic characteristics of multi-staged rocket-boosted maneuvering aerial targets. These equations form the core of a Fortran simulation package named FLISIM. FLISIM is currently installed on a VAX 11/780 computer at DRES, and has been extensively utilized in ROBOT-X flight control algorithm development, mission profile definition, and in comparision with flight test data.

The FLISIM package is currently being adapted for use in the DRES real time simulation facility (SIMFAC). SIMFAC has been configured around a Masscomp 5500S minicomputer operating in a UNIX environment.

The current software, although flexible in its implementation, is relatively slow and is thus unsuitable for use in real time. As part of the SIMFAC implementation, steps are being taken to modify the code for efficient execution in a real time environment. These modifi-

cations will also improve the efficiency of the VAX 11/780 code which is used strictly in applications that are not real time.

In order to facilitate broader application of the simulation package, in the longer term modifications are under consideration that will remove some of the assumptions and restrictions applicable to the current versions. These modifications could include the following:

a) Removal of the flat, nonrotating Earth assumption.
b) Addition of the capability to model internal rigid rotors.
c) Modeling of fall-away rocket motor stages.
d) Modeling of different types of propulsion systems.

REFERENCES - VOLUME 1

1. Markov, A.B., **A Nonlinear Six Degree-of-Freedom Ballistic Aerial Target Simulation Model Volume 1 - Theoretical Development; Volume 2 - BALSIM Userbook (U)**, Suffield Memorandum No. 1081, February 1984. UNCLASSIFIED.

2. Markov, A.B., **The Landing Approach in Variable Winds: Curved Glidepath Geometries and Worst-Case Wind Modeling**, UTIAS Report No. 254, University of Toronto, 1981.

3. Gagnon, B., **Simulation Based Evaluation of the Modified Maximum Likelihood Estimation Software (MMLE5) for Airplane Aerodynamic Parameter Identification**, Boeing of Canada R&D Contract Report BCW-TR-86-134, DSS File No. 01SG.97702-R-5-0367, July 1986. UNCLASSIFIED.

4. Etkin, B., **Dynamics of Atmospheric Flight**, John Wiley & Sons Inc., Toronto, 1972.

5. McRuer, D., Ashkenas, I. and Graham, D., **Aircraft Dynamics and Automatic Control**, Princeton University Press, New Jersey, 1973.

6. Hoak, D.E. and Finck, R.D., **USAF Stability and Control DATCOM**, Air Force Flight Dynamics Laboratory Project No. 8219, Task No. 821901, October 1960 (revised April 1978). UNCLASSIFIED.

7. Anonymous, **Design of Aerodynamically Stabilized Free Rockets - Engineering Design Handbook**, AMC Pamphlet AMCP 706-280, US Army Materiel Command, July 1968.

8. Torenbeek, E., **Synthesis of Subsonic Airplane Design**, Delft University Press, 1981.

9. Reid, L.D. and Graf, W.O., **Design and Development of a Low Cost Maneuverable Rocket Boosted Target - Control Law Synthesis, Phase 2**, UTIAS Contract Report, R&D Contract No. 01SG.97702-R-3-6715, November 1983. UNCLASSIFIED.

10. Anonymous, **IMSL Library Reference Manual**, Vols. 1-3, Edition 8, IMSL, Inc., June 1980.

11. Gear, C.W., **Numerical Initial Value Problems in Ordinary Differential Equations**, Prentice-Hall, 1971.

TABLE I

SUMMARY OF DRES SIX DEGREE-OF-FREEDOM
AND ASSOCIATED SOFTWARE PACKAGES

NAME	DESCRIPTION	REMARKS
BALSIMV3	• Free flight, ballistic 6 DOF package. • Vehicle constrained to launch rail until T-bolt clears.	• Used on ROBOT-5, ROBOT-7F, ROBOT-7R, ROBOT-9.
BALSIMV5	• Free flight, ballistic 6 DOF package. • Geared to rocket-boosted systems. • Vehicle has guide bolt but it is not modeled as a T-bolt.	• As above.
FLISIMV1	• Maneuvering vehicle 6 DOF package. • Geared to rocket-boosted aerial targets, but readily configured to other propulsion methods. • Modular structure allows complete modeling of control laws, autopilot nonidealities and sensor nonidealities. • Wind, turbulence models incorporated. • Servo dynamics model incorporated. • Nonlinear aerodynamic model (Model AERO1).	• Used on ROBOT-X, ROBOT-LRX, ROBOT-9. • Modified version used in MMLE study (Reference 3).
FLISIMV2	• As above except that the nonlinear aerodynamic model is Model AERO2.	• ROBOT-X
PREAER1	• Aerodynamic model generation program for FLISIMV1, DATCOM methods.	• Used on ROBOT-X, ROBOT-LRX, R^2P^2, HULK.
PREAER2	• Aerodynamic model generation program for FLISIMV1, hybrid DATCOM/wind tunnel test data methods.	• Used on ROBOT-X in conjunction with wind tunnel test data.
MICONSIM	• Real time ROBOT-X mission controller training program.	• Uses simulation files generated by FLISIMV1 and FLISIMV2.

TABLE I

SUMMARY OF DRES SIX DEGREE-OF-FREEDOM
AND ASSOCIATED SOFTWARE PACKAGES
(continued)

NAME	DESCRIPTION	REMARKS
NATMOD	• Natural mode program (open-loop or closed-loop). • Generates system eigenvalues and eigenvectors.	• Makes use of aerodynamic files generated by PREAER1 or PREAER2. • Used in ROBOT-X, R^2P^2 and HULK.
TRIMV1	• Determines steady-state trim conditions.	• Makes use of aerodynamic files generated by PREAER1 or PREAER2. • Used by ROBOT-X, R^2P^2.
PLOTBALSM	• Plotting package for BALSIMV3 and BALSIMV5.	• Developed around PLOT 10 subroutines.
PLTSIMV1	• Plotting package for FLISIMV1 and FLISIMV2.	• As above.
RBTPLOTV2	• Plotting package for PREAER1 and PREAER2.	• As above.

TABLE II

AERO1 AERODYNAMIC MODEL BASELINE PARAMETERS

LONGITUDINAL		LATERAL	
i	VARIABLE	i	VARIABLE
1	C_{D_1}	1	C_{y_β}
2	C_{L_1}	2	C_{l_β}
3	$C^N_{m_1}$	3	$C^N_{n_\beta}$
4	C_{D_q}	4	C_{y_p}
5	C_{L_q}	5	$C^N_{l_p}$
6	$C^N_{m_q}$	6	$C^N_{n_p}$
7	$C_{D_{\dot\alpha}}$	7	C_{y_r}
8	$C_{L_{\dot\alpha}}$	8	$C^N_{l_r}$
9	$C^N_{m_{\dot\alpha}}$	9	$C^N_{n_r}$
10	$C_{D_{\delta_E}}$	10	$C_{y_{\delta_A}}$
11	$C_{L_{\delta_E}}$	11	$C^N_{l_{\delta_A}}$
12	$C^N_{m_{\delta_E}}$	12	$C^N_{n_{\delta_A}}$
13	$C_{D_{i_H}}$	13	$C_{y_{\delta_R}}$
14	$C_{L_{i_H}}$	14	$C^N_{l_{\delta_R}}$
15	$C^N_{m_{i_H}}$	15	$C^N_{n_{\delta_R}}$

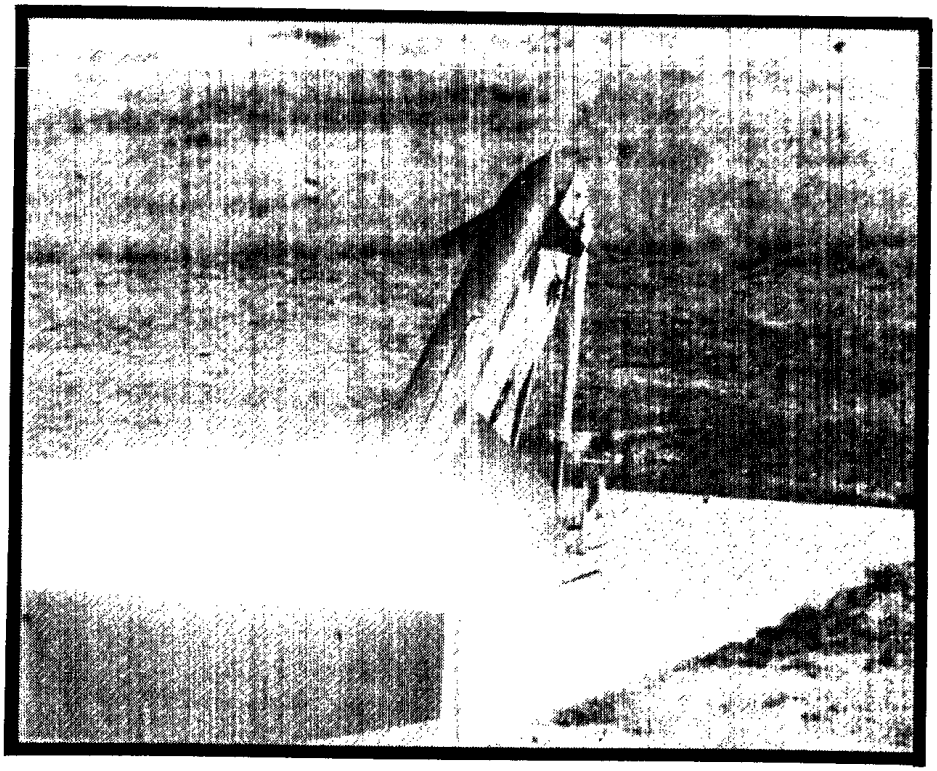

t = 0 seconds

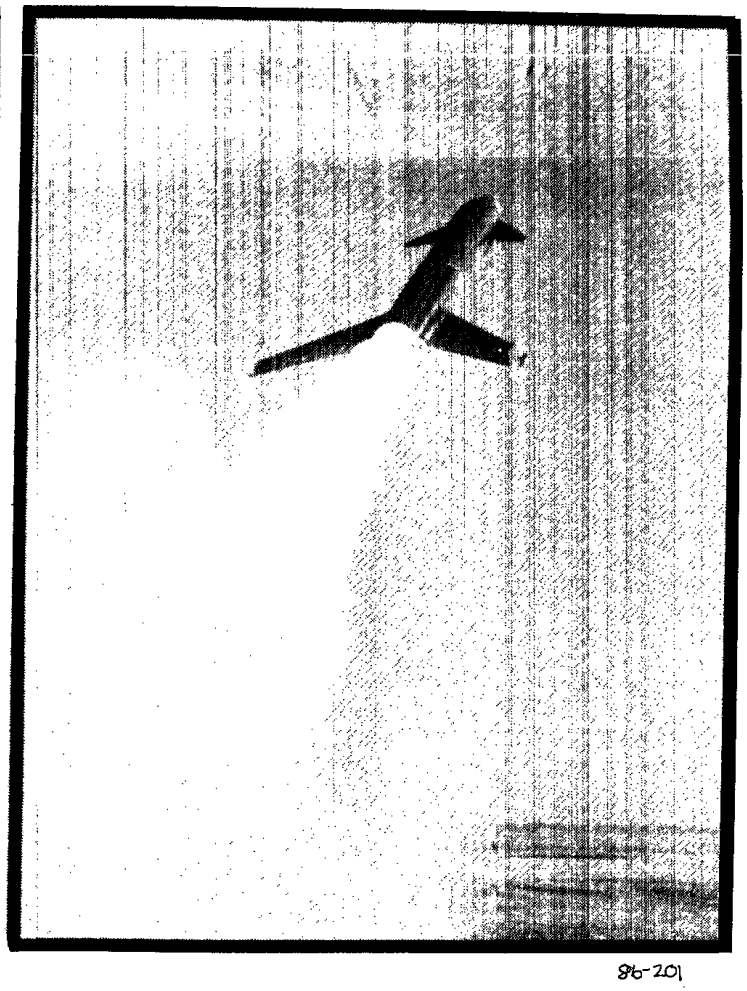

t = 0.65 seconds

Figure 1

THE ROBOT-X AERIAL TARGET SYSTEM
Flight 3 Launch – 29 August, 1986
(Taken with 70 mm Hulcher Camera Running at 40 frames per second)

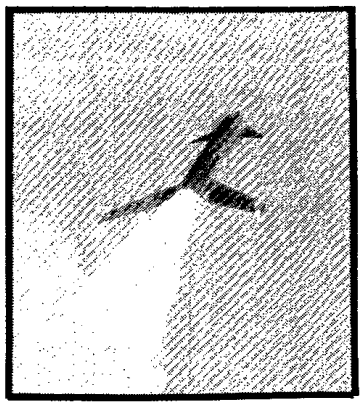

ROBOT-X

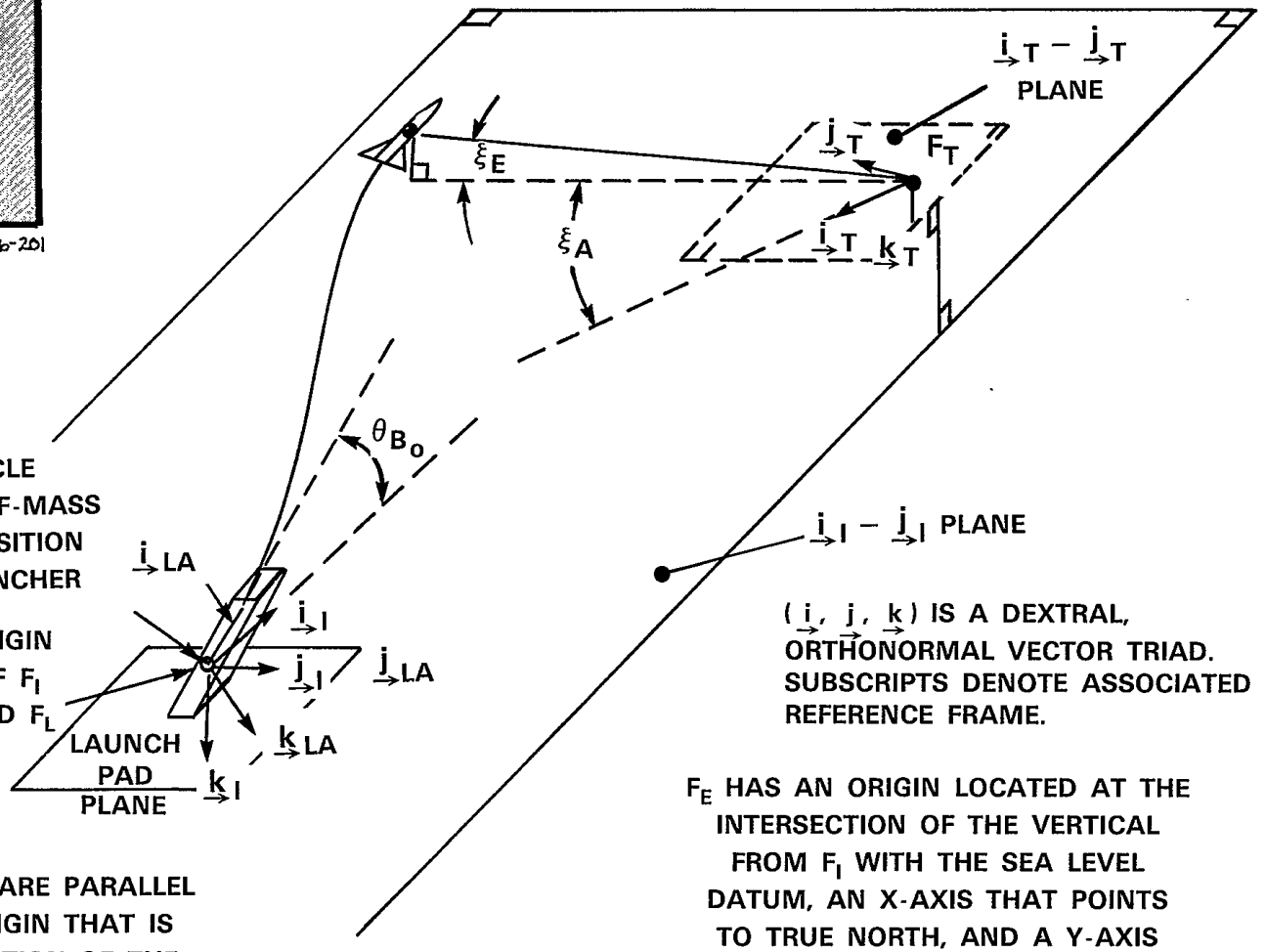

F_I HAS AXES THAT ARE PARALLEL TO F_E BUT AN ORIGIN THAT IS ON THE REST POSITION OF THE VEHICLE ON THE LAUNCHER.

$(\underset{\rightarrow}{i}, \underset{\rightarrow}{j}, \underset{\rightarrow}{k})$ IS A DEXTRAL, ORTHONORMAL VECTOR TRIAD. SUBSCRIPTS DENOTE ASSOCIATED REFERENCE FRAME.

F_E HAS AN ORIGIN LOCATED AT THE INTERSECTION OF THE VERTICAL FROM F_I WITH THE SEA LEVEL DATUM, AN X-AXIS THAT POINTS TO TRUE NORTH, AND A Y-AXIS THAT POINTS TO TRUE EAST.

Figure 2

DEFINITION OF EARTH-FIXED REFERENCE FRAMES

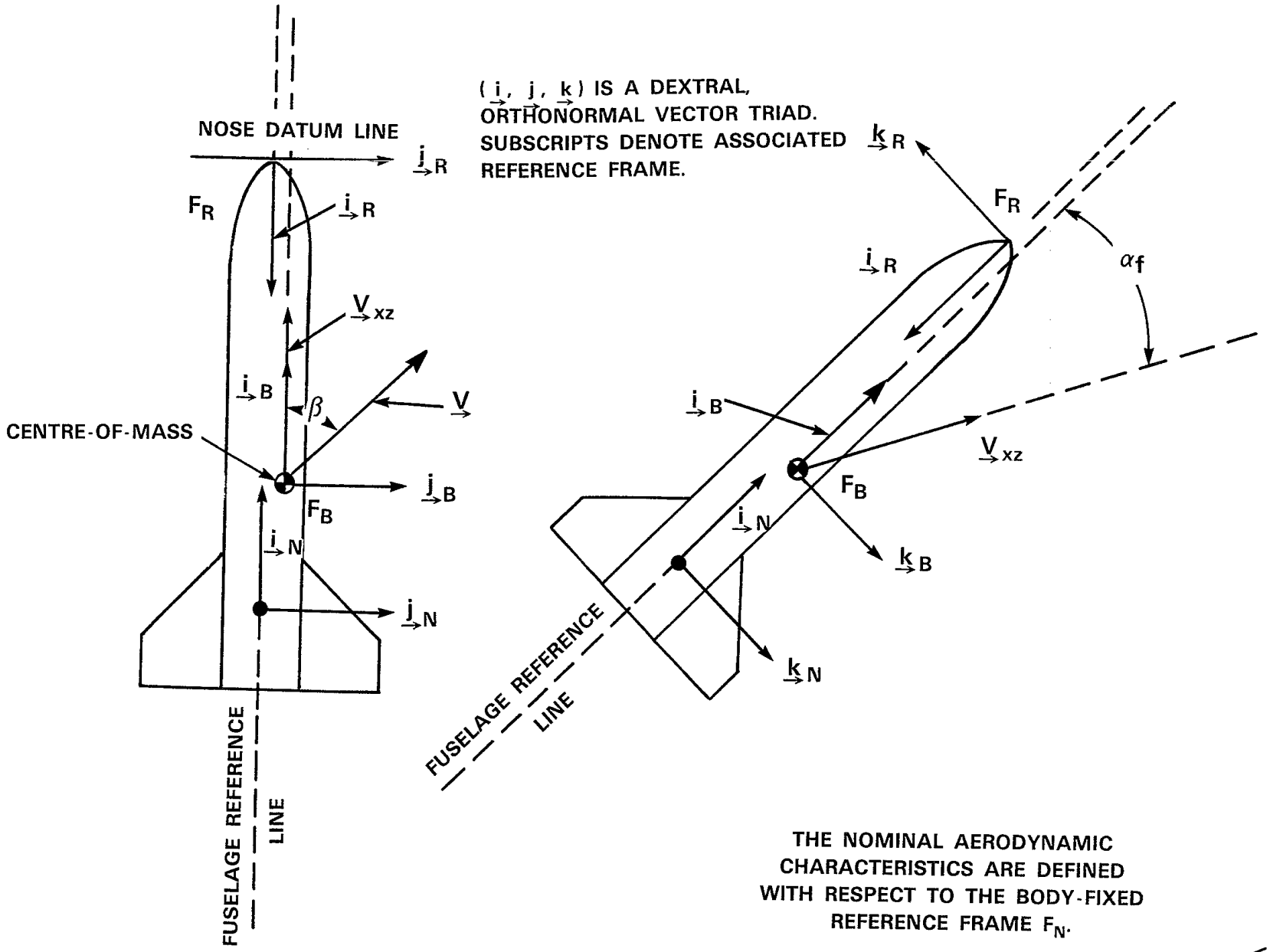

Figure 3

DEFINITION OF BODY-FIXED REFERENCE FRAMES AND AERODYNAMIC ANGLES

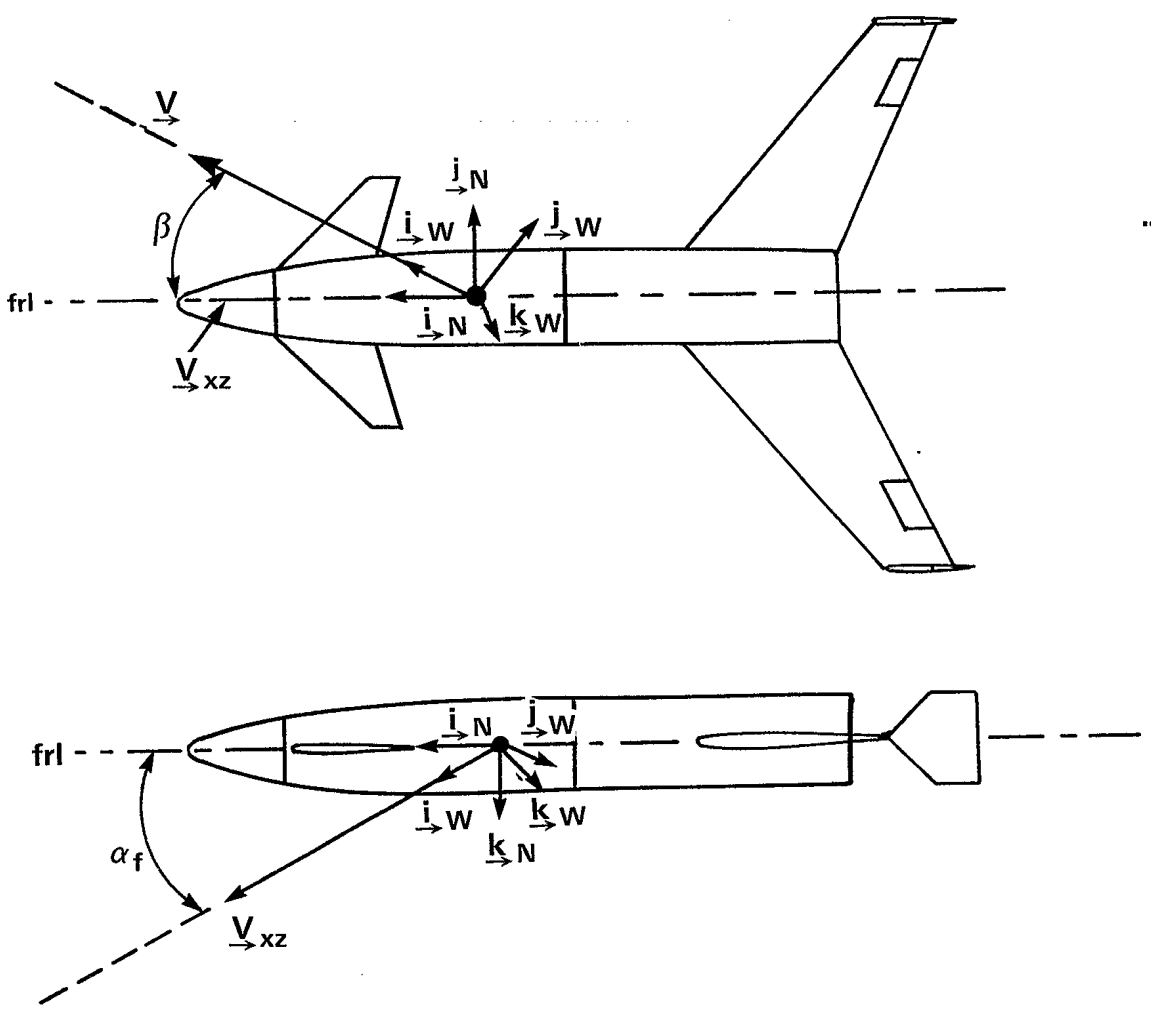

Figure 4

DEFINITION OF WIND AXES

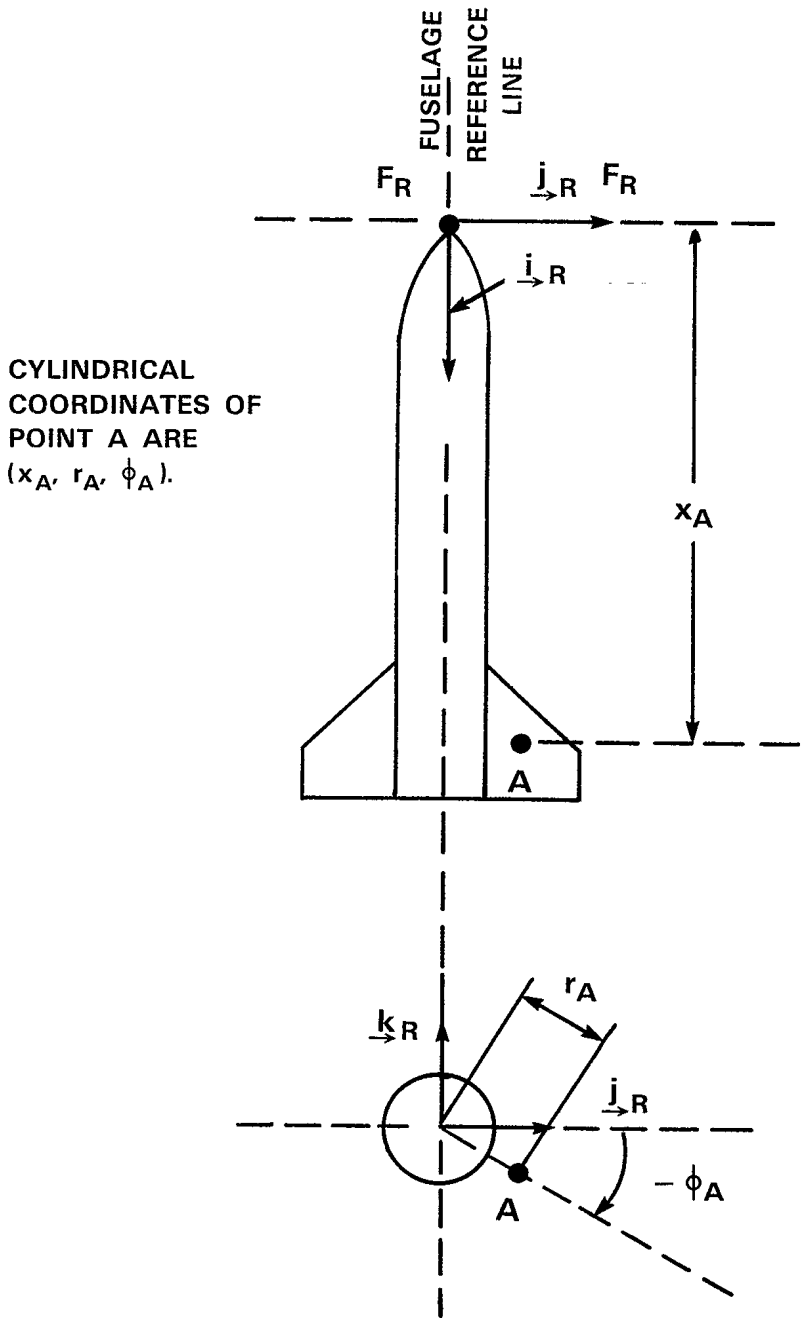

Figure 5

VEHICLE CYLINDRICAL COORDINATE SYSTEM

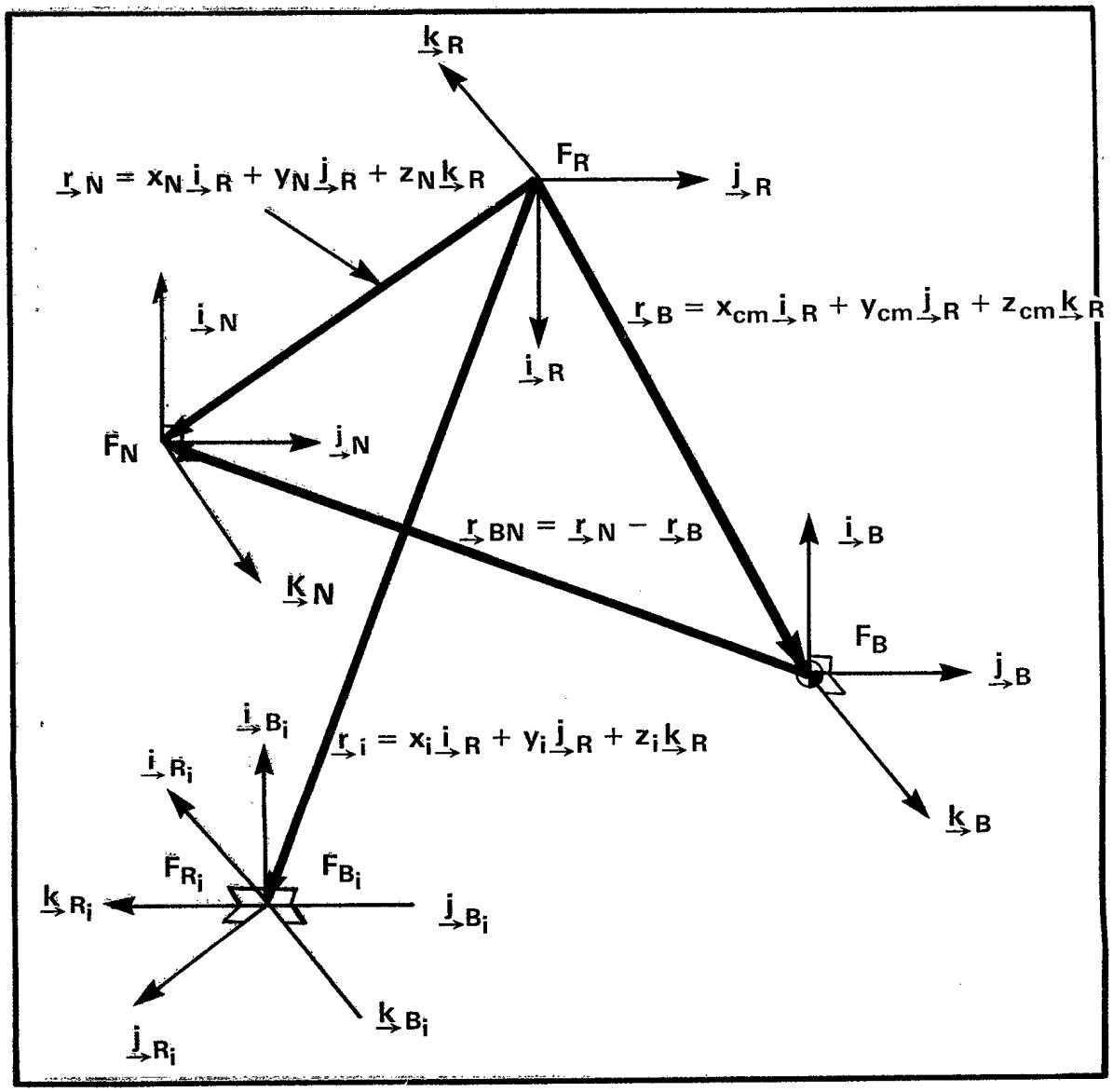

NOTES

(i) The origin of F_B is at the vehicle centre-of-mass.

(ii) The origin of F_R is on the vehicle datum point and does not move.

(iii) The orientation of F_B is related to the orientation of F_R through 180° rotation about $\underset{\rightarrow}{j}_R$.

(iv) The axes of F_N and F_{B_i} are parallel to F_B.

(v) The origin of F_{B_i} and F_{R_i} are at the centre-of-mass of the i-th airframe component.

(vi) F_{R_i} is of arbitrary orientation. F_{R_i} is obtained from F_R through the ordered Euler rotations (ϕ_{R_i}, θ_{R_i}, δ_{R_i}).

Figure 6

GENERALIZED COMPONENT REFERENCE FRAMES AND GEOMETRIES

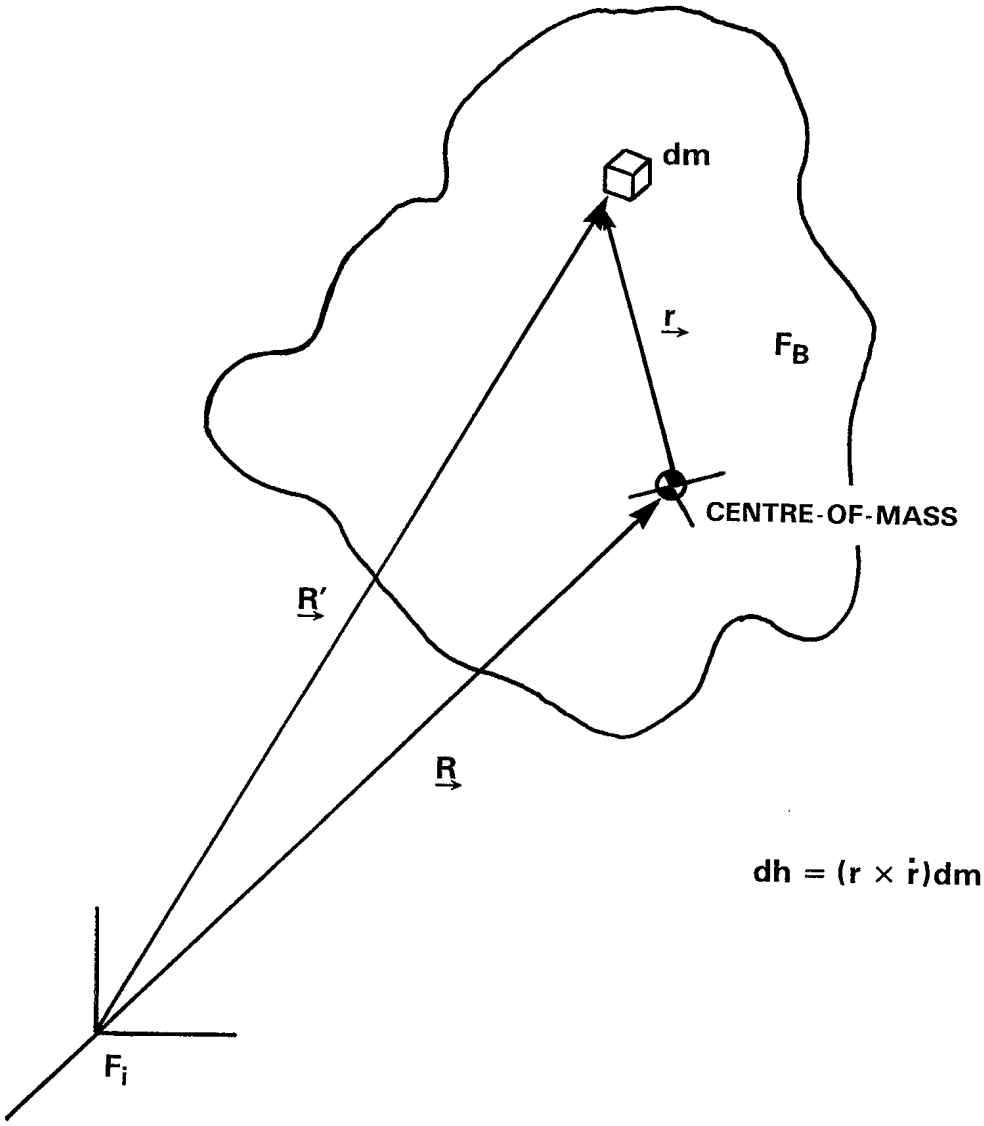

Figure 7

ANGULAR MOMENTUM CONTRIBUTION OF THE MASS ELEMENT dm

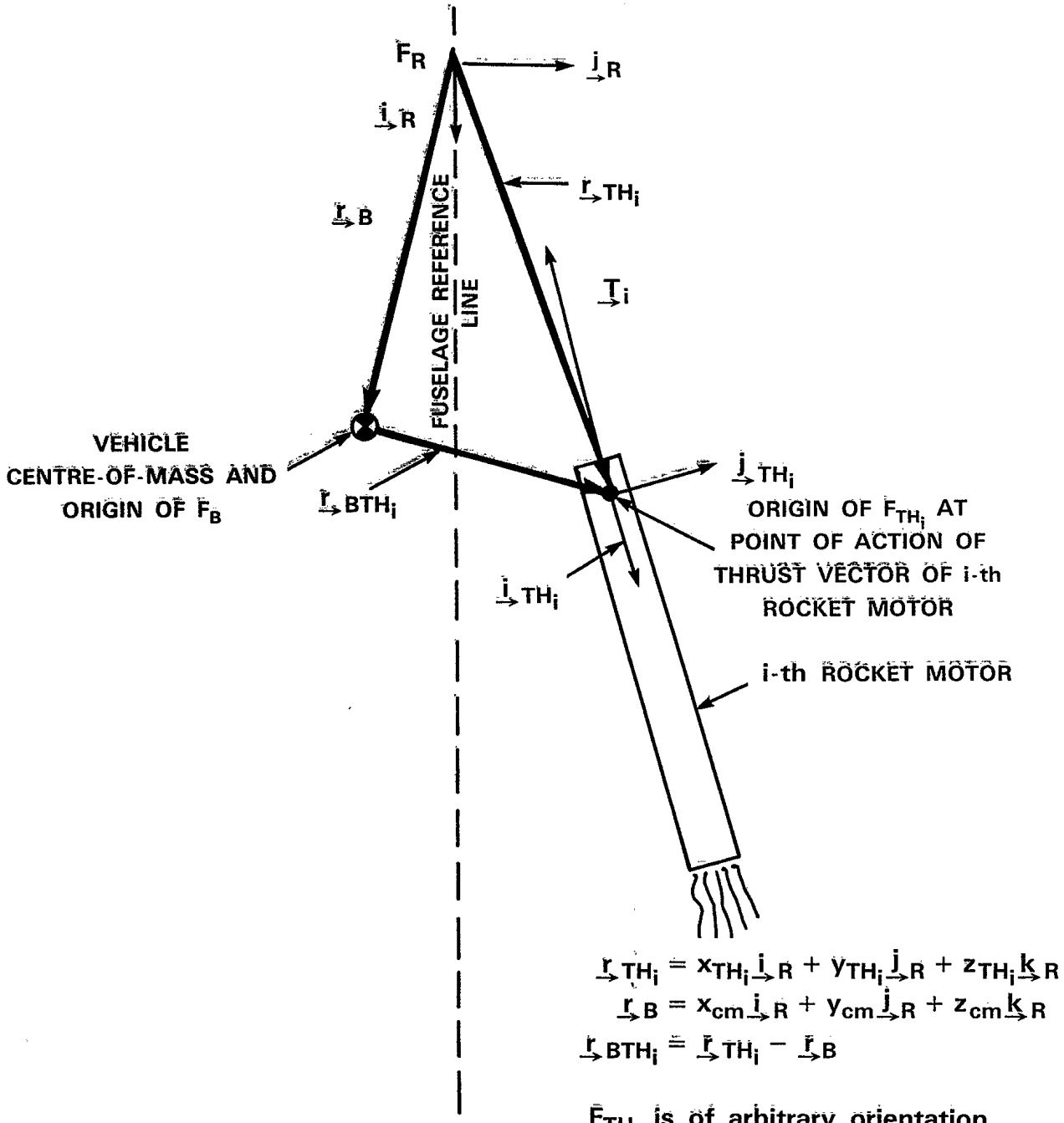

$$\underrightarrow{r}_{TH_i} = x_{TH_i}\underrightarrow{i}_R + y_{TH_i}\underrightarrow{j}_R + z_{TH_i}\underrightarrow{k}_R$$

$$\underrightarrow{r}_B = x_{cm}\underrightarrow{i}_R + y_{cm}\underrightarrow{j}_R + z_{cm}\underrightarrow{k}_R$$

$$\underrightarrow{r}_{BTH_i} = \underrightarrow{r}_{TH_i} - \underrightarrow{r}_B$$

F_{TH_i} is of arbitrary orientation

F_{TH_i} is obtained from F_R through the ordered Euler rotations $(\phi_{TH_i}, \theta_{TH_i}, \delta_{TH_i})$.

Figure 8

DEFINITION OF REFERENCE FRAME F_{TH_i}

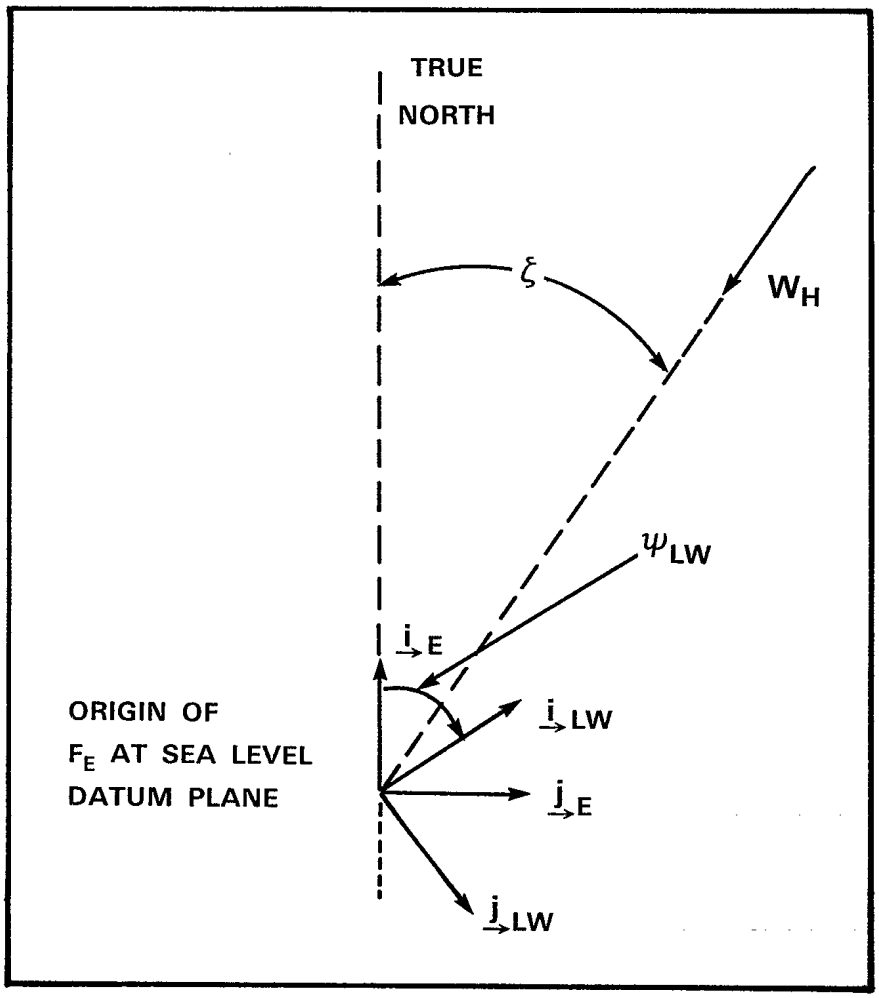

Figure 9

WIND DIRECTION ξ DEFINITION

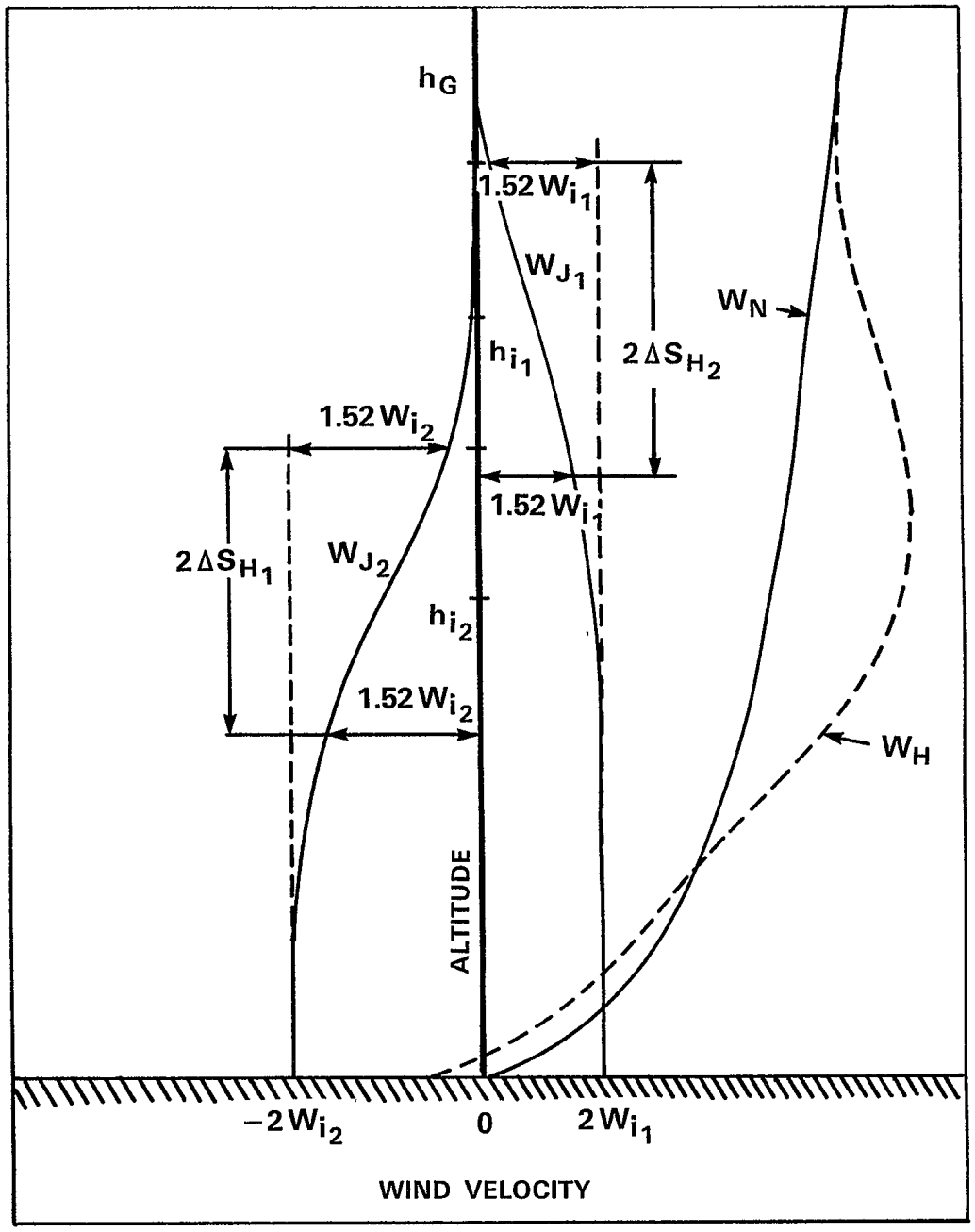

Figure 10

HORIZONTAL MEAN WIND SPEED CHARACTERISTICS FOR MODEL I

(Taken from Reference 2)

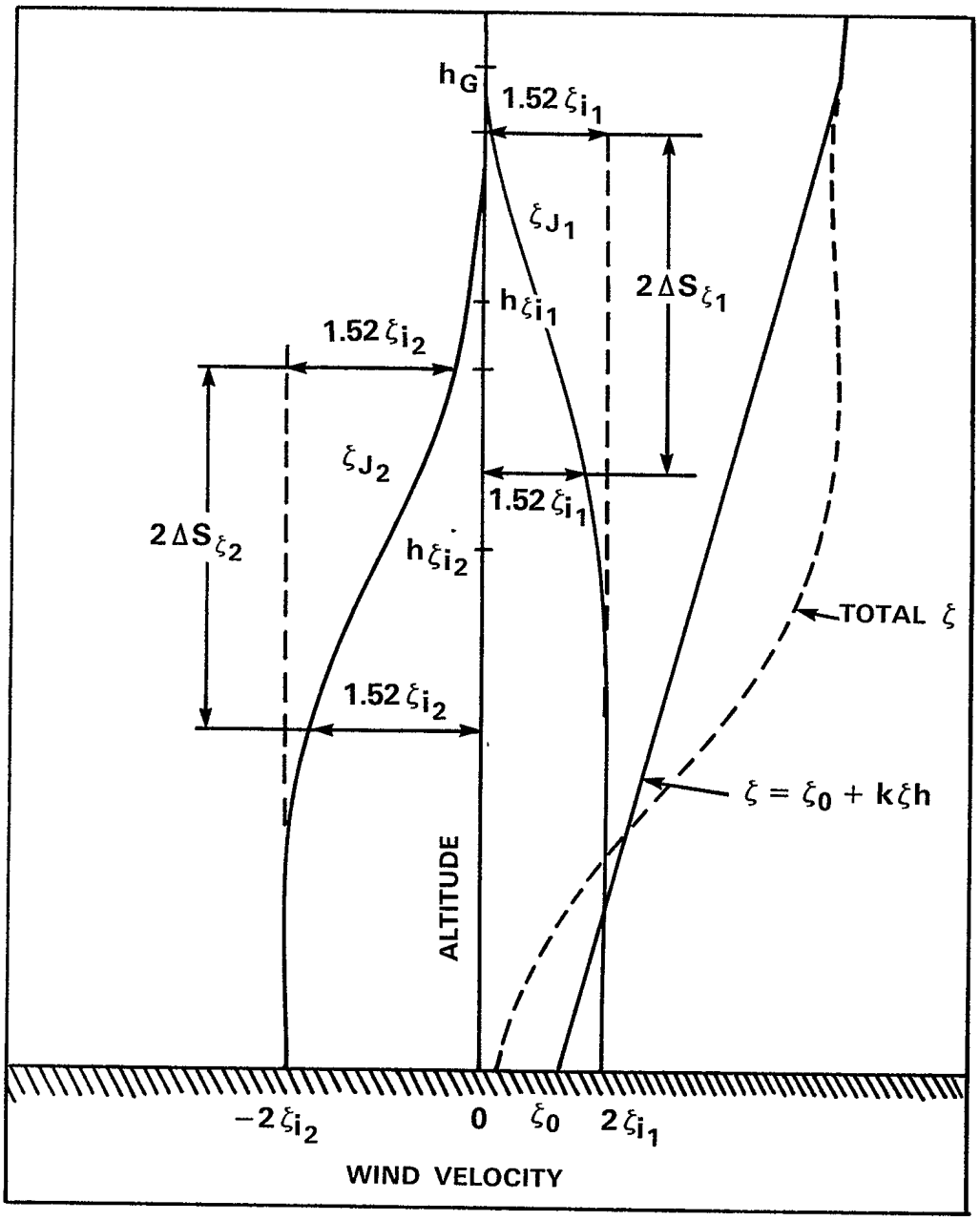

Figure 11

HORIZONTAL MEAN WIND DIRECTION CHARACTERISTICS FOR MODEL I

(Taken from Reference 2)

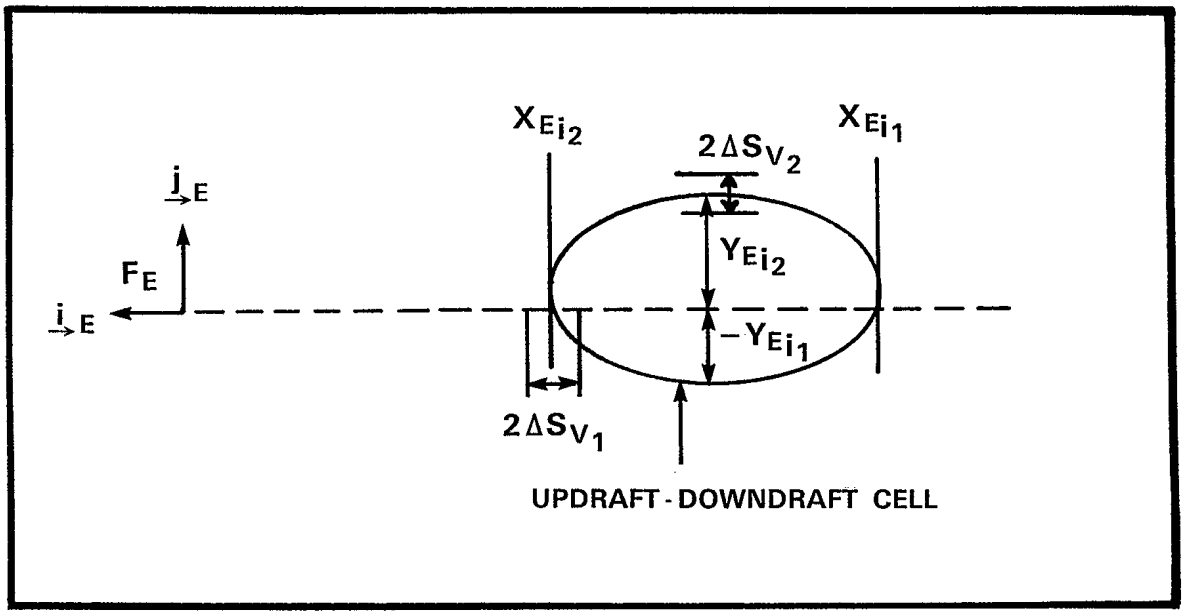

Figure 12

UPDRAFT-DOWNDRAFT CELL GEOMETRY

(Taken from Reference 2)

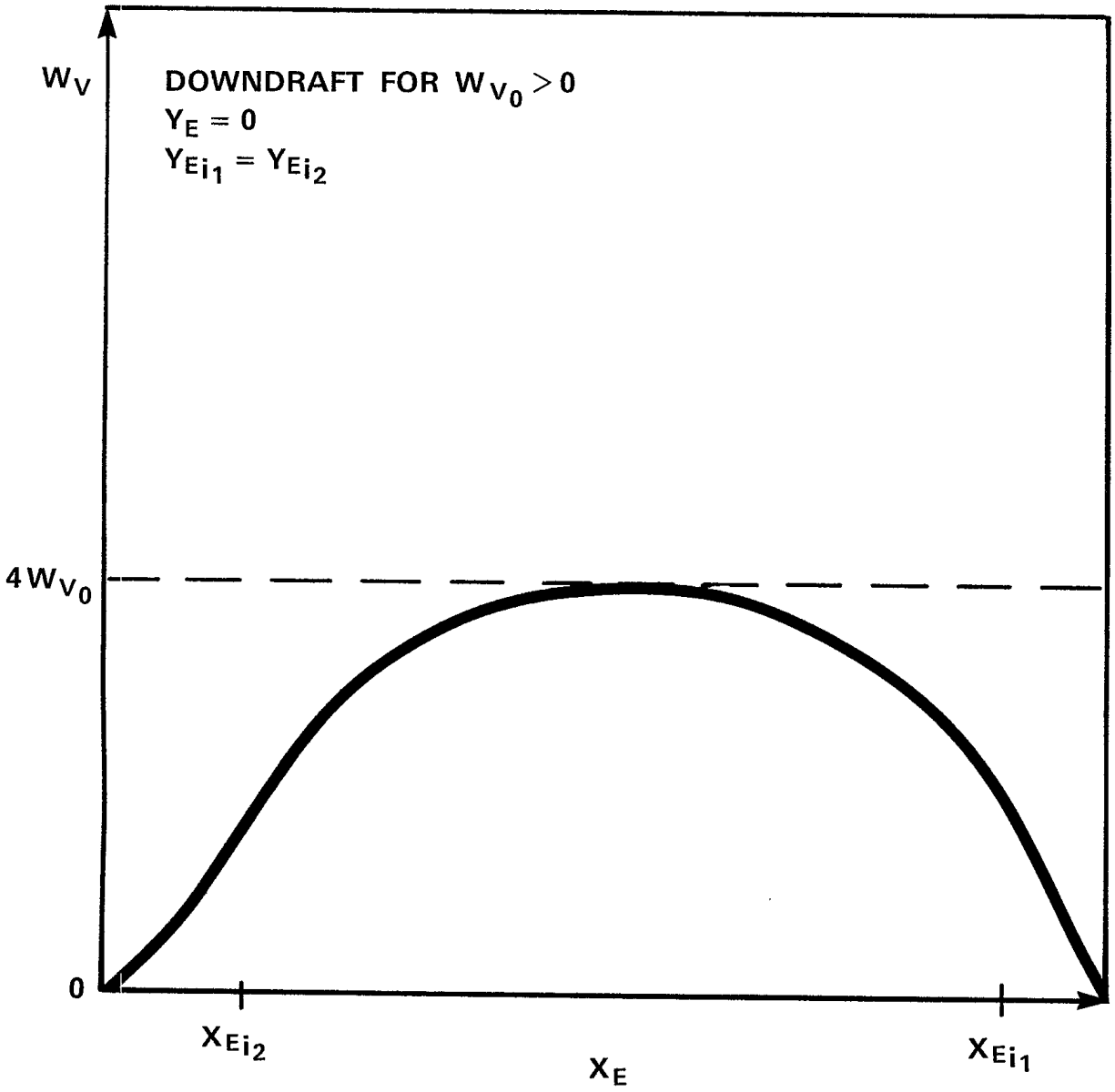

Figure 13

UPDRAFT-DOWNDRAFT MEAN WIND SPEED FOR MODEL I

(Taken from Reference 2)

F_B is a body-fixed reference frame defined in Figure 3.

F_{LA} is a launcher fixed reference frame whose initial orientation coincides with F_B

s = distance vehicle has moved along launcher rail relative to rest position

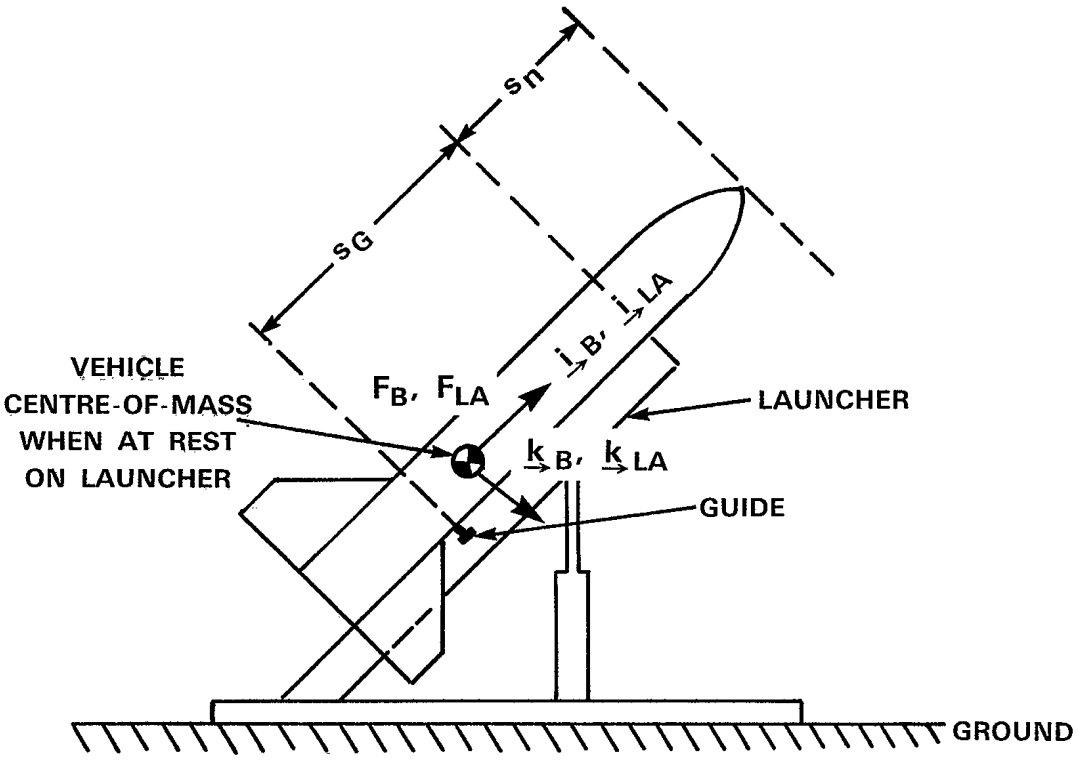

Figure 14

VEHICLE CONSTRAINTS WHILE ON LAUNCHER

$(\underrightarrow{i}, \underrightarrow{j}, \underrightarrow{k})$ is a dextral, orthonormal vector triad. Subscripts denote associated reference frame.

$$\underrightarrow{R} = x_I \underrightarrow{i}_I + y_I \underrightarrow{j}_I + z_I \underrightarrow{k}_I$$
$$\underrightarrow{R}_{IT} = x_{IT} \underrightarrow{i}_I + y_{IT} \underrightarrow{j}_I + z_{IT} \underrightarrow{k}_I$$
$$\underrightarrow{R}_T = x_T \underrightarrow{i}_T + y_T \underrightarrow{j}_T + z_T \underrightarrow{k}_T$$

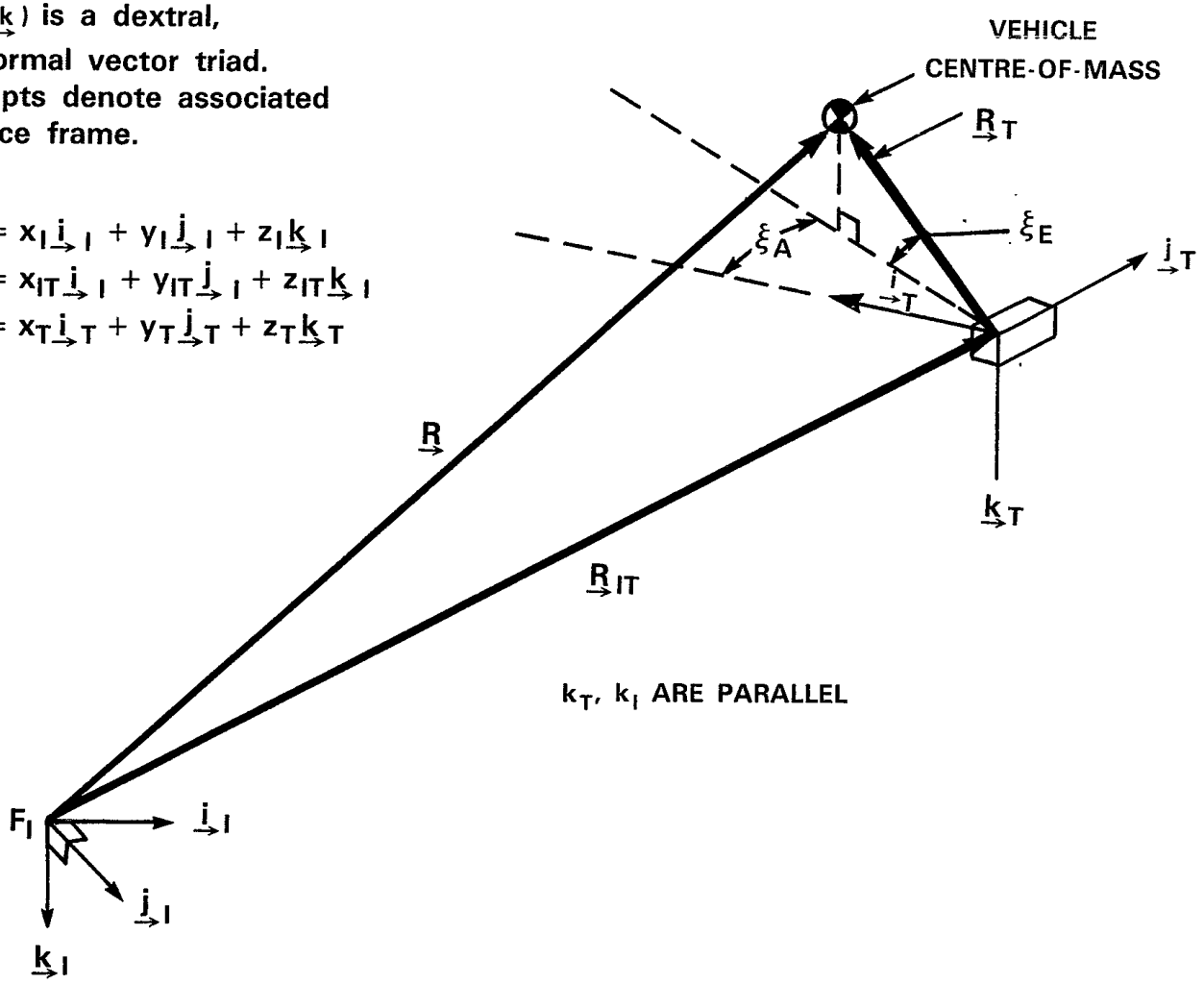

Figure 15

ASPECT ANGLE GEOMETRY

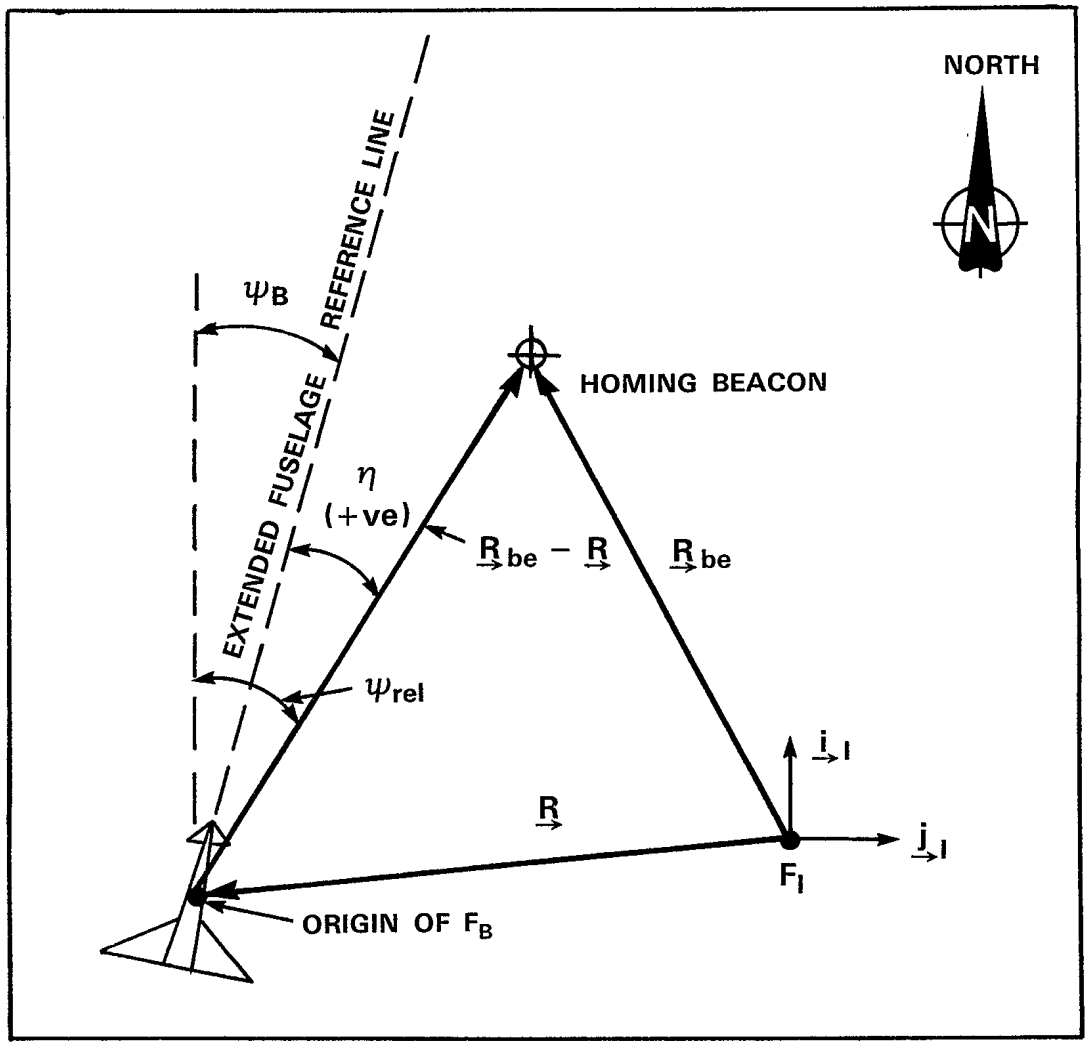

$$\underrightarrow{R}_{be} = x_{I_{be}}\underrightarrow{i}_I + y_{I_{be}}\underrightarrow{j}_I + (h_{0_{ASL}} - h_{be_{ASL}})\underrightarrow{k}_I$$

$$\underrightarrow{R} = x_I\underrightarrow{i}_I + y_I\underrightarrow{j}_I + z_I\underrightarrow{k}_I$$

Figure 16

HOMING ANGLE GEOMETRY

UNCLASSIFIED
This Sheet Security Classification

DOCUMENT CONTROL DATA - R & D
(Security classification of title, body of abstract and indexing annotation must be entered when the overall document is classified)

1 ORIGINATING ACTIVITY
Defence Research Establishment Suffield
Box 4000, Medicine Hat, AB T1A 8K6

2a. DOCUMENT SECURITY CLASSIFICATION
unclassified

2b. GROUP

3 DOCUMENT TITLE
A NONLINEAR SIX DEGREE-OF-FREEDOM FLIGHT SIMULATION MODEL (U)
VOLUME 1 - THEORETICAL DEVELOPMENT

4 DESCRIPTIVE NOTES (Type of report and inclusive dates)
Suffield Report No. 446

5. AUTHOR(S) (Last name, first name, middle initial)
Markov, A.B.

6. DOCUMENT DATE
May 1990

7a. TOTAL NO. OF PAGES

7b. NO. OF REFS
Volume 1 - 11

8a. PROJECT OR GRANT NO.
031SE

8b CONTRACT NO.

9a. ORIGINATOR'S DOCUMENT NUMBER(S)
SR 446

9b. OTHER DOCUMENT NO.(S) (Any other numbers that may be assigned this document)

10. DISTRIBUTION STATEMENT
Volumes 1 & 2 - Unlimited Distribution
Volume 3 - Limited Distribution

11. SUPPLEMENTARY NOTES

12. SPONSORING ACTIVITY
Defence Research Establishment Suffield
Box 4000, Medicine Hat, AB T1A 8K6

13. ABSTRACT

Six degree-of-freedom, rigid body equations of motion are described suitable for modeling the dynamic characteristics of multistaged rocket-boosted maneuvering aerial targets such as the DRES developed ROBOT-X. These equations of motion form the core of a Fortran simulation package called FLISIM. FLISIM is currently installed on a VAX 11/780 computer and allows for modeling of vehicle thrust and structural asymmetries, time-varying mass and inertia characteristics, autopilot control laws, autopilot update rates, autopilot sensor nonidealities, nonlinear aerodynamic characteristics, variable wind conditions, turbulence, nonstandard atmospheric conditions, stage and individual motor failures, different rocket motor types, and parachute deceleration dynamics. The FLISIM software package has been developed in two versions (FLISIMV1 and FLISIMV2) using two different aerodynamic models. Both are written in VAX 11 Fortran and run under the VMS Operating System. FLISIM is fully supported with a plotting software package (PLTSIM) developed around Tektronix PLOT 10 core software.

Volume 1 describes the development of the equations of motion. Volume 2 is the FLISIM software userbook. Volume 3 contains FLISIM source code listings.

DRDS
78-079

KEY WORDS

aerial targets
aerodynamics
control dynamics
CRV-7
drones
equations of motion
flight dynamics
flight mechanics
ROBOT-X
rocket-boosted target
simulation
six degree-of-freedom
unmanned aerial vehicles

90-03585
65834

INSTRUCTIONS

1 ORIGINATING ACTIVITY Enter the name and address of the organization issuing the document.

2a DOCUMENT SECURITY CLASSIFICATION Enter the overall security classification of the document including special warning terms whenever applicable.

2b GROUP Enter security reclassification group number. The three groups are defined in Appendix 'M' of the DRB Security Regulations.

3 DOCUMENT TITLE Enter the complete document title in all capital letters. Titles in all cases should be unclassified. If a sufficiently descriptive title cannot be selected without classification, show title classification with the usual one-capital-letter abbreviation in parentheses immediately following the title.

4 DESCRIPTIVE NOTES Enter the category of document, e.g. technical report, technical note or technical letter. If appropriate, enter the type of document, e.g. interim, progress, summary, annual or final. Give the inclusive dates when a specific reporting period is covered.

5 AUTHOR(S) Enter the name(s) of author(s) as shown on or in the document. Enter last name, first name, middle initial. If military, show rank. The name of the principal author is an absolute minimum requirement.

6 DOCUMENT DATE Enter the date (month, year) of Establishment approval for publication of the document.

7a TOTAL NUMBER OF PAGES The total page count should follow normal pagination procedures, i.e., enter the number of pages containing information.

7b NUMBER OF REFERENCES Enter the total number of references cited in the document.

8a PROJECT OR GRANT NUMBER If appropriate, enter the applicable research and development project or grant number under which the document was written.

8b. CONTRACT NUMBER If appropriate, enter the applicable number under which the document was written.

9a ORIGINATOR'S DOCUMENT NUMBER(S) Enter the official document number by which the document will be identified and controlled by the originating activity. This number must be unique to this document.

9b. OTHER DOCUMENT NUMBER(S): If the document has been assigned any other document numbers (either by the originator or by the sponsor), also enter this number(s).

10. DISTRIBUTION STATEMENT: Enter any limitations on further dissemination of the document, other than those imposed by security classification, using standard statements such as:

(1) "Qualified requesters may obtain copies of this document from their defence documentation center."

(2) "Announcement and dissemination of this document is not authorized without prior approval from originating activity."

11. SUPPLEMENTARY NOTES: Use for additional explanatory notes.

12. SPONSORING ACTIVITY: Enter the name of the departmental project office or laboratory sponsoring the research and development. Include address.

13. ABSTRACT: Enter an abstract giving a brief and factual summary of the document, even though it may also appear elsewhere in the body of the document itself. It is highly desirable that the abstract of classified documents be unclassified. Each paragraph of the abstract shall end with an indication of the security classification of the information in the paragraph (unless the document itself is unclassified) represented as (TS), (S), (C), (R), or (U).

The length of the abstract should be limited to 20 single-spaced standard typewritten lines; 7½ inches long.

14. KEY WORDS: Key words are technically meaningful terms or short phrases that characterize a document and could be helpful in cataloging the document. Key words should be selected so that no security classification is required. Identifiers, such as equipment model designation, trade name, military project code name, geographic location, may be used as key words but will be followed by an indication of technical context.